



THE UNIVERSITY OF
WAIKATO
Te Whare Wānanga o Waikato

Research Commons

<http://waikato.researchgateway.ac.nz/>

Research Commons at the University of Waikato

Copyright Statement:

The digital copy of this thesis is protected by the Copyright Act 1994 (New Zealand).

The thesis may be consulted by you, provided you comply with the provisions of the Act and the following conditions of use:

- Any use you make of these documents or images must be for research or private study purposes only, and you may not make them available to any other person.
- Authors control the copyright of their thesis. You will recognise the author's right to be identified as the author of the thesis, and due acknowledgement will be made to the author where appropriate.
- You will obtain the author's permission before publishing any material from the thesis.

Examination of the Molecular Mass of Polyhydroxypolyamides

A thesis submitted in partial fulfilment
of the requirements for the degree
of
Masters of Science in Chemistry
at
The University of Waikato
by
Martyn Faville

The University of Waikato
2010



THE UNIVERSITY OF
WAIKATO
Te Whare Wānanga o Waikato

Abstract

The work described in this thesis investigated the use of size exclusion chromatography (SEC) to fractionate a variety of different polyhydroxypolyamide (PHPA) samples for analysis by matrix assisted laser desorption ionisation-time of flight spectrometry (MALDI-TOF). The molecular weights obtained via MALDI-TOF were then compared to those obtained by ^1H nuclear magnetic resonance (NMR) end-group analysis.

Deionised water was used as the solvent for SEC fractionation using KS sugar columns KS-804 and 805 in series. An issue with PHPA is the possibility that they may hydrolyse in water and also under elevated temperature. Since deionised water was used to prepare each sample and they were run through columns which were under elevated temperatures (50°C) hydrolysis could occur during fractionation by SEC. Through ^1H NMR degradation experiments at room temperature and at 50°C , it was observed that degradation would not be a problem.

Analysis of each PHPA sample on each KS sugar column showed fractions in the V_0 region. These fractions make up the majority of the composition of unfractionated PHPA samples. There are two possible explanations for these fractions in this region, these are; 1) smaller ionised molecular weight PHPA polymers and 2) extremely high molecular weight PHPA polymer fractions. From the resulting SEC, MALDI and ^1H NMR T_2 relaxation rate measurements, it was concluded that these fractions are extremely high molecular weight polymer fractions.

The size of these PHPA fractions means molecular weights cannot be determined for these fractions and for unfractionated PHPA samples due to the limitations of MALDI-TOF spectrometry and ^1H NMR end group analysis. However MALDI-TOF and ^1H NMR end-group analysis do give good predictions for low molecular weight PHPA fractions which are in agreement with each other.

Acknowledgements

I would firstly like to express my personal gratitude to my supervisor Assoc. Prof. Marilyn Manley-Harris. Her professional support, encouragement and constant motivation throughout this project has been invaluable. It's been a pleasure working with you and I look forward to what the future may bring.

To Professor Donald Kiely who not only has provided the opportunity for me to undertake this project, but also has spent a vast amount of years producing the research that is the ground work and background to this project. I would also like to extend my immense gratitude to Dr. Tyler N. Smith and Dr. Michael R. Hinton, for not only providing me with the polymers for this project, but also with their valuable advice.

I would like to thank everyone in the chemistry department at The University of Waikato, the other academic staff, the technicians and the other students whom I've had the pleasure of knowing. Special thanks to Professor Alistair Wilkins for sharing his vast experience and knowledge of NMR. The hours that he has spent helping me understand and teaching me how to run relaxation rate measurements has been invaluable. I would also like to say a massive thanks to everyone in my lab, E3.24, for not only putting up with me and listening to all my stories and ramblings, but providing me with an escape from the HPLC room (aka The Black Hole) and from my writing. I would also like to acknowledge the scholarships that I have been fortunate to receive over my masters; The Sir Edmond Hillary Scholarship and University of Waikato Science and Engineering Masters Fees Award.

Thanks to all my friends, if it wasn't for all your guy's encouragement and conversations I might have lost my sanity a long time ago. To my siblings Stewart, Suzanne and David; I thank you all for the valuable parts you all have played in helping me and from taking my mind off my thesis. I would like to give a special thanks to my brother Richard for giving up large amounts of his time to not only read my thesis, but also to guide me through the writing process.

Lastly to my Mum and Dad, the support you guys have given me not only during my MSc, but over my whole education has been amazing. You guys have shared a hard long road with me to get to this point and no amount of words can describe how much I've appreciated everything you guys have done for me in that time.

Table of Contents

| | |
|--|-------|
| Abstract | ii |
| Acknowledgements | iii |
| Table of Contents | v |
| List of Figures | x |
| List of Tables..... | xv |
| List of Abbreviations..... | xviii |
| 1 Introduction | 1 |
| 1.1 Polymers | 1 |
| 1.2 Different ways of Describing the Size of a Polymer | 1 |
| 1.2.1 Degree of Polymerisation..... | 1 |
| 1.2.2 Terminology of Average Molecular Weight..... | 2 |
| 1.2.2.1 Number Average Molecular Weight (M_n) | 3 |
| 1.2.2.2 Weight Average Molecular Weight (M_w)..... | 3 |
| 1.2.2.3 z-Average Molecular Weight (M_z) | 4 |
| 1.2.2.4 Viscosity Average Molecular Weight (M_v) | 5 |
| 1.2.3 Polydispersity Index..... | 5 |
| 1.3 Applications for Measuring Average Molecular Weights..... | 6 |
| 1.3.1 Size Exclusion Chromatography (SEC)..... | 6 |
| 1.3.1.1 Advantages of Using SEC to Analysis Polymers | 7 |
| 1.3.1.2 Disadvantages of Using SEC to Analysis Polymers..... | 8 |
| 1.3.2 Matrix-Assisted Laser Desorption Ionisation (MALDI) | |
| Spectrometry | 10 |
| 1.3.2.1 Advantages of Using MALDI to Analysis Polymers | 11 |
| 1.3.2.2 Disadvantages of Using MALDI to Analysis Polymers..... | 12 |
| 1.3.3 Light Scattering (LS) of Polymer Solutions | 16 |
| 1.3.3.1 Advantages of Using LS to Analysis Polymers Solutions..... | 17 |
| 1.4 NMR Relaxation Theory for Polymers in Solution..... | 19 |
| 1.4.1 Basic Relaxation Theory | 20 |
| 1.4.2 Relaxation Mechanisms of Polymers in Solution | 21 |
| 1.4.2.1 Dipole-Dipole Interactions (DD) | 22 |
| 1.4.2.2 Quadrupolar Interactions Relaxation | 24 |

| | | |
|-----------|---|----|
| 1.4.2.3 | Chemical Shift Anisotropy (CSA) Relaxation..... | 25 |
| 1.4.2.4 | Paramagnetic Relaxation | 26 |
| 1.4.2.5 | Other Relaxation Mechanisms Relaxation | 27 |
| 1.4.3 | Measurements of Relaxation Rates..... | 28 |
| 1.4.3.1 | Spin-Lattice Relaxation (T_1)..... | 28 |
| 1.4.3.1.1 | How Spin-Lattice Relaxation (T_1) is Measured..... | 28 |
| 1.4.3.2 | Spin-Spin Relaxation (T_2)..... | 30 |
| 1.4.3.2.1 | How Spin-Spin Relaxation (T_2) is Measured..... | 31 |
| 1.4.4 | Factors that Affect T_1 and T_2 Relaxation Rates of Polymers in Solution | 33 |
| 1.4.4.1 | Modelling of a Polymers Molecular Dynamics in Solution | 34 |
| 1.4.4.2 | Effect of Molecular Weight | 35 |
| 1.4.4.3 | Effect of Temperature | 37 |
| 1.4.4.4 | NMR Frequency | 39 |
| 1.5 | Polyhydroxypolyamides (PHPA) | 40 |
| 1.5.1 | History of PHPA | 40 |
| 1.5.2 | Kiely's Studies of PHPA..... | 41 |
| 1.5.3 | Techniques used for Molecular Weight Determination..... | 42 |
| 1.6 | Aim of Research..... | 45 |
| 2 | Experimental | 46 |
| 2.1 | Materials..... | 46 |
| 2.2 | Instrumental..... | 46 |
| 2.2.1 | Matrix-assisted Laser Desorption Ionisation Time of Flight (MALDI-TOF) | 46 |
| 2.2.2 | Size Exclusion Chromatography (SEC)..... | 47 |
| 2.2.3 | Nuclear Magnetic Resonance (NMR)..... | 47 |
| 3 | Results and Discussion..... | 49 |
| 3.1 | Dextrans as Models for Polyhydroxypolyamides | 49 |
| 3.2 | Hydrolysis of Polyhydroxypolyamides | 50 |
| 3.3 | MALDI-TOF Spectrometry of Dextrans and Unfractionated Polyhydroxypolyamides..... | 53 |
| 3.3.1 | MALDI-TOF Spectra of Dextrans | 53 |
| 3.3.2 | MALDI-TOF Spectra of Spiked Dextrans..... | 59 |
| 3.3.3 | MALDI-TOF Spectra of Unfractionated Polyhydroxypolyamides | 63 |

| | | |
|---------|---|-----|
| 3.4 | SEC of Dextrans and Polyhydroxypolyamides | 66 |
| 3.4.1 | Characteristics of SEC Columns Used..... | 66 |
| 3.4.2 | SEC of Unfractionated Polyhydroxypolyamides | 68 |
| 3.4.3 | Calibration Curves for SEC Columns KS-804 and 805 in series ... | 80 |
| 3.5 | Measurements of NMR Relaxation Times | 82 |
| 3.6 | Analysis of Fractionated PHPAs | 83 |
| 3.6.1 | Poly(tetramethylene D-glucaramide) Post-polymer | 86 |
| 3.6.1.1 | Introduction..... | 86 |
| 3.6.1.2 | Fractionation by SEC..... | 87 |
| 3.6.1.3 | Maldi-TOF of Fractions..... | 88 |
| 3.6.1.4 | NMR Spectroscopy..... | 93 |
| 3.6.1.5 | Conclusions..... | 96 |
| 3.6.2 | Poly(tetramethylene D-glucaramide) Pre-polymer..... | 97 |
| 3.6.2.1 | Introduction..... | 97 |
| 3.6.2.2 | Fractionation by SEC..... | 98 |
| 3.6.2.3 | MALDI-TOF of Fractions | 100 |
| 3.6.2.4 | NMR Spectroscopy..... | 103 |
| 3.6.2.5 | Conclusions..... | 104 |
| 3.6.3 | Poly(3',6'-dioxaoctamethylene D-glucaramide) Pre-polymer | 105 |
| 3.6.3.1 | Introduction..... | 105 |
| 3.6.3.2 | Fractionation by SEC..... | 106 |
| 3.6.3.3 | MALDI-TOF of Fractions | 108 |
| 3.6.3.4 | NMR Spectroscopy..... | 113 |
| 3.6.3.5 | Conclusions..... | 115 |
| 3.6.4 | Poly(ethylene D-glucaramide) Post-polymer | 117 |
| 3.6.4.1 | Introduction..... | 117 |
| 3.6.4.2 | Fractionation by SEC..... | 118 |
| 3.6.4.3 | MALDI-TOF of Fractions | 119 |
| 3.6.4.4 | NMR Spectroscopy..... | 123 |
| 3.6.4.5 | Conclusions..... | 124 |
| 3.6.5 | Poly(ethylene xylaramide) Pre-polymer (A)..... | 126 |
| 3.6.5.1 | Introduction..... | 126 |
| 3.6.5.2 | Fractionation by SEC..... | 127 |
| 3.6.5.3 | MALDI-TOF of Fractions | 128 |

| | | |
|---------|--|-----|
| 3.6.5.4 | NMR Spectroscopy..... | 132 |
| 3.6.5.5 | Conclusions..... | 134 |
| 3.6.6 | Poly(ethylene xylaramide) pre-polymer (B)..... | 136 |
| 3.6.6.1 | Introduction..... | 136 |
| 3.6.6.2 | Fractionation by SEC..... | 137 |
| 3.6.6.3 | MALDI-TOF of Fractions | 139 |
| 3.6.6.4 | NMR Spectroscopy..... | 142 |
| 3.6.6.5 | Conclusions..... | 144 |
| 3.7 | Relaxation Rates and Molecular Weight of Individual Polymers and Mixtures of Polymer Fractions of Varying Molecular Weight..... | 145 |
| 4 | Conclusions..... | 152 |
| 4.1 | Degradation of PHPA | 152 |
| 4.2 | Analysis of PHPA Fractions..... | 152 |
| 4.2.1 | PHPA Fractions collected around V_0 Region in SEC..... | 152 |
| 4.2.2 | MALDI and ^1H NMR End-group Analysis of each PHPA Fraction 153 | |
| 4.3 | Further Work that can be done | 155 |
| 4.3.1 | Light Scattering..... | 155 |
| 4.3.2 | Determination of Non-polymer Organic Material from PHPA polymers in Smaller Fractions | 155 |
| 5 | Appendix..... | 156 |
| 5.1 | Equations used to Calculate Molecular Weight of Polymers in Solution for Laser Light Scattering | 156 |
| 5.2 | Explanation on how Polymers Molecular Weights are Determined using Universal Calibration Curve | 157 |
| 5.3 | Raw Data for Each Polyhydroxypolyamide ^1H NMR Degradation Experiments..... | 158 |
| 5.3.1 | Poly(tetramethylene D-glucaramide) post-polymer | 158 |
| 5.3.1.1 | Degradation Experiments at Room Temperature | 158 |
| 5.3.1.2 | Degradation Experiments at 50°C | 159 |
| 5.3.2 | Poly(tetramethylene D-glucaramide) pre-polymer..... | 160 |
| 5.3.2.1 | Degradation Experiments at Room Temperature | 160 |
| 5.3.2.2 | Degradation Experiments at 50°C | 161 |
| 5.3.3 | Poly(3',6'-dioxaoctamethylene D-glucaramide) pre-polymer | 162 |

| | | |
|---------|---|-----|
| 5.3.3.1 | Degradation Experiments at Room Temperature | 162 |
| 5.3.3.2 | Degradation Experiments at 50°C | 163 |
| 5.3.4 | Poly(ethylene D-glucaramide) post-polymer | 164 |
| 5.3.4.1 | Degradation Experiments at Room Temperature | 164 |
| 5.3.4.2 | Degradation Experiments at 50°C | 165 |
| 5.3.5 | Poly(ethylene xylaramide) pre-polymer (A)..... | 166 |
| 5.3.5.1 | Degradation Experiments at Room Temperature | 166 |
| 5.3.5.2 | Degradation Experiments at 50°C | 167 |
| 5.3.6 | Poly(ethylene xylaramide) pre-polymer (B) | 168 |
| 5.3.6.1 | Degradation Experiments at Room Temperature | 168 |
| 5.3.6.2 | Degradation Experiments at 50°C | 169 |
| 5.4 | Raw Data for Poly(tetramethylene D-glucaramide) post-polymer Temperature Experiments | 170 |
| 5.5 | Raw Data for T_1 and T_2 Relaxation Rate Measurements for each Poly(tetramethylene D-glucaramide) post-polymer Fraction..... | 171 |
| 5.6 | Raw Data for T_2 Relaxation Rate Measurements for each Poly(3',6'- dioxaoctamethylene D-glucaramide) pre-polymer Fraction..... | 172 |
| 5.7 | Raw Data for T_2 Relaxation Rate Measurements for each Dextran | 173 |
| 5.8 | Commands to Reduce the Effect of HOD water Peak on T_2 Relaxation Rate Measurements | 174 |
| 5.9 | Pulse Programs used to measure T_1 Relaxation Rate | 174 |
| 5.10 | Pulse Programs used to measure T_2 Relaxation Rate | 176 |
| 6 | References | 178 |

List of Figures

| | |
|--|----|
| Figure 1.1: Representative differential weight distribution curves, a) Narrow, b) Broad and c) Binomial distribution curves | 2 |
| Figure 1.2: Molecular Weight Distributions | 6 |
| Figure 1.3: Illustration of a pack SEC column with gel pores and individual polymer molecules either permeating the pores or being excluded..... | 7 |
| Figure 1.4: Principles of MALDI before and after ionisation..... | 10 |
| Figure 1.5: Mass distribution of polystyrene sample with nominal molecular weight of 330,000, which A) is the 2+ ion and B) has a single charge | 11 |
| Figure 1.6: Molecular weight distribution of a polymer with a polydispersity >1.2 | 13 |
| Figure 1.7: Setup of an Online and Direct Deposition SEC/MALDI TOF MS.... | 13 |
| Figure 1.8: The resulting molecular weight distribution of PMMA sample in the MALDI compared with GPC (SEC) | 14 |
| Figure 1.9: Resulting MALDI spectra of PMMA obtained with different laser powers: A) 46%, B) 50% and C) 54% | 15 |
| Figure 1.10: Illustration of light scattering technique which uses a multiple detectors surrounding the polymer sample | 16 |
| Figure 1.11: Planes in which T_1 and T_2 are measured in..... | 21 |
| Figure 1.12: Pulse program used to measure T_1 relaxation rates in the NMR..... | 28 |
| Figure 1.13: Typical results for a T_1 experiment in the NMR obtained by varying τ | 29 |
| Figure 1.14: Pulse program used to measure T_2 relaxation rates in the NMR using A) Carr-Purcell pulse program and A) Carr-Purcell-Meiboom-Gill's pulse program | 32 |
| Figure 1.15: Typical results for a T_2 experiment using Carr-Purcell-Meiboom-Gill's pulse program in the NMR obtained by varying n | 33 |
| Figure 1.16: Resulting trend for A) T_1 relaxation rates with increasing polymer molecular weight and B) T_2 relaxation rates with increasing polymer molecular weight and temperature | 36 |
| Figure 1.17: Relaxation models of A) T_1 and B) T_2 relaxation rates vs correlation times | 38 |

| | |
|--|----|
| Figure 1.18: Resulting T_1 relaxation rate of PIP with molecular weight of 305,000 with increasing temperature and NMR frequency | 39 |
| Figure 1.19: Resulting T_1 relaxation rates for different molecular weight PDMS at increasing NMR frequency | 39 |
| Figure 1.20: General Structure for a PHPA based on a hexaric acid..... | 40 |
| Figure 1.21: Range of PHPA based on A) galactaric acid, B) D-mannaric acid, C) D-glucaric, and D) xylaric acid..... | 42 |
| Figure 1.22: A block copolymer PHPA with galactaric acid, xylaric acid and 2,6-dioxaoctane-1,8-diamine, this has shown to have good film forming ability..... | 42 |
| Figure 1.23: A) Poly(hexamethylene D-galactaramide) showing two terminal CH_2 protons and six non terminal CH_2 protons next to the amide and B) ^1H NMR spectra of poly(hexamethylene D-galactaramide) in TFA- d_1 showing the terminal CH_2 protons and the non terminal CH_2 protons next to the amides | 43 |
| Figure 3.1 – Partial Structure of Dextran | 49 |
| Figure 3.2: A) Change in DP determined by end-group analysis of Poly(tetramethylene D-glucaramide) post-polymer at room temperature B) Change in DP determined by end-group analysis of Poly(tetramethylene D-glucaramide) post-polymer at room temperature, red region is estimated time period taken to prepare sample for the HPLC..... | 51 |
| Figure 3.3: Change in DP determined by end-group analysis of Poly(tetramethylene D-glucaramide) post-polymer at 50 °C..... | 52 |
| Figure 3.4: Change in DP determined by end-group analysis of Poly(tetramethylene D-glucaramide) post-polymer at 50 °C red region is estimated time period polymer spent in column | 53 |
| Figure 3.5: MALDI-TOF Mass spectra for A) Dextran 1200 in sDHB matrix, B) Dextran 1200 in THAP matrix, C) Dextran 4440 in sDHB matrix, D) Dextran 4440 in THAP matrix and E) Dextran 9890 in sDHB matrix..... | 55 |
| Figure 3.6: Dextran 4440 detected using A) Reflectron Mode, and B) Linear Mode. | 57 |
| Figure 3.7: Repeating Unit of Poly(ethylene xylaramide). | 58 |
| Figure 3.8: MALDI-TOF massSpectra for A) Dextran 1200 spiked with 2mM of NaCl B) Dextran 1200 spiked with 2mM of KCl THAP C) Unspiked Dextran 1200..... | 60 |

| | |
|---|----|
| Figure 3.9: MALDI-TOF Mass Spectra of Unfractionated A) Poly(tetramethylene D-glucaramide) Post-polymer, B) poly(tetramethylene-D-glucaramide pre-polymer, C) Poly(3',6'-dioxaoctamethylene D-glucaramide) pre-polymer, D) poly(ethylene D-glucaramide) Post-polymer, E) Poly(ethylene xylaramide) pre-polymer (A), and F) Poly(ethylene xylaramide) pre-polymer (B) in THAP Matrix. | 64 |
| Figure 3.10: SEC Chromatograms of Poly(tetramethylene D-glucaramide) Post-polymer on each individual KS columns. | 68 |
| Figure 3.11: SEC Chromatograms of Poly(tetramethylene D-glucaramide) Pre-polymer on each individual KS columns. | 70 |
| Figure 3.12: SEC Chromatograms of Poly(3',6'-dioxaoctamethylene D-glucaramide) pre-polymer on each individual KS columns..... | 72 |
| Figure 3.13: SEC Chromatograms of Poly(ethylene D-glucaramide) Post-polymer on each individual KS columns. | 74 |
| Figure 3.14: SEC Chromatograms of Poly(ethylene xylaramide) pre-polymer (A) on each individual KS columns. | 76 |
| Figure 3.15: SEC Chromatograms of Poly(ethylene xylaramide) pre-polymer (B) on each individual KS columns. | 78 |
| Figure 3.16: Calibration curve of Dextrans Molecular Weight versus their Retention Time on on KS-804 and 805 SEC columns in series. | 81 |
| Figure 3.17: A) Structure of the Poly(tetramethylene d-glucaramide) post-polymer repeating unit. B) Fully Labelled ¹ H NMR Spectrum of Poly(tetramethylene d-glucaramide) Post-polymer. | 86 |
| Figure 3.18: SEC Chromatogram of Poly(tetramethylene D-glucaramide) Post-polymer on columns KS-804 and KS-805 in series. | 87 |
| Figure 3.19: Mass Spectra of Poly(tetramethylene D-glucaramide) Post-polymer Fractions from SEC (see also Figure 3.18) | 89 |
| Figure 3.20: NMR of A) Fraction A 128 scans, B) Fraction B 129 scans, C) Fraction C 1000 scans, D) Fraction D 1000 scans, E) Fraction E 4000 scans and F) Fraction F 1000 scans. | 93 |
| Figure 3.21: Effect upon DP calculated by End-group analysis of varying the temperature of the ¹ H NMR experiment for unfractionated poly(tetramethylene D-glucaramide) post-polymer. | 95 |
| Figure 3.22: Structure of the Poly(tetramethylene D-glucaramide) pre-polymer repeating unit..... | 97 |

| | |
|---|-----|
| Figure 3.23: Fully Labelled ^1H NMR Spectrum of Poly(tetramethylene D-glucaramide) Pre-polymer..... | 98 |
| Figure 3.24 : SEC Chromatogram of Poly(tetramethylene D-glucaramide) Pre-polymer on columns KS-804. | 99 |
| Figure 3.25: Mass Spectra of Poly(tetramethylene D-glucaramide) Pre-polymer Fractions from SEC (see also Figure 3.24) | 102 |
| Figure 3.26: NMR of A) Fraction A 1000 scans, B) Fraction B 1000 scans, C) Fraction C 2000 scans, D) Fraction D 1000 scans and E) Fraction E 1500 scans | 103 |
| Figure 3.27: Structure of the Poly(3',6'-dioxaoctamethylene D-glucaramide) Pre-polymer repeating unit. | 105 |
| Figure 3.28: Fully Labelled ^1H NMR Spectrum of Poly(3',6'-dioxaoctamethylene D-glucaramide) Pre-polymer. | 106 |
| Figure 3.29: SEC Chromatogram of Poly(3',6'-dioxaoctamethylene D-glucaramide) Pre-polymer on columns KS-804 and KS-805 in series. | 107 |
| Figure 3.30: Mass Spectra of Poly(3',6'-dioxaoctamethylene D-glucaramide) Pre-polymer Fractions from SEC (see Figure 3.29). | 109 |
| Figure 3.31: NMR of A) Fraction A 500 scans, B) Fraction B 500 scans, C) Fraction C 4500 scans, D) Fraction D 1000 scans, E) Fraction E 1000 scans F) Fraction F 500 scans and Fraction G 10,000 scans..... | 113 |
| Figure 3.32: A) Structure of the Poly(ethylene D-glucaramide) post-polymer repeating unit. B) Fully Labelled ^1H NMR Spectrum of Poly(ethylene D-glucaramide) Post-polymer. | 117 |
| Figure 3.33: SEC Chromatogram of Poly(ethylene D-glucaramide) Post-polymer on columns KS-804 and KS-805 in series. | 118 |
| Figure 3.34: Mass Spectra of Poly(ethylene D-glucaramide) Post-polymer Fractions from SEC (see Figure Figure 3.33). | 120 |
| Figure 3.35: NMR of A) Fraction A 4000 scans, B) Fraction B 4500 scans, C) Fraction C 6000 scans, D) Fraction D 4000 scans, E) Fraction E 4000 scans and F) Fraction F 7560 scans. | 124 |
| Figure 3.36: Structure of the Poly(ethylene xylaramide) Pre-polymer (A) repeating unit..... | 126 |
| Figure 3.37: Fully Labelled ^1H NMR Spectrum of Poly(ethylene xylaramide) Pre-polymer (A)..... | 127 |

| | |
|---|-----|
| Figure 3.38: SEC Chromatogram of Poly(ethylene xylaramide) Pre-polymer (A) on columns KS-804 and KS-805 in series. | 128 |
| Figure 3.39: Mass Spectra of Poly(ethylene xylaramide) Pre-polymer (B) Fractions from SEC (see Figure Figure 3.38) | 130 |
| Figure 3.40: NMR of A) Fraction A 1000 scans, B) Fraction B 1000 scans, C) Fraction C 500 scan and D) Fraction D 1500 scans..... | 132 |
| Figure 3.41: A) ^1H and B) ^{13}C NMR of Fraction C. | 133 |
| Figure 3.42: Repeating Unit of polyethylene glycol..... | 133 |
| Figure 3.43: Hypothesised structure of the repeating unit possibly observed in Fraction C..... | 134 |
| Figure 3.44: Structure of the Poly(ethylene xylaramide) Pre-polymer (B) repeating unit | 136 |
| Figure 3.45: Fully Labelled ^1H NMR Spectrum of Poly(ethylene xylaramide) Pre-polymer (B). | 137 |
| Figure 3.46: SEC Chromatogram of Poly(ethylene xylaramide) Pre-polymer (B) on columns KS-804 and KS-805 in series. | 138 |
| Figure 3.47: Mass Spectra of Poly(ethylene xylaramide) Pre-polymer (B) Fractions from SEC (see Figure Figure 3.46). | 140 |
| Figure 3.48: NMR of A) Fraction A 1250 scans, B) Fraction B 1250 scans, C) Fraction C 500 scan and D) Fraction D 1500 scans..... | 142 |
| Figure 3.49: Fully labelled ^1H NMR of Dextrans | 146 |
| Figure 3.50: A) T_2 data for the fractionated dextrans plotted against molecular mass at 30°C B) The region 0 to 41,000 expanded..... | 149 |

List of Tables

| | |
|--|----|
| Table 1.1: Some polymer standards used for SEC calibration | 9 |
| Table 1.2: Properties of some common NMR active Nuclei | 20 |
| Table 1.3: Molecular weights calculated by ¹ H NMR end-group analysis and GPC | 45 |
| Table 3.1: Polytools™ Calculations of Mn using Peak Height and Peak Integral for Dextrans 1200, 4440 and 9890..... | 56 |
| Table 3.2: Hypothesised structures between 800m/z and 1250m/z. | 61 |
| Table 3.3: ICP-MS data of the Concentration (ppb) of Sodium and Potassium in each PHPA samples. | 62 |
| Table 3.4: Polytools™ Calculations of M _n using Peak Height and Peak Integral and ¹ H End Group Calculations of M _n for each unfractionated PHPA sample. ... | 65 |
| Table 3.5: Manufacturer's Exclusion Limit and Retention Time of 2M Dextran and Glucose of each Shodex KS series SEC column..... | 67 |
| Table 3.6: Integrated Areas of labelled peaks in SEC chromatograms of unfractionated poly(tetramethylene-D-glucaramide post-polymer on the KS series SEC columns..... | 69 |
| Table 3.7: Integrated Areas of labelled peaks in SEC chromatograms of unfractionated poly(tetramethylene-D-glucaramide pre-polymer on the KS series SEC columns..... | 71 |
| Table 3.8: Integrated Areas of labelled peaks in SEC chromatograms of unfractionated poly Poly(3',6'-dioxaoctamethylene D-glucaramide) pre-polymer on the KS series SEC columns..... | 73 |
| Table 3.9: Integrated Areas of labelled peaks in SEC chromatograms of unfractionated poly(ethylene D-glucaramide) Post-polymer on the KS series SEC columns. | 75 |
| Table 3.10: Integrated Areas of labelled peaks in SEC chromatograms of unfractionated poly(ethylene xylaramide) pre-polymer (A) on the KS series SEC columns. | 77 |
| Table 3.11: Integrated Areas of labelled peaks in SEC chromatograms of unfractionated poly(ethylene xylaramide) pre-polymer (B) on the KS series SEC columns. | 79 |

| | |
|---|-----|
| Table 3.12: Retention Time of 2M Dextran and Glucose of Shodex KS-804 and 805 SEC column in series. | 80 |
| Table 3.13: M_n Calculations by ^1H NMR end group analysis of each PHPA sample Prior to fractionation by | 84 |
| Table 3.14 – M_n Calculations by ^1H NMR end group analysis of each unfractionated PHPA sample on a 300 MHz Bruker NMR spectrometer using a QMP and Dual probe and on a 400 MHz Bruker NMR spectrometer using a Inverse Dual and Dual probe..... | 85 |
| Table 3.15: Integrated Areas of labelled peaks in SEC chromatogram of unfractionated poly(tetramethylene-D-glucaramide post-polymer on KS-804 and 805 SEC columns in series..... | 88 |
| Table 3.16: MALDI-TOF Laser Power used to ionise the Poly(tetramethylene D-glucaramide) Post-polymer Fractions. | 90 |
| Table 3.17: Polytools™ Calculations of M_n using Peak Height and Peak Integral and ^1H End Group Calculations of M_n for each Poly(tetramethylene D-glucaramide) Post-polymer Fraction..... | 92 |
| Table 3.18: T_1 and T_2 relaxation time measurements for each individual poly(tetramethylene D-glucaramide) post-polymer fraction. | 96 |
| Table 3.19: Integrated areas of labelled peaks in SEC chromatogram of unfractionated poly(tetramethylene-D-glucaramide Pre-polymer on KS-804 and 805 SEC columns in series..... | 99 |
| Table 3.20: MALDI-TOF Laser Power used to ionise Poly(tetramethylene D-glucaramide) Pre-polymer Fractions..... | 100 |
| Table 3.21: Polytools™ Calculations of M_n using Peak Height and Peak Integral and ^1H End Group Calculations of M_n for each Poly(tetramethylene D-glucaramide) Pre-polymer Fraction. | 101 |
| Table 3.22: Integrated Areas of labelled peaks in SEC chromatogram of unfractionated Poly(3',6'-dioxaoctamethylene D-glucaramide) Pre-polymer on KS-804 and 805 SEC columns in series. | 107 |
| Table 3.23: MALDI-TOF Laser Power used to Ionise Poly(3',6'-dioxaoctamethylene D-glucaramide) Post-polymer Fractions. | 110 |
| Table 3.24: Polytools™ Calculations of M_n using Peak Height and Peak Integral and ^1H End Group Calculations of M_n for each Poly(3',6'-dioxaoctamethylene D-glucaramide) Pre-polymer Fraction. | 112 |

| | |
|---|-----|
| Table 3.25: T_1 and T_2 relaxation time measurements for each individual poly(3',6'-dioxaoctamethylene D-glucaramide) pre-polymer fraction. | 114 |
| Table 3.26: Integrated Areas of labelled peaks in SEC chromatogram of unfractionated Poly(ethylene D-glucaramide) Post-polymer on KS-804 and 805 SEC columns in series..... | 119 |
| Table 3.27: MALDI-TOF Laser Power used to Ionise Poly(ethylene D-glucaramide)Post-polymer Fractions. | 121 |
| Table 3.28: Polytools™ Calculations of M_n using Peak Height and Peak Integral and 1H End Group Calculations of M_n for each Poly(ethylene D-glucaramide) Post-polymer Fraction..... | 122 |
| Table 3.29: Integrated Areas of labelled peaks in SEC chromatogram of unfractionated Poly(ethylene xylaramide) Pre-polymer (A) on KS-804 and 805 SEC columns in series..... | 128 |
| Table 3.30: MALDI-TOF Laser Power used to Ionise Poly(ethylene xylaramide) Pre-polymer (A) Fractions. | 129 |
| Table 3.31: Polytools™ Calculations of M_n using Peak Height and Peak Integral and 1H End Group Calculations of M_n for each Poly(ethylene xylaramide) Pre-polymer (B) Fraction..... | 131 |
| Table 3.32: Integrated Areas of labelled peaks in SEC chromatogram of unfractionated Poly(ethylene xylaramide) Pre-polymer (B) on KS-804 and 805 SEC columns in series..... | 139 |
| Table 3.33: MALDI-TOF Laser Power used to Ionise Poly(ethylene xylaramide) Pre-polymer (B) Fraction | 140 |
| Table 3.34: Polytools™ Calculations of M_n using Peak Height and Peak Integral and 1H End Group Calculations of M_n for each Poly(ethylene xylaramide) Pre-polymer (B) Fraction..... | 141 |
| Table 3.35: T_2 Relaxation Rates for Unfractionated poly(ethylene xylaramide) pre-polymer (A) and (B). | 143 |
| Table 3.36: T_2 relaxation rates for each individual Fractionated Dextrans and the two mixtures..... | 147 |
| Table 3.37: Calculations of M_n for each Dextran Mixture..... | 150 |

List of Abbreviations

| | |
|------------------|---|
| Da | Daltons |
| D ₂ O | Deuterated Water |
| DP | Degree of Polymerisation |
| D.I.water | Deionised Water |
| GPC | Gel Permeation Chromatography |
| HPLC | High Pressure Liquid Chromatography |
| Hz | Hertz |
| MALDI-TOF | Matrix Assisted Laser Desorption Ionisation – Time of Flight |
| M _n | Number Average Molecular Weight |
| M _w | Weight Average Molecular Weight |
| M _z | z-average Molecular Weight |
| M _v | Viscosity Average Molecular Weight |
| MWD | Molecular Weight Distribution |
| mL | Millilitres |
| m/z | Mass to Charge Ratio |
| NMR | Nuclear Magnetic Resonance |
| PHPA | Polyhydroxypolyamide |
| PIP | Polyisoprene |
| ppm | Parts Per Million |
| SEC | Size Exclusion Chromatography |
| T ₁ | Spin-Lattice Relaxation |
| T ₂ | Spin-Spin Relaxation |

1 Introduction

1.1 Polymers

Polymers are extensively used in today's world. Chemists, biochemists and chemical engineers are all in some way involved in polymer science or technology. As such, some people have now come to refer to this as the polymer age [1]. The word *polymer* stands for poly meaning many and mers meaning units. It was derived from the ancient Greek words of poly and meros which mean respectively many and parts.

1.2 Different ways of Describing the Size of a Polymer

1.2.1 Degree of Polymerisation

There are a variety of ways that can be used to quantify the size of a polymer. The primary measurement of a polymer's size is the degree of polymerization (DP). DP refers to the number of repeating units that are present in a polymer's chain.

A major drawback associated with polymers is that it is almost impossible to terminate growing polymers at a specific size [2]. A typical polymer system will therefore have a distribution of polymer chains with differing lengths. Consequently the quoted DP value actually represents the *average* DP over the polymer system [2-7].

1.2.2 Terminology of Average Molecular Weight

For a heterodispersed polymer system, only an average molecular weight can be used to quantify the molecular weight. The average molecular weight of a polymer system can be expressed in numerous ways; the four main measurements being 1) number average molecular weight (M_n), 2) weight average molecular weight (M_w), 3) z-average molecular weight (M_z), and 4) viscosity average molecular weight (M_v) [2-7, 9].

It should be appreciated that the distribution of polymer molecular weights can vary within a polymer system. Three types of distribution curves that can be used to describe these variations; 1) relatively broad, 2) relatively narrow, and 3) bimodal curves (Figure 1.1) [8-10]. From these curves, several mathematical moments can be used to derive equations from which the average molecular weight for a polymer system can be calculated.

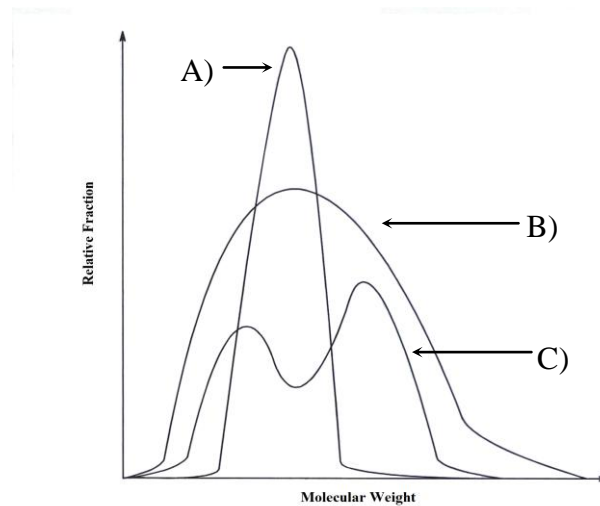


Figure 1.1: Representative differential weight distribution curves, a) Narrow, b) Broad and c) Binomial distribution curves (Charraher, 2008 [8])

1.2.2.1 Number Average Molecular Weight (M_n)

The first distribution moment describes the number average molecular weight (M_n). M_n is also commonly referred to as the arithmetic mean and is the easiest of the average molecular weights to calculate. The general equation for M_n is given by:

$$M_n = \frac{\sum w_i}{\sum \frac{w_i}{M_i}} = \frac{\sum N_i \times M_i}{\sum N_i} = DP \times M_r \quad (1.1)$$

where N_i is the number of polymer chains, w_i is the polymer sample weight, M_i is the polymer molecular weight, and M_r is the repeating unit molecular weight.

The values obtained for M_n are independent of a polymer's molecular size, but are dependent on the number of chains present in the polymer system. It should also be noted that values calculated for M_n for a polymer system are highly sensitive to the presence of smaller molecular weight polymers. For a more elegant explanation of the basis for M_n , interested readers are directed to Seymour and Carraher [8]. Some of the common experimental methods for determining M_n are; 1) SEC, 2) membrane osmometry, 3) vapour phase osmometry, 4) end-group analysis and 5) MALDI-TOF spectrometry.

1.2.2.2 Weight Average Molecular Weight (M_w)

The second distribution moment describes the weight average molecular weight (M_w). M_w is closely related to the bulk properties of a polymer system [1, 2, 8]. The general equation used to calculate M_w is as follows:

$$M_w = \frac{\sum w_i M_i}{\sum w_i} = \frac{\sum N_i \times M_i^2}{\sum N_i M_i} \quad (1.2)$$

Compared to M_n , M_w is more dependent on the polymer chain lengths that are present in a polymer system. Therefore, M_w will be highly sensitive to the presence of larger molecular weight polymers. For a more elegant explanation of the basis for M_w interested readers are again directed to Seymour and Carraher's [8]. Some of the common experimental method for determining M_w are; 1) light scattering and 2) segmental velocity.

1.2.2.3 z-Average Molecular Weight (M_z)

The third distribution moment describes the z-average molecular weight (M_z). Whereas M_w is closely related to a polymer's bulk properties, M_z it is closely related to the melt elasticity of a polymer. The general equation used to calculate M_z is given as follows:

$$M_z = \frac{\sum w_i M_i^2}{\sum w_i} = \frac{\sum N_i \times M_i^3}{\sum N_i M_i^2} \quad (1.3)$$

Some of the common experimental methods for determining M_z are; 1) sedimentation equilibrium and 2) SEC with the combination of a laser light scattering detector [1, 2, 8, 10]. Note that it is possible to determine higher order distribution moments. These can be calculated using the following general equation:

$$M = \frac{\sum N_i \times M_i^{\alpha+1}}{\sum N_i M_i^\alpha} \quad (1.4)$$

where α is the distribution moment order. However, as the main polymer properties are related to the first three moments, it is unnecessary to calculate these higher order moments.

1.2.2.4 Viscosity Average Molecular Weight (M_v)

Viscosity average molecular weight (M_v) differs slightly from the other three molecular weight measurements in that it is not calculated by the general equation given by eqn. (1.5). In order to calculate M_v , constants need to be found experimentally using polymers of known molecular weights. The general equation for M_v is given by the following equation:

$$M_v = \left[\frac{\sum N_i \times M_i^{1+a}}{\sum N_i M_i} \right]^{\frac{1}{a}} \quad (1.5)$$

where a is the constant that must be determined experimentally, and depends on the polymer/solvent pair used in the viscosity experiments. However, molecular weights obtained for M_v are less precise than molecular weights found for other average molecular weights. This is because M_v is highly dependent on the solvent used to measure viscosity. The only experimental method for determining M_v is intrinsic viscosity.

1.2.3 Polydispersity Index

For a heterodispersed polymer system, the following relationship holds between the average molecular weights: $M_n \leq M_v \leq M_w \leq M_z$. This relationship can also be illustrated on a molecular weight distribution (MWD) curve (Figure 1.2). To measure the polydispersity of a heterodispersed polymer system, the ratio of M_w/M_n , is used. This is commonly referred to as the polydispersity index. The polydispersity index will be greater than or equal to unity. Higher polydispersity index values indicate a wider range of M_i values. Conversely, polymer systems where the polydispersity index approaches unity (i.e., $M_n = M_v = M_w = M_z$) indicate no variation between the M_i values. These are referred as monodispersed polymer systems, with an example being proteins [2].

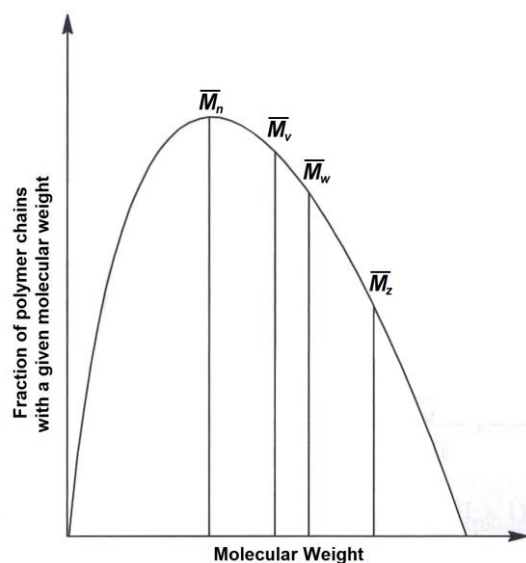


Figure 1.2: Molecular Weight Distributions (Charraher, 2008 [8])

1.3 Applications for Measuring Average Molecular Weights

A number of different methods have been used to measure the average molecular weight for polymer's. From the classical applications of intrinsic viscosity, osmometry and light scattering to the more modern applications of electrospray MS and MALDI-TOF, all these applications have shown advantages and disadvantages for determining a polymer's average molecular weight. This discussion will be limited to methods used in this study or by Kiely and co-workers in their various publications.

1.3.1 Size Exclusion Chromatography (SEC)

Since the early 1960's, the use of SEC has been extensively used in the characterization of both synthetic and natural polymers [11]. The primary benefit of this technique, which is also commonly referred to as Gel Permeation Chromatography (GPC), is that it is applicable to polymer molecules of any size. The wide variety of applications of SEC, along with the relative ease in running this technique, makes it the most important tool for characterizing industrial polymer systems.

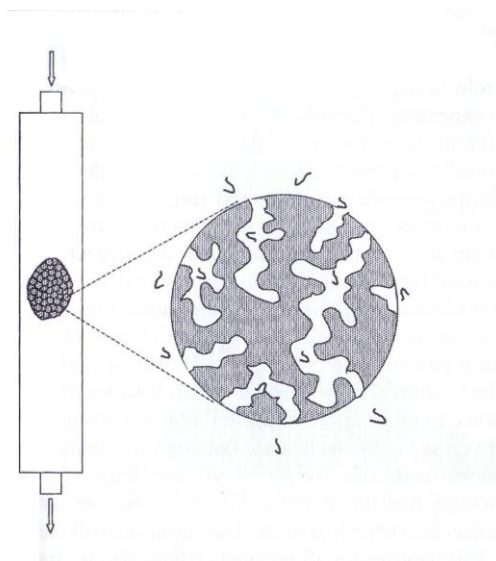


Figure 1.3: Illustration of a pack SEC column with gel pores and individual polymer molecules either permeating the pores or being excluded (Hiemenz & Lodge, 2007 [1])

Separation of a polymer system using SEC is dependent on either the polymer's hydrodynamic volume or size. Separation of polymer samples by SEC is achieved by passing the polymer, carried by a solvent of choice, through the SEC column. These columns are packed with rigid gels which contain pores that can vary in size between $10\text{-}10^4 \text{ \AA}$ [1]. It is the size of these pores that dictates the size of the polymer that can permeate within the given SEC column. The specific size of these pores which allow the polymer to permeate into the gel pores are also known as the *exclusion limit*. Therefore, as the polymer sample travels through the columns, the smaller size polymer molecules will permeate the gel pores (Figure 1.3). Larger polymer molecules, will either semi-permeate the gel pores or travel through the columns without permeating into any pores (Figure 1.3)

1.3.1.1 Advantages of Using SEC to Analysis Polymers

The main advantage of using SEC to investigate polymer systems is that it is independent of the chemical properties of the polymer being analysed. This is because unlike other chromatography techniques, in which the chemical properties of a polymer are important, polymers in the SEC have no chemical interaction with the columns gel surface [1, 11]. Instead, separation of the

different sized polymer molecules that are present in a sample is based on each molecule's hydrodynamic volume or molecular size. It should be noted that this is not the case for all polymers. Non-specific interactions, for example ion exclusion, can be an issue.

When calibrated using a suitable polymer standard, SEC can be used to determine the molecular distributions. However, as will be explained in subsequent sections this is not the most advantageous method for determining molecular weights for polymer samples (see Section 1.3.1.2)

SEC has the added advantage in that it can provide data from a variety of detectors, thereby providing a richer data set. There are four classes of detectors that are commonly used for SEC; 1) the refractive index (RI), 2) the absorption (UV-vis), 3) laser light scattering (LLS) and, 4) on-line viscometer (V) detectors [1, 2]. When used in combination with each other, these detectors are capable of determining information such as concentration, viscosity and molecular weight. Furthermore, the use of multiple detectors provides the means by which a polymer's average molecular weight can be determined without having to use known polymer standards for calibration.

Finally, SEC can be used in combination with MALDI-TOF spectrometry to determine the average molecular weights from a MWD. Both on-line [12] and off-line [12-14] SEC/MALDI techniques have been developed to study molecular weights of polymers. As for the previously mentioned detectors, MALDI-TOF spectrometry is an alternative way of determining molecular weight for polymer's MWD's without having to use known polymer standards for calibration.

1.3.1.2 Disadvantages of Using SEC to Analysis Polymers

Despite the aforementioned advantages of using SEC, there are drawbacks to using this technique. It is not an absolute method and generally requires calibration from a polymer standard of known molecular weight. The process of calibration can inadvertently introduce errors in the calculated M_n [2, 11, 15] as

there are only a limited amount of polymer standards that are commercially available.

Table 1.3 illustrates example some of the most common standards available for calibration. The main types of homo- polymer standards available commercially are of linear type. This is the major disadvantage for SEC as there are many different types of branched or hetero- and co-polymers. The use of these restricted polymer standards to predict the molecular weight of these types of polymers is not advantageous. This is because polymers may have different hydrodynamic behaviour to those of the standards, hence retention times will not correlate.

This issue can be overcome by using either the 1) universal calibration curve (see Appendix 5.2 for explanation on how universal calibration curve is used to determine molecular weight of a polymer), 2) SEC coupled with two detectors simultaneously (see Section 1.3.1.1) or 3) off-line/on-line SEC/MALDI techniques, which is explained in further detail below (see also Section 1.3.1.1) [12, 13, 16]. Note that the universal calibration curve, despite being able to approximate a polymer's molecular weight, is prone to drawbacks. However, the use of either methods 2) and 3) from above alleviates the problem of having to use polymer standards for calibration.

| Standards | Type of Solvents Typically used for SEC Analysis of these Standards |
|------------------------------------|---|
| Polystyrene | Organic |
| Polyethylene | Organic |
| Poly(vinyl chloride) | Organic |
| Poly(1,2-butyleneglycol phthalate) | Organic |
| Poly(methyl methacrylate) | Organic |
| Dextrans | Aqueous |

Table 1.1: Some polymer standards used for SEC calibration

1.3.2 Matrix-Assisted Laser Desorption Ionisation (MALDI) Spectrometry

Mass spectrometry has been used for the study of synthetic polymers since the 1960's [17]. However, early mass spectrometry techniques were limited by what information they could provide about a polymer sample. This is because they were hard ionisation techniques [2, 8, 18]. This limiting issue was overcome with the discovery of Matrix-assisted laser desorption ionisation, MALDI. Introduced in 1988 by Tanaka, Hillenkamp and co-workers [18], MALDI is a soft ionization technique which allows for the desorption and ionisation of varying sized molecules [19, 20]. MALDI can potentially provide a vast amount of information about a polymer's structure, MWD and molecular weight which was previously unattainable by other mass spectrometry techniques. For these reasons, MALDI has become the most commonly used ionisation technique for analysing synthetic polymers.

There are two types of mass analyser commonly used together with MALDI; 1) quadrupole detection and 2) time of flight (TOF). MALDI uses a vast array of different matrices to co-crystallise with the polymer sample. These matrices efficiently absorb the UV component of the laser and transfer it to the sample. This allows for the polymer sample to be ionized, through the capture of either a proton H^+ , metal ion (e.g., sodium, potassium, lithium) or some other species, to form positively or negatively charged ion adducts (Figure 1.4) [20]. Absorbance of the laser's UV component by the matrix not only aids in polymer ionisation, but also prevents fragmentation of the polymer.

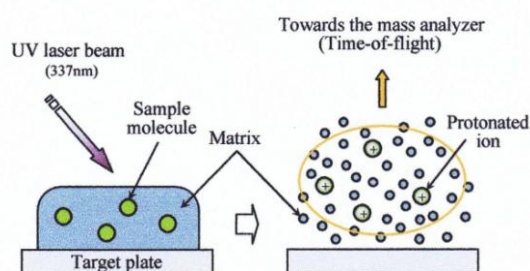


Figure 1.4: Principles of MALDI before and after ionisation

1.3.2.1 Advantages of Using MALDI to Analysis Polymers

There are many advantages in using MALDI to analyse synthetic polymers. Spectra obtained via MALDI are often simple and can provide an accurate, fast and direct MWD for a polymer sample. The spectra produced by MALDI consist predominantly of singularly charged polymer molecule ions that have very little, if any, fragmentation [12, 16]. The information provided by this analysis not only includes the polymer's repeating unit, end groups and other modification of an individual oligomer, but also M_n and M_w . This information is dependent on the mass analyser providing sufficient separation of individual polymer ions.

Through many empirical studies, MALDI has been demonstrated to produce fairly accurate molecular weights for polymer samples that have low to moderate molecular weights, with narrow polydispersity (≤ 1.2), relative to other techniques [12, 14, 21, 22]. These studies have also shown that MALDI has the ability to determine polymer molecular weights that are greater than 100,000. To date, there have only been a few cases reported with polymer molecular weight greater than 100,000 [23]. Techniques have been developed by Schreimer and co-workers which enable measurements of polymer M_n values greater than 100,000 [23]. From their research, they have established the highest molecular weight ever measured for a polymer in the MALDI of 1.5 million for polystyrene [12, 23].

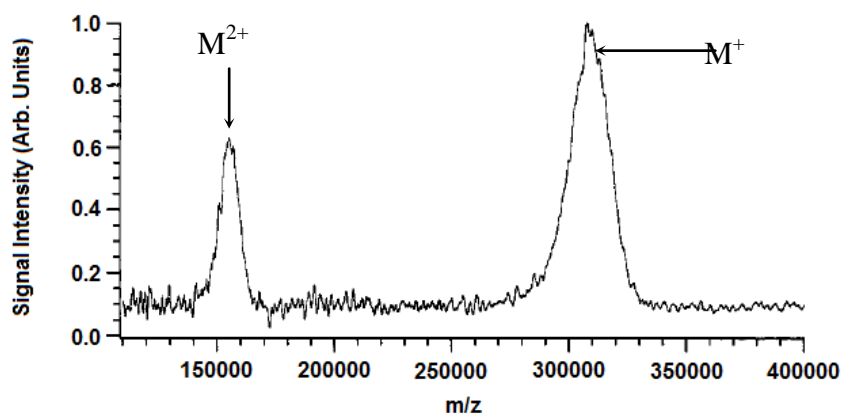


Figure 1.5: Mass distribution of polystyrene sample with nominal molecular weight of 330,000, which A) is the 2+ ion and B) has a single charge (Schreimer & Li, 1996 [23])

1.3.2.2 Disadvantages of Using MALDI to Analysis Polymers

One of the main disadvantages of using MALDI is that the resolution and sensitivity of a polymers mass spectrum decreases as the polymers molecular weight increases (Figure 1.5) [12, 23]. Information provided for a polymer in the MALDI, such as repeating units, end groups and other oligomer modifications, are also affected by the decrease in resolution and sensitivity [12, 16, 23]. In these cases it is still possible to determine a polymer's molecular weight. Furthermore, the mass accuracy diminishes as the polymer molecular weight increases, and calibration with a standard is usually required.

The limitations that are observed for high molecular weight polymers are due to instrumental and fundamental limitations making analysis of such polymers difficult. Furthermore, there can be an upper limit to the mass ions that can be produced for a selected polymer sample. This upper limit may be caused by chemistry/photochemistry effects of the polymers sample being analysed [23]. Several investigators have suggested that sample preparation, and not instrumental limitations, is the principle impediment to analysing high molecular weight polymers [23].

As previously stated, MALDI performs best for M_n calculations of polymers samples that have narrow polydispersity (≤ 1.2). For polymer systems with polydispersity greater than this, the MALDI fails to produce reliable molecular weight distributions (Figure 1.6). Results from experimental studies have shown that smaller mass polymers are preferentially desorbed and ionized in the MALDI [14, 20, 25]. For polymer systems of broad polydispersity, this causes suppression of the desorption and ionisation of higher mass polymers in the MALDI [12, 15, 16]. However, this limitation can be overcome by fractionating broadly polydispersed polymers into lower polydispersed fractions using SEC. This process is known as the off-line SEC/MALDI method. As the polydispersity of each sample is reduced, MALDI can once again be employed to accurately analyse the individual fractions.

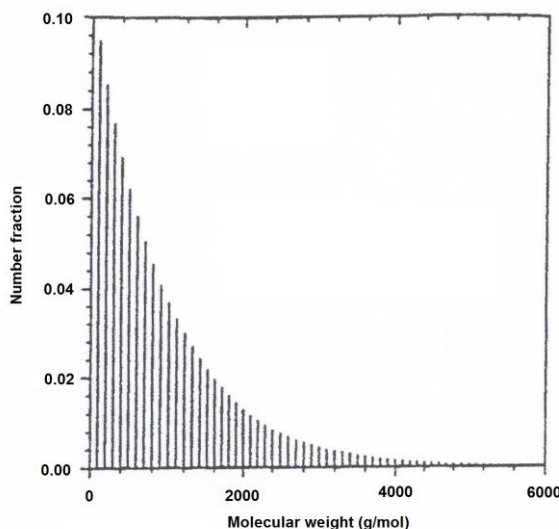


Figure 1.6: Molecular weight distribution of a polymer with a polydispersity >1.2 (Jackson et al, 1996 [24])

It should be appreciated however that this off-line SEC/MALDI method is time consuming. In order to reduce analysis time, attempts have recently been made to develop an on-line SEC/MALDI instrument. This is a direct deposit method in which fractions from the SEC and matrix are directly and automatically deposited onto a MALDI target plate (Figure 1.7) [26].

It has been suggested that MALDI could become a viable alternative to SEC, due to the lack of fragmentation of molecular species observed during analysis [12, 16]. It is however currently appreciated that MALDI is quantitatively less reliable than SEC and other chromatography techniques [15]. Furthermore, MWD obtained via MALDI are generally viewed as being less reliable than that obtained via other techniques [15, 21].

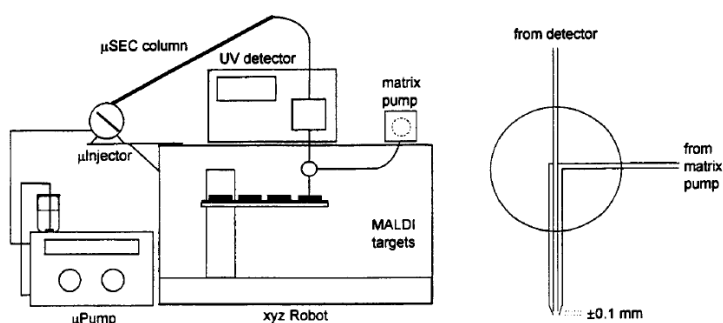


Figure 1.7: Setup of an Online and Direct Deposition SEC/MALDI TOF MS (Nielen, 1998 [26])

Experimental studies have shown that there is a difference between the MWD obtained via MALDI and SEC (Figure 1.8) [15]. From the studies, it was observed that the MWD obtained from MALDI was displaced further towards the lower mass region relative to SEC. There are numerous suggestions for this discrepancy [15] with the main hypotheses being 1) the type of matrix used [12, 16], 2) the dynamic range of the detectors used [12, 16], 3) the post-acceleration voltage and fragmentation, and 4) the preferential volatilisation of smaller molecular weight polymers when using different laser powers. These results were elegantly illustrated by Lehrle and Saron in their research using poly(methyl methacrylate) (PMMA) [15].

An understanding of the polymer system and the choice of laser power is an important factor in acquiring quality MALDI spectra [12, 15, 16]. Many studies have shown the effects that laser power has on a polymer sample's MWD [12, 16]. These studies show that the experimental parameters that provide maximum sensitivity (ion yield) do not necessarily provide the most representative MWD for that polymer sample [15]. There is a trade off between increasing laser power to obtain enough intensity, with limiting laser powers so as to not fragment or distort the polymer sample [15] (Figure 1.9).

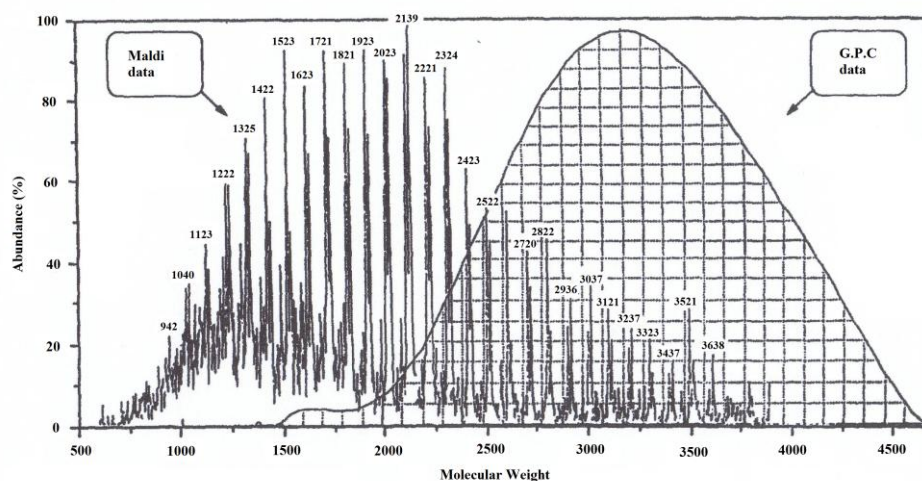


Figure 1.8: The resulting molecular weight distribution of PMMA sample in the MALDI compared with GPC (SEC) (Lehrle & Sarson, 1996 [15])

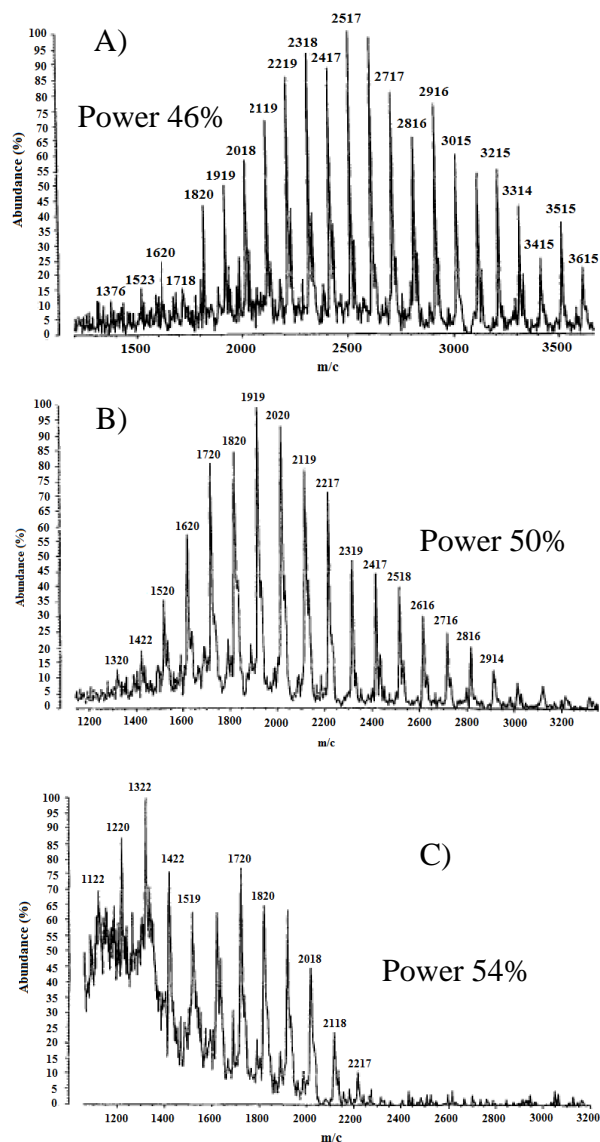


Figure 1.9: Resulting MALDI spectra of PMMA obtained with different laser powers: A) 46%, B) 50% and C) 54% (Lehrle & Sarson, 1996 [15])

It has also been noted that the matrices affect the MWD obtained by MALDI. It has been demonstrated that certain matrices used in MALDI analysis perform poorly on certain polymer samples [23]. This is mainly due to the unfavourable chemical, or photochemical, reactions that are induced between the matrix and the polymer sample; a reaction that can occur either during preparation of the sample, or during ionization when in the MALDI.

1.3.3 Light Scattering (LS) of Polymer Solutions

LS has become one of the most widely used applications for determining the molecular weight of polymer solutions. Originally LS was developed to study the scattering caused by gas particles [1, 10, 27, 28]. However, during the 1940's LS scattering was successfully adapted by Debye to analyse polymer solutions [1, 10, 28]. Since then LS techniques have become a powerful tool in determining a polymer molecule's size and shape [1].

LS techniques use a light beam which is passed through a polymer solution. This causes oscillation of the dipoles that are formed between the electrons in the polymer and solvent. The effect of this oscillation is that energy is re-radiated from the sample as scattered light (Figure 1.10) [10]. Early LS photometers used high pressure mercury lamps and filters to obtain a monochromatic beam as the radiation source. Modern LS photometers use lasers which produce higher quality monochromatic beams than mercury lamp equivalents.

The intensity of the scattering signal detected for LS experiments are dependent upon several factors, the most important being 1) the concentration of the polymer solution, 2) the size of the polymer, and 3) the polarisability of the scattered polymer molecules. It also should be noted that the refractive index detected from

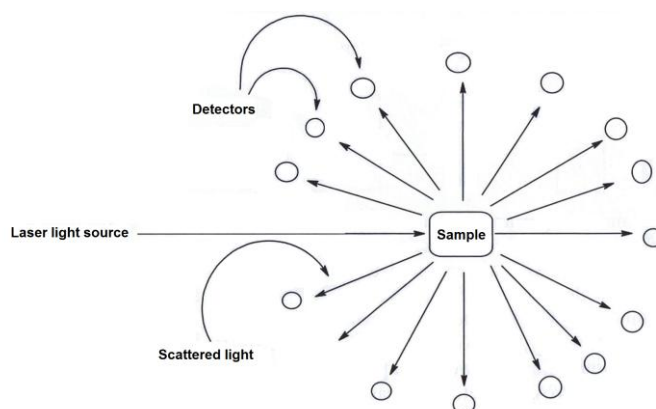


Figure 1.10: Illustration of light scattering technique which uses a multiple detectors surrounding the polymer sample (Charraher, 2008 [8])

a polymer solution is also dependant on the solution concentration and vibration intensity of the polymer. The combination of these material properties can be utilised to calculate the molecular weight of varying polymer solutions (see Appendix A for equations).

1.3.3.1 Advantages of Using LS to Analysis Polymers Solutions

LS is one of the most powerful tools that can be used by polymer chemists to obtain absolute M_w measurements [8, 29-32] and characterise polymers [8, 31, 33]. Compared to other M_n measurement techniques, such as SEC and MALDI, LS increases in sensitivity as a polymer's size increases [8]. This gives LS the ability to determine a polymer's molecular shape. Many empirical studies have utilized LS not only to determine molecular weights of synthetic polymer, but also as a classical method for verifying the accuracy of newer techniques in calculating polymer molecular weights. One such study, undertaken by Zhu and co-workers, used known molecular weight standards of polystyrene to test the accuracy of molecular weight as determined by MALDI [34].

Currently there are several photometers that are available for LS analysis. These types of photometers are 1) low angle laser light scattering (LALLS), 2) multi-angle angle laser light scattering (MALLS), 3) right angle laser light scattering (RALLS) and 4) dynamic laser light scattering [35, 36]. These detectors have the advantage in that they reduce the scattering particle factor (P_θ), a parameter in the equations used to calculate M_w , to 1. This has the effect of simplifying the calculations that are made by the photometers to determine M_w (see also Appendix 5.1 for equations).

One of the biggest advantages of using LALLS, MALLS and RALLS is their ability to be coupled to SEC as detectors. A combination of SEC with one of these laser light scattering detectors (LLS) provides a large amount of information about a polymer sample. Examples of such information include the polymer's size, shape and MWD. The SEC/LLS combination setup has the ability of determining various molecular weights, in addition to M_w , such as M_n and M_z .

Due to its ease of use, reduced cost, and the variety of polymer samples that can be analyzed, the SEC/LLS setup is now observed as the most effective for determining the molecular weight of polymer solutions. The accuracy of this setup was verified by Nielen & Malucha [13] who used SEC/RALLS to determine the molecular weights from known polymer standards.

An added advantage of the SEC/LLS setup is that the SEC columns act as filters to remove any dust particles present in the polymer sample prior to analysis. As will be seen in subsequent sections (see Section 1.4.3.2) dust particles are a major limitation to LS analysis. Removal of these dust particles from the polymer solution prior to analysis by LS is essential.

1.4.3.2 Disadvantages of Using LS to Analyse Polymers Solutions

The major limitation with using LS is that it is essential that the preparations are *dust free* [1, 28]. If dust particles are present in the polymer solution, and are larger than the polymer molecules themselves, they will scatter the light more strongly than the polymer molecule of interest. Dust removal is harder for some solvents than others. Dust removal using polar solvents for example, such as water and tetrahydrofuran (THF), has been found to be more difficult than using non-polar solvents such as toluene and cyclohexane.

There are three main ways of removing these dust particles from a polymer sample. These methods include 1) filtration, 2) centrifugation and 3) by using SEC. The first two methods are seen to be less than advantageous because they are concentration-dependent processes, and the concentration of a polymer sample will vary [1, 28]. However, as previously mentioned (see Section 1.3.3.1), the SEC/LLS setup has the added advantage of using the SEC columns to act as a filter for dust removal [1].

Despite the advantages of combining the LS and SEC methods, there are still issues inherent in this setup. One such issue is that it is difficult to measure the molecular weight of polymer solutions for $M_n < 1000$ as high concentrations of

the polymer solution are required to produce a detectable LS signal. The reason for this is that the scattering signal is proportional to c/M_w , for a given polymer solution concentration [36].

When using LS alone, it is difficult and time consuming to measure a polymer's molecular weight [1, 10]. This is because calibrations of variable quantities in both the polymer solvent and the instruments are required [1, 28]. The major variable quantities that require calibration are the solution's refractive index (n), concentration (c), light source wavelength (λ), and the rate of change of refractive index as a function of concentration (d_n/d_c) [1, 2, 8]. Care must be taken in calibrating these variables because this can lead to inaccurate results when calculating the molecular weight for a polymer solution [1, 2, 8].

1.4 NMR Relaxation Theory for Polymers in Solution

NMR spectroscopy has for many years been used to study the dynamics of polymers in solution. Originally it was thought that the restricted chain motion of high molecular weight polymers would result in the rapid relaxation of excited NMR spin states, and that only low intensity broad line signals would therefore be observed. Fortunately this did not prove to be the case. In general well resolved, sharp line spectra can be obtained [37, 38]. It is now known that relaxation pathways associated with the re-orientation in solution of atoms of the polymer chain is only a small contribution to the relaxation of atoms of polymeric chains.

The dominant relaxation pathways in high molecular weight polymers are those associated with localised atomic motions such as rapid librational motions, gauche-trans isomerisation processes and segmental motions [37, 38]. Relaxation via rapid librational motions or gauche-trans isomerisation pathways is only significant for polymers which have high molecular weights ($M_w > 10^4$).

In medium to low molecular weight polymers segmental relaxation processes are the predominant relaxation process. Segmental relaxation of high molecular weight polymers occurs more slowly than in lower molecular weight polymers.

1.4.1 Basic Relaxation Theory

The basic theory of relaxation can be explained thus; when a magnetic pulse (usually a rf pulse) is applied to an NMR active nucleus, this perturbs all the spin populations from their natural, thermally controlled, equilibrium state [37-39]. The rate at which the spin populations return to its equilibrium states provides information about the molecular dynamics and the inter-nuclear distances between interacting nuclei.

A variety of NMR-active nuclei (e.g. ^1H , ^{13}C , ^{15}N , etc) can be present in natural and synthetic polymers. Common nuclei and some of their properties are shown in Table 1.2. A knowledge of the relaxation rates of these nuclei affords an insight into the dynamic properties and molecular weight of polymers.

| Nucleus | Spin Quantum Number (I) | Magnetic Moment (μ) | Gyromagnetic Ratio (γ) | Electric Quadrupole Moment (eQ) |
|-----------------|-------------------------|---------------------------|---------------------------------|---------------------------------|
| ^1H | 1/2 | 4.8374 | 26.7520 | - |
| ^2D | 1 | 1.2126 | 4.1067 | 0.00277 |
| ^{13}C | 1/2 | 1.2166 | 6.7265 | - |
| ^{15}N | 1/2 | -0.4905 | -2.7108 | - |
| ^{19}F | 1/2 | 4.5533 | 25.1670 | - |
| ^{31}P | 1/2 | 1.9600 | 10.8290 | - |

Table 1.2: Properties of some common NMR active Nuclei

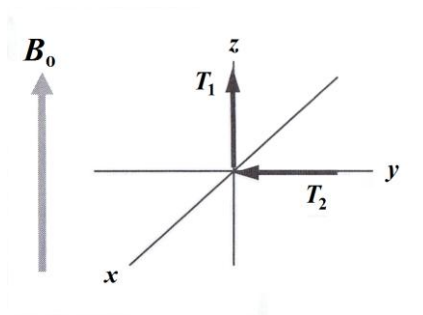


Figure 1.11: Planes in which T_1 and T_2 are measured in

The relaxation of an excited nucleus is primarily attributable to interactions between it, and the molecular motions of other polymer nuclei (atoms). This is because atomic fluctuations of these nuclei modulate the magnetic field that is experienced by nearby atoms [38]. The fluctuations that occur in a local magnetic field occur over a broad range of frequencies. The gross chemical structure and molecular environment of atoms in a polymer chain determine the nature and magnitude of fluctuations that occur in a local magnetic field [38].

In NMR experiments there are two types of relaxation processes that are important, namely the spin-lattice relaxation process, (T_1 process) and spin-spin relaxation process (T_2 process). Spin-lattice relaxation corresponds to the rate at which a polymers spin system takes to recover to equilibrium along the longitudinal z-axis (Figure 1.11), while spin-spin relaxation corresponds to the rate at which a polymer's spin system magnetisation decays to zero in the transverse x-y plane (Figure 1.11). T_1 and T_2 rate constants give complementary information about a polymers molecular dynamics.

1.4.2 Relaxation Mechanisms of Polymers in Solution

To fully understand the resulting relaxation rate measurements observed for both T_1 and T_2 relaxation, the relaxation mechanisms behind these values must be understood.

When a polymer spin system is perturbed by a magnetic pulse from its thermal equilibrium state several relaxation mechanisms characterise the pathways which a polymer spin system uses to return back to its thermal equilibrium state [37, 38]. Relaxation mechanisms or interaction pathways for a polymer in solution include dipole-dipole interactions (DD), quadrupolar interactions (Q), chemical shift anisotropy (CSA), and paramagnetic relaxation (PARA) pathways. Other, less significant, relaxation mechanisms (pathways) are also known [37, 38]. The preferred relaxation mechanism of an excited polymer spin system is dependent on the chemical environment and the nuclei (be it ^1H , ^{13}C , ^{15}N , etc) in the polymer chain.

The sum of all applicable relaxation mechanisms contribute to give the overall observed relaxation rates for both T_1 and T_2 relaxation process. The respective equations used to describe the sum of these interactions are given by:

$$T_1: \quad \frac{1}{T_1} = \frac{1}{T_1^{DD}} + \frac{1}{T_1^{CSA}} + \frac{1}{T_1^Q} + \frac{1}{T_1^{PARA}} + \frac{1}{T_1^{OTHER}} \quad (1.6)$$

$$T_2: \quad \frac{1}{T_2} = \frac{1}{T_2^{DD}} + \frac{1}{T_2^{CSA}} + \frac{1}{T_2^Q} + \frac{1}{T_2^{PARA}} + \frac{1}{T_2^{OTHER}} \quad (1.7)$$

1.4.2.1 Dipole-Dipole Interactions (DD)

Dipole-dipole interactions also known as dipole coupling are the most common and usually the most effective relaxation mechanism for a polymer molecule. The dipole-dipole interaction mechanism is most important for nuclei that have $I = 1/2$, such nuclei include ^1H and ^{13}C . The relaxation via dipole-dipole interactions is the direct result of through space interactions between NMR active nuclei [38]. The rate that is observed for spin-lattice and spin-spin relaxation from dipole-dipole relaxation is dependent on several factors. These include the strength of the dipole coupling and the distance between NMR-active nuclei and also it is dependent on the NMR properties of an NMR-active nuclei, such as their magnetic moment and their gyromagnetic ratio (also known as magnetogyric ratio) (Table 1.2) [37, 38].

$$DC \propto \frac{\mu_1 + \mu_2}{r^3} \quad (1.8)$$

The dipole coupling strength depends on both intermolecular distance between the two NMR-active nuclei involved and the magnetic moments they possess. The strength of the dipole coupling energy is given by equation 1.8, where μ_1 and μ_2 are the magnetic moments of the two nuclei in question and r is the inter-nuclear distance [38]. Nuclei such as ^1H and ^{19}F are more effective at causing relaxation than other NMR-active nuclei. This is because they have larger magnetic moments (Table 1.2) than other NMR-active nuclei and this allows them to have a stronger dipole coupling.

The dipole coupling between two neighbouring nuclei decreases with increasing distance [38]. If the inter-nuclear distance between two nuclei increased for example from 1 to 2.5\AA this would cause the dipole coupling to reduce significantly. This means that the dipole coupling is more effective in causing relaxation of nuclei that are located in the same molecule [38]. The overall total of dipole coupling is the sum of all the surrounding nearby nuclei.

There are two type of dipole-dipole interactions that can cause relaxation, these are homonuclear and heteronuclear dipole-dipole interactions. Homonuclear arise from the interaction of nuclei that are the same, this dipole-dipole interaction mainly affects spin-lattice relaxation rates [38]. For polymer molecules the most common homonuclear dipole-dipole interaction occurs between a pair of ^1H [38].

Heteronuclear dipole coupling arise from the interaction of two different nuclei and affects both spin-lattice and spin-spin relaxation rates. Heteronuclear dipole relaxation mechanism are most commonly observed for ^1H that are directly bonded to a ^{13}C in a polymer molecule [38]. The following equations describe the interactions quantitatively:

$$T_I^{DD}:$$

Homo:

$$\frac{1}{T_1^{DD}} = \frac{n}{20} \left(\frac{\mu_0}{4\pi} \right)^2 \frac{\gamma_H^4 \hbar}{r^6} \{J(0) + 3J(\omega_H) + 6J(2\omega_H)\} \quad (1.9)$$

Hetro:

$$\frac{1}{T_1^{DD}} = \frac{n}{10} \left[\frac{\mu_0}{4\pi} \right] \frac{\gamma_C^2 \gamma_H^2 \hbar^2}{r^6} \{J(\omega_H - \omega_C) + 3J(\omega_C) + 6J(\omega_H + \omega_C)\} \quad (1.10)$$

$$\begin{aligned} \frac{1}{T_2^{DD}} = \frac{n}{20} \left(\frac{\mu_0}{4\pi} \right)^2 \frac{\gamma_C^2 \gamma_H^2 \hbar}{r^6} \{ & 4J(0) + J(\omega_H - \omega_C) + 3J(\omega_C) \\ & + 6J(\omega_H) + J(\omega_H + \omega_C) \} \end{aligned} \quad (1.11)$$

where n is the number of protons, μ_0 is the vacuum magnetic permeability, γ_C and γ_H are the magnetogyric ratios of carbon and hydrogen, ω_C and ω_H are the frequencies of carbon and hydrogen and r is the inter-nuclear distance.

Equations 1.9, 1.10 and 1.11 are shown to be proportional to the inverse sixth power of the intermolecular distance [37], this is why the dipole coupling diminishes as r increases. Also each equation shows that the relaxation rates are dependent on the size of the magnetogyric ratio, that is each equation is proportional to γ^2 [37, 38]. This means the higher the magnetogyric ratio the more effective the relaxation [38]. Using the magnetic properties of different NMR-active nuclei it is possible to understand how effective relaxation will be. Using these magnetic properties its observed that a ^1H pair or a pair containing a ^1H and another nuclei will provide a greater dipole-dipole interactions than other NMR-active nuclei. It is also expected that will also give significant dipole-dipole interactions will occur for ^{19}F nuclei and its neighbouring nuclei as well [37, 38].

1.4.2.2 Quadrupolar Interactions Relaxation

Relaxation via quadrupolar interactions is usually not very important for polymers [38]. Quadrupolar interactions are mostly important for NMR-active nuclei that

have electronic quadrupole moment such as D [38]. The relaxation by quadrupolar interactions is dependent on two factors; 1) the quadrupole moment of the nuclei and 2) the electrical field gradient (EFG). In a polymer molecule if a nuclei has a spin that is greater than a 1/2 it is said that the electronic charges have a non-spherical distribution .

Nuclei with non-spherical electronic charges distribution now have a electronic quadrupole moment (alternatively it can also be known as electronic magnetic moment). The effectiveness of relaxation via quadrupolar interactions related to the electronic quadrupole moments magnitude. Relaxation via quadrupolar interactions is caused by the electronic quadrupole moment of a nuclei interacting with the fluctuating EFG around the nucleus, causing changes in the spin state providing an efficient relaxation. The following equations describe this effect:

$$T_1: \quad \frac{1}{T_1^Q} = \frac{3\pi^2}{10} \left(\frac{e^2 q Q}{h} \right)^2 (1 + \xi) \{J(\omega_D) + 4J(\omega_D)\} \quad (1.12)$$

$$T_2: \quad \frac{1}{T_2^Q} = \frac{3\pi^2}{20} \left(\frac{e^2 q Q}{h} \right)^2 (1 + \xi) \{3J(0) + 5J(\omega_D) + 2J(\omega_D)\} \quad (1.13)$$

where ξ is the asymmetry of the electric field gradient and $(e^2 q Q / h)$ is the quadrupole coupling constant.

1.4.2.3 Chemical Shift Anisotropy (CSA) Relaxation

The CSA relaxation mechanism is the only relaxation mechanism for molecules that is dependent on the size and strength of the magnetic field [37, 38]. The magnetic field makes a stronger contribution to the relaxation of nuclei as it increases. For polymers in solution CSA is averaged out. Relaxation of polymers in solution by CSA is only important in the absence of no other relaxation mechanism. For the NMR-active nuclei such as ^{13}C , ^{19}F , ^{15}N and ^{31}P , relaxation via CSA is a main contributor to relaxation, as they have a large chemical shift range [37]. This is particularly true for ^{13}C nuclei because some polymer's may

contain anisotropic groups such as aromatics and carbonyl which do not have a ^1H directly attached [37].

For the relaxation of these NMR-active nuclei, electronic shielding of the nucleus (i.e. the chemical shift) dictates how much magnetic field the nucleus experiences [37, 38]. A nucleus with a non-spherical electronic distribution produces an electronic current which causes a secondary magnetic field. This secondary magnetic field has a perpendicular component to the magnetic field, therefore relaxation via CSA is caused when this perpendicular component fluctuates while the molecule rotates [37, 38]. To understand the effect that chemical shift anisotropy has on spin-lattice and spin-spin relaxation rates, equations have been theorised:

$$T_1: \quad \frac{1}{T_1^{\text{CSA}}} = \frac{2}{15} \omega_C^2 \Delta\sigma^2 J(\omega_C) \quad (1.14)$$

$$T_2: \quad \frac{1}{T_2^{\text{CSA}}} = \frac{1}{45} \omega_C^2 \Delta\sigma^2 \{4J(0) + 3J(\omega_C)\} \quad (1.15)$$

where
$$\Delta\sigma = \sigma_{33} + \frac{1}{2}(\sigma_{11} + \sigma_{22}) \quad (1.16)$$

1.4.2.4 Paramagnetic Relaxation

The principal theory of paramagnetic relaxation is similar to that of dipole-dipole interactions [37]. Paramagnetic relaxation, is caused by dipole interactions with an unpaired electron rather than another nucleus [37, 38]. For both spin-lattice relaxation and spin-spin relaxation, an unpaired electron is more efficient at causing relaxation than a ^1H which is known to have the highest magnetic moment out of all the NMR-active nuclei. This is because the magnetic moment for an electron is ~ 700 times larger than that of a ^1H , therefore causing more efficient relaxation [37]. This means a molecule containing an unpaired electron,

paramagnetic relaxation will be the dominant mechanism, this is known to be particularly true for small molecules.

For polymers paramagnetic relaxation is usually not a problem as polymer's generally do not contain unpaired electrons [37, 38]. However contamination with a paramagnetic species can lead to incorrect relaxation rates, this then leads to misleading conclusions about a polymers molecular structure and dynamics. This is because these species can cause the relaxation of a polymer to be artificially shortened. This is particularly a problem for sections with long relaxation time as they compete with dipole interactions or chemical shift anisotropy relaxation which are a usually the main mechanism for relaxation for these sections.

For polymers the most common source of contamination is paramagnetic oxygen. It is imperative that paramagnetic oxygen is remove from samples that have long relaxation times before relaxation rates are measured [37, 38]. There are currently two methods commonly utilised to remove paramagnetic oxygen from a polymer sample. These are; 1) bubbling an inert gas (usually dry argon or nitrogen) through the sample prior to running of relaxation experiment, or alternatively 2) repeated freeze-thaw cycles under vacuum [38].

1.4.2.5 Other Relaxation Mechanisms Relaxation

There are a few other relaxation mechanisms that can cause some relaxation in a polymers molecule; these include spin-rotation and scalar rotational. However these relaxation mechanisms are usually not that important and have little effect for the relaxation of polymer molecules [38].

1.4.3 Measurements of Relaxation Rates

1.4.3.1 Spin-Lattice Relaxation (T_1)

Spin-lattice relaxation also commonly known as longitudinal relaxation is designated by the symbol T_1 , it is the easiest of the two NMR relaxation applications to be measured. The main affect T_1 has in an NMR spectrum is that it influences the relative intensities of signal [37-40]. The reason spin-lattice relaxation has an influence over peak intensities is that the signal intensity of an NMR peak is proportional to longitudinal magnetisation [37, 38, 40].

T_1 relaxation rate is dependent upon several factors. These include 1) the mobility of the molecular chain containing the nucleus in question, 2) the proximity of the nearest neighbouring nuclei 3) the size of the NMR magnetic field used 4) temperature and 5) the molecular weight of the polymer.

1.4.3.1.1 How Spin-Lattice Relaxation (T_1) is Measured

The time taken by the spin system to return to equilibrium along the z-axis, after it has been perturbed is used to define the spin-lattice relaxation time for a specific system for a polymer. The most commonly used technique to determine T_1 values is the inversion-recovery pulse sequence. This pulse sequence is depicted in Figure 1.12.

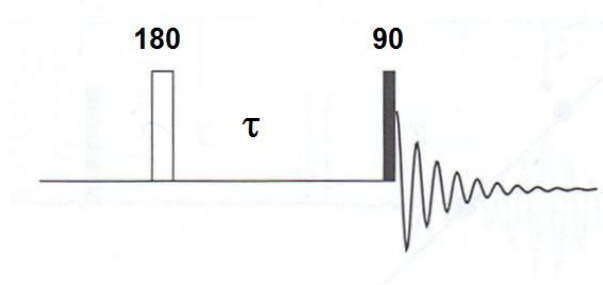


Figure 1.12: Pulse program used to measure T_1 relaxation rates in the NMR (Mirau, 2005 [38])

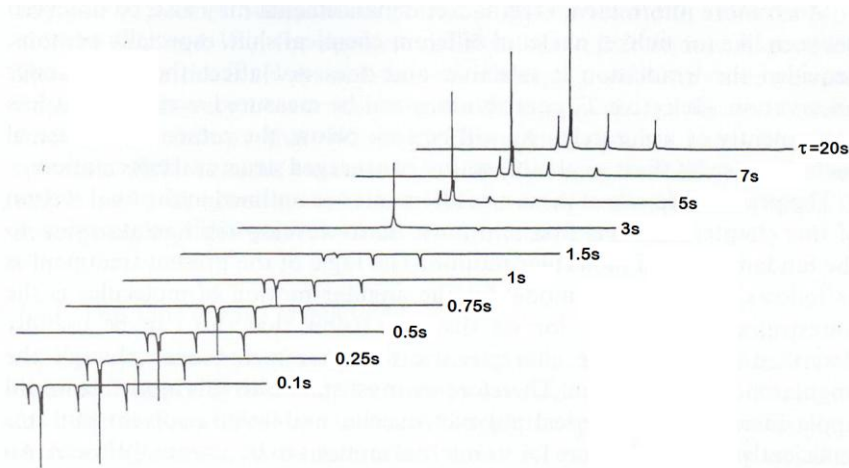


Figure 1.13: Typical results for a T_1 experiment in the NMR obtained by varying τ (Ibbett, 1993 [37])

Initially a 180° pulse is applied to a polymer spin system, followed by a 90° pulse. If the interval between the initial 180 degree pulse and the subsequent 90° pulse is very short the combination of the two pulses equates to a 270° pulse which effectively inverts the observed signal relative to that which would have been observed if only a single 90 degree pulse had been applied. If τ is too long the system will recover from the 180° pulse and will behave as if it has been subjected to a single 90° pulse.

Typically a series of inversion -recovery experiments are run with a range of τ values ranging from a few μsec (effectively zero) to a value 5-10 times greater than the T_1 value of target nuclei. A typical set of profiles from an inversion recovery experiment is illustrated in Figure 1.13.

It can be shown that the intensity of the magnetization vector in the Z direction (the longitudinal direction) at time τ is given by the expression:

$$M_z = M_0(1 - 2e^{(-\tau/T_1)})$$

where M_z = observed intensity for a τ value

M_0 = equilibrium value (long τ value)

T_1 = the longitudinal spin-lattice relaxation rate

$$\text{i.e.: } M_z = M_0 - 2 M_0 e^{(-\tau/T_1)}$$

$$M_z - M_0 = -2 M_0 e^{(-\tau/T_1)}$$

$$\text{thus: } M_0 - M_z = 2 M_0 e^{(-\tau/T_1)}$$

$$\log_e (M_0 - M_z) = \log_e (2 M_0) (-\tau / T_1)$$

Hence a plot of $\log_e (M_z - M_z^0)$ against τ will give a straight line, since T_1 and $\log_e(2)$ are constants and it can be shown that the point at which this line crosses the origin (i.e. the point at which the term $\log_e (M_z - M_0) = 0$ corresponds to $0.691 T_1$ [41]. This point can be visually identified for target species by inspection of the data shown in Figure 1.13.

In practical terms, NMR software is available which automatically calculates the best fit decay curve using either peak areas, or signal heights, and the T_1 value for the fitted curve

An important consideration when using the inversion recovery sequence is that the 90° pulse angle must be accurately known prior to T_1 measurements being undertaken, otherwise the use of incorrect 90 and 180° pulse times will lead to inaccurate measurements of spin-lattice relaxation times. It is also important that for accurate T_1 measurements the longest τ value used should be at least 3 times, and preferably five time longer than the longest T_1 value in order to ensure complete relaxation of all spin systems to their equilibrium state [41]. Practically it was found the NMR software produced more consistent T_1 values if inversion-recovery experiments included 2 or more τ values in the range $3-5 T_1$ or greater, together with 2 short τ values of the order $0.1-0.5 T_1$ and 2-3 τ values in the range $0.5-3 T_1$.

1.4.3.2 Spin-Spin Relaxation (T_2)

Spin-spin relaxation, also commonly known as transverse relaxation, is designated by the symbol T_2 [37, 38, 40]. The measurements of spin-spin relaxation (T_2) is technically more demanding than is the case for T_1 values.

T_2 relaxation processes have been found to affect linewidths (broadness) of a polymers peak in an NMR spectra [37, 38]. In turn this affects the resolution of lines in polymer NMR spectra [37, 38, 40]. The line width (resolution) of an NMR signal is inversely related to T_2 (see Equation 1.17) [37, 38].

$$\Delta\nu_{1/2} = \frac{1}{\pi T_2} \quad (1.17)$$

It is also well known that T_2 relaxation has an effect on the sensitivity. For an NMR pulse the sensitivity is given by a ratio of signal to noise (S/N) [40]. The equation to explain this ratio is the following equation:

$$S / N = NT_2 \gamma_{exc} \left(\frac{\sqrt[3]{B_0 \gamma_{det} \sqrt{ns}}}{T} \right) \quad (1.18)$$

where n is the number of spins in the system, B_0 is external magnetic field, ns is number of scans T is sample temperature and $\gamma_{exc}/\gamma_{det}$ is the magnetogyric ratio of excited and detected nucleus respectively. T_2 relaxation rate determines the linewidth.

Like T_1 , there are many factors related to the solution dynamics and alternative relaxation pathways that can effect T_2 . One, or all, of these factors can affect the overall linewidth of a polymers NMR signal. For instance T_2 increases when chain motion is restricted. This leads to a decreased linewidth thereby increasing the observed resolution of an NMR signal.

1.4.3.2.1 How Spin-Spin Relaxation (T_2) is Measured

T_2 values characterise the rate at which at magnetisation dissipates to zero in the transverse x-y plane after the application of a 90 degree pulse. Theoretically, observed signal linewidths can be used to determine T_2 values using the equation:

$$T_2 = \frac{1}{\pi\delta\nu_{1/2}} \quad (1.19)$$

where $\delta\nu_{1/2}$ is the observed linewidth.

However experimentally measuring T_2 using linewidths proved to be difficult due to the contribution of magnetic field inhomogeneity relaxation effects to line broadening. Thus only an apparent spin-spin relaxation rate (T_2^*) can be determined from linewidth measurement since both T_2 and inhomogeneous broadening ($1/T_2^{inhomo}$) effect contribute to this measurement according to the following equation:

$$\frac{1}{T_2^*} = \frac{1}{T_2} + \frac{1}{T_2^{inhomo}} \quad (1.20)$$

To remove these magnetic field inhomogeneities, Meiboom-Gill modified the spin echo pulse program developed by Carr-Purcell (Figure 1.14a) to include a repetitive [t-180]_n loop (Figure 1.14b). In the Carr-Purcell pulse program τ is varied to find T_2 , whereas in Meiboom-Gill's pulse T_2 is determined by varying the number of times the [t-180]_n loop cycles around.

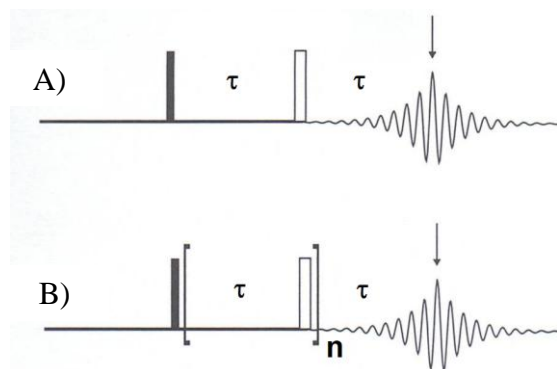


Figure 1.14: Pulse program used to measure T_2 relaxation rates in the NMR using A) Carr-Purcell pulse program and A) Carr-Purcell-Meiboom-Gill's pulse program (Mirau, 2005 [38])

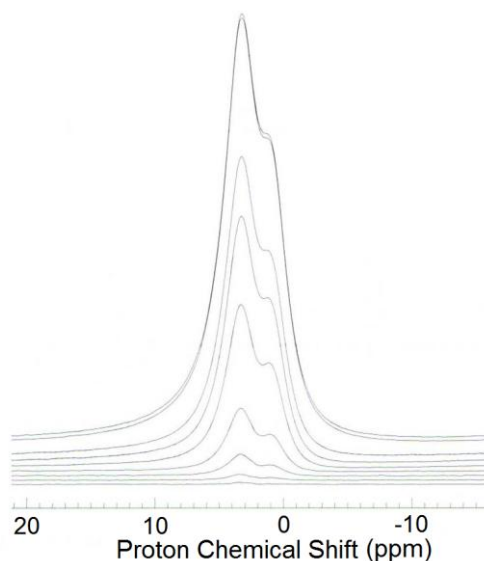


Figure 1.15: Typical results for a T_2 experiment using Carr-Purcell-Meiboom-Gill's pulse program in the NMR obtained by varying n (Mirau, 2005 [38])

Typical results from a spin-spin relaxation experiment are shown in Figure 1.15 where the maximum signal was determined using a low 'n' value and the minimum signal was determined using a large 'n' value. Practically strict attention to baseline correction is required to obtain reliable T_2 data [37, 38].

1.4.4 Factors that Affect T_1 and T_2 Relaxation Rates of Polymers in Solution

As previously mentioned chain motion of a polymer has a major affect on T_1 and T_2 , as relaxation measurements are extremely sensitive to changes in chain motion. There are many factors that can influence and affect the relaxation of a polymer's chain motion but the main factors include the molecular weight of a polymer, the temperature the NMR is set at, the magnetic field of the NMR used to examine the polymers relaxation rate and also the chemical environment the nuclei are in.

1.4.4.1 Modelling of a Polymers Molecular Dynamics in Solution

Interpreting T_1 and T_2 on their own is very difficult. The use of relaxation mechanisms, correlation times and molecular models can help to interpret the effect that molecular weight and temperature and magnetic field have on the chain motion of a polymer and thus relaxation rates. A single measurement alone will not give any information about a polymer molecular motion and correlation time for relaxation rates. Multiple measurements as a function of magnetic field and temperature however will [37, 38].

Section 1.4.1 introduced and explained the basic concept of relaxation. Extending this concept further, the relaxation that occurs after thermal equilibrium is perturbed is dependent on the spectral densities ($J(\omega)$). Spectral densities are a function in all the relaxation mechanisms. The reason why spectral densities are so prominent in relaxation of polymer is because at a particular frequency, spectral densities help describe the power available to cause relaxation [37, 38]. The spectral density is given by the Fourier transform of the correlation function, where the correlation function helps give correlation times for a chains motion. Correlation times for the molecular chain motion is given by the total area under the curve that is produced for $G(t)$. The correlation time is an important variable as it gives an indication of the molecular motion of a polymer chain and the effects changing one of the rate dependent variables causes. The different localised atomic motions of rapid librational motions, gauche-trans isomerisation and segmental motion all give different correlation times [37, 38]. For short correlation times these corresponds to a rapid molecular motion as observed for rapid librational motions or gauche-trans isomerisation, for longer correlation times these correspond to a restricted molecular motion as observed for segmental motion.

To provide and understand information about a polymer's relaxation rate and their correlation times, different models are employed with different spectral densities to help model the relaxation that is occurring. There are two types of models that are used; 1) models based on the polymer structure, such models include the Hall-

Helfand theory, isotropic rotational motion and diamond-lattice, 2) models based on conformational transitions, models used for this include Cole-Cole, Fuoss-Kirkwood and $\log\text{-}\chi^2$ distribution functions [37, 38]. An example of the most basic spectral density function is given by the isotropic rotational function:

$$J(\omega) = \frac{\tau_c}{1 + \omega^2 \tau_c^2} \quad (1.21)$$

where τ_c is the rotational correlation time.

1.4.4.2 Effect of Molecular Weight

At a constant temperature both T_1 and T_2 , these relaxation rates will only increase with the mobility of a polymer's chain motion [37, 38, 42]. As previously mentioned, increasing the molecular weight of a polymer causes the chain motion relaxation to change from a combination of rapid librational motions, gauche-trans isomerisation and segmental motion to just segmental motion. This change in chain motion causes both T_1 and T_2 to either decrease or increase depending on the chemical environment of the section of the polymer structure that is being analysed.

The effect of molecular weight of polymers on T_1 has been tested and is well known [38]. Figure 1.16A illustrates the effect of T_1 relaxation time as a function of molecular weight for a methine and methylene signal for a polystyrene. This is used to explain the effect of chain motion on T_1 measurements. For a low molecular weight polymer, the chain motion is quite mobile and produces a higher T_1 relaxation rate. Conversely, higher molecular weight polymers results in a decreased T_1 relaxation rate because mobility is more restricted. However, there is a critical point where the T_1 relaxation rate becomes insensitive to changes in molecular weight. This is the basis for the hypothesis that segmental relaxation is the main relaxation in high molecular weight polymers [38].

This phenomenon was also illustrated by Kimmich and colleagues [42] on T_2 relaxation measurements (see also Figure 1.16B). The work performed on polyisobutane of different molecular weights showed that, similar to the T_1 measurements, T_2 measurements decreased as the molecular weight increased. Moreover, the graphs of T_2 relaxation rates again had a critical point where the relaxation rate was insensitive to the increase in molecular weight. These observations lead to the conclusion that segmental relaxation was the only cause of relaxation of high molecular weight polymers.

These results observed for T_1 and T_2 for varying molecular weights are only applicable to polymers whose molecular chain motions are known to be less restricted. However for some polymers, at a single temperature T_1 increases with rather than decreases with molecular weight. For these polymers not enough information about the effect of molecular weight on the chain motion can be obtained at one single temperature and frequency.

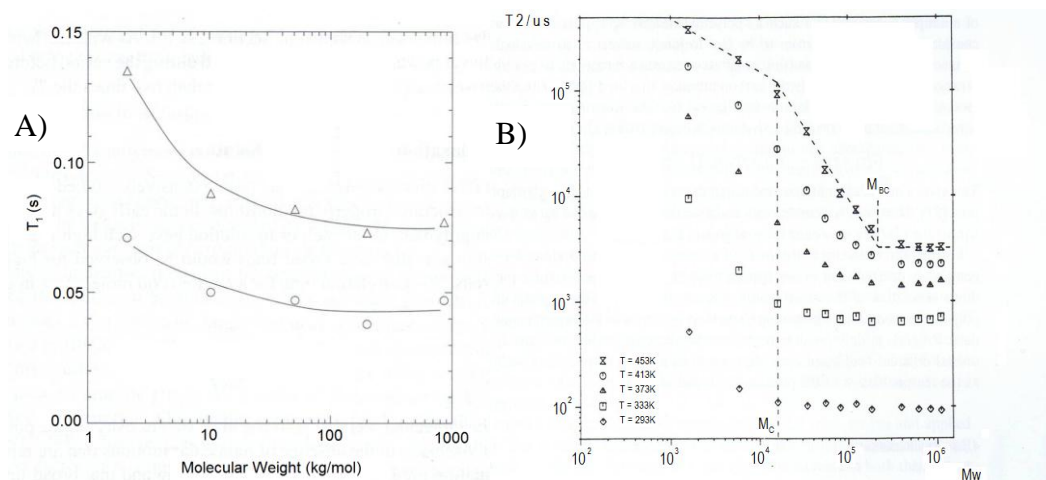


Figure 1.16: Resulting trend for A) T_1 relaxation rates with increasing polymer molecular weight (Mirau, 2005 [38]) and B) T_2 relaxation rates with increasing polymer molecular weight and temperature (Kimmich et al, 1988[42])

1.4.4.3 Effect of Temperature

For T_1 and T_2 relaxation rates measurements at a single temperature for certain polymers may not provide enough information about the effect molecular weight has on the polymer chain motion [38, 42]. The relaxation rates for high molecular weight polymers have been found to be dependent on temperature. This is because polymer chain motion is a thermally active process, meaning high molecular weight polymers are less restricted at higher temperatures, and hence are capable of greater chain motion. This means changes in correlation times can occur, leading to changes in the measured T_1 and T_2 relaxation rates.

Changes in temperature have major affect on the resolution of a polymer's NMR. For example, high molecular weight polymers produce a poorly resolved NMR spectrum at a given temperature; however, by elevating the temperature, it is possible for the NMR spectra to be resolved [37, 38, 42]. This can also be shown using the isotropic rotational motion model, where there is no observable minimum, so measured T_2 relaxation rates reduce with increased correlation time [38] (Figure 1.17B). Kimmich also showed the effects that temperature has on T_2 relaxation time. Upon increasing the temperature from 293K to 454K (Figure 1.16B), the T_2 rates for all of the polyisobutene polymers increased. This was particularly apparent for polymers with molecular weights greater than 10^4 (Figure 1.16B) [42].

For polymers that have more restricted molecular chain motions, T_1 relaxation rates measured can give complicated results. For instance T_1 relaxation rates for high molecular weight polymers can be observed to be similar to those measured for low molecular weight polymers. This phenomenon is observed for the C1-H signal for fractionated dextran samples of varying molecular weights. Using the isotropic rotational motion model for T_1 relaxation rates a simple explanation can be obtained.

For this relaxation model a minimum is observed (Figure 1.17A). This minimum in this model is attributed to equation 1.21 having different contributions on the

relaxation rate in the fast- and slow-motion limit [38]. Changes in temperature and the use of this minimum can be used to help define the molecular chain motion in a section of a polymer. For instance when the temperature is increased, if T_1 decreases, correlation time is concluded to be long, meaning the molecular motion for this part of the chain is restricted[38]. However if T_1 increases correlation time is short, so molecular motion for that part of the chain is less restricted [38].

Weber and Kimmich elegantly showed this for polyisoprene ($M_w = 305,000$) over a range of temperatures and magnetic fields [43]. With this fraction of polyisoprene its chain motion is more restricted than its lower molecular weight counterparts, so it has a longer correlation time. It was shown that with increasing temperature, T_1 decreases until it get to a temperature where it crosses the minimum to the faster side relative to the minimum where it continues to increase (Figure 1.18).

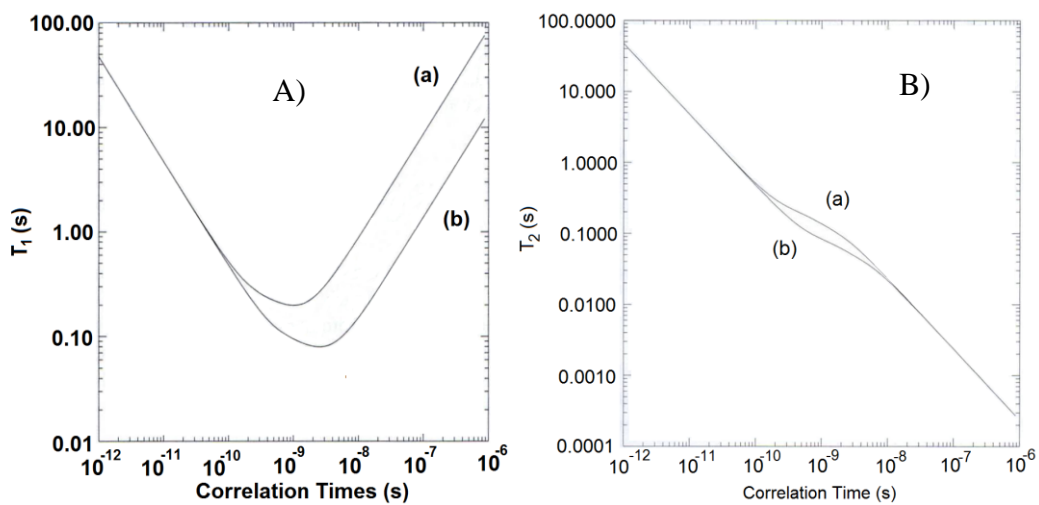


Figure 1.17: Relaxation models of A) T_1 and B) T_2 relaxation rates vs. correlation times (Mirau, 2005 [38])

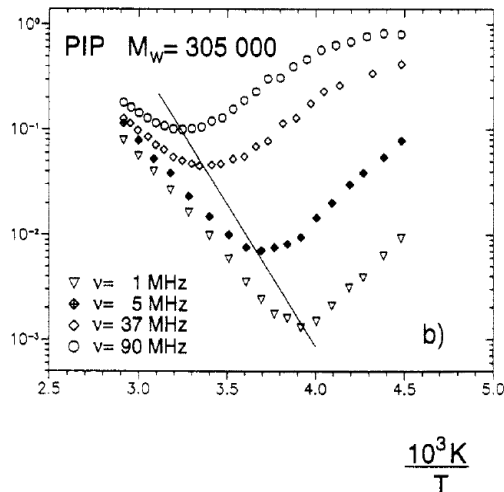


Figure 1.18: Resulting T_1 relaxation rate of PIP with molecular weight of 305,000 with increasing temperature and NMR frequency (Kimmich *et al*, 1993 [43])

1.4.4.4 NMR Frequency

Change in NMR frequency have more effect on T_1 than T_2 . This is because T_1 relaxation rates are very sensitive to molecular motions that occur near or at the NMR frequency. Increasing the NMR frequency causes chain motion to become less restricted causing T_1 for high molecular weight polymers to increase. From the work of both Weber and Kimmich *at el.* it can be observed that frequency that the T_1 relaxation rates for all the fractions are the same (Figure 1.19).

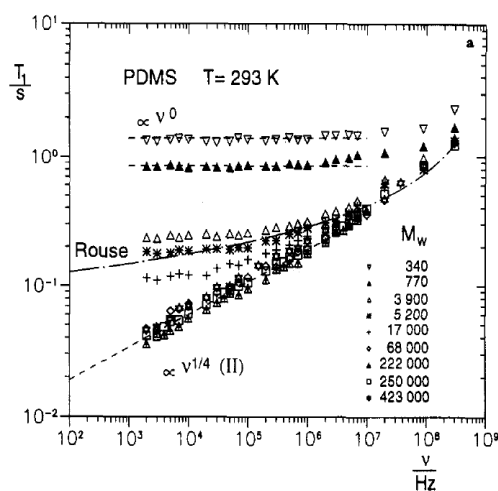


Figure 1.19: Resulting T_1 relaxation rates for different molecular weight PDMS at increasing NMR frequency (Kimmich *et al*, 1993 [43])

1.5 Polyhydroxypolyamides (PHPA)

1.5.1 History of PHPA

Nylons and other synthetic polymers have numerous practical applications that extend into everyday life. Synthetic polymers of this type have been commercially viable over the last century due to mass production on an industrial scale [5, 44]. However these synthetic polymers are non-biodegradable and require non-renewable resources, in the form of fossil fuels, for their production. As the world's crude oil supplies diminish, combined with the increased awareness of such polymer's low biodegradability, the use of petroleum-based polymers is starting to become nonviable. This therefore necessitates research into biodegradable polymers based on monomers that are sourced from alternative, renewable sources.

One area that has been the focus of significant research over recent years is polyhydroxypolyamides (PHPA), commonly referred to as hydroxylated nylons. First synthesised in the 1970's [45-47], PHPA are synthetic polyamides that are produced from aldaric acids and primary diamines [45-49]. These polymers are observed to be structurally similar to that of nylons, the only point of difference being that nylon's dibasic acid is replaced with an aldaric acid (carboxylic acid). The general structure of a PHPA polymer is shown in Figure 1.20.

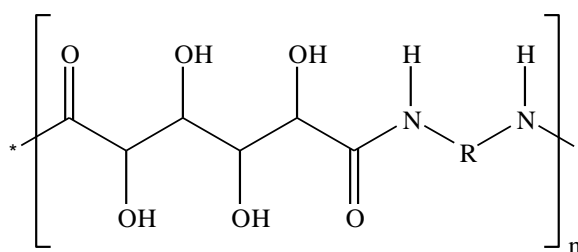


Figure 1.20: General Structure for a PHPA based on a hexaric acid

PHPA are based on carbohydrates which are a renewable resource. Furthermore, these polymers are more biodegradable than traditional petroleum-based polymers [4, 5, 44, 45]. Because of these properties, PHPA have been viewed as a more appropriate alternative to petroleum-derived polymers.

If PHPA are to successfully compete commercially with petroleum-derived polymers, the raw manufacturing materials must be abundant and of low cost. Minimisation of the number of steps involved in the synthesis of PHPA must also be addressed. From a non-commercial perspective, method development must be undertaken to overcome the numerous protection/deprotection steps that are often associated with carbohydrate chemistry. Further to this, processes need to be created so as to avoid extensive purification of the polymer after synthesis, which significantly increases production duration and costs.

1.5.2 Kiely's Studies of PHPA

The first PHPA that was produced using unprotected, activated aldaric acids was discovered by Ogata and co-workers at the beginning of the 1970's [45-47]. Since the mid 1990's, Kiely *et. al* [44] have extended this research in an attempt to produce commercially viable PHPA. Their investigations into unprotected carbohydrates and simple chemistry are aimed at developing procedures which would lower PHPA production costs and increase their process efficiency [45-49].

Further to this, Kiely and colleagues have continued to extend their work in this area by developing methods for producing stereoregular head-tail PHPA [47]. Their research has not only extended our knowledge of PHPA, but also the range of known PHPA synthesised using D-mannaric acid [46], D-glucaric [46, 49, 50], galactaric acid [46] and xylaric acid [46] (Figure 1.21). Their research has led to the use of computer aided structural molecular modelling [51] and conformational analysis via MM3(96) software [51]. Such techniques are used to better understand the observed variances in the physical properties of carbohydrate-derived PHPA.

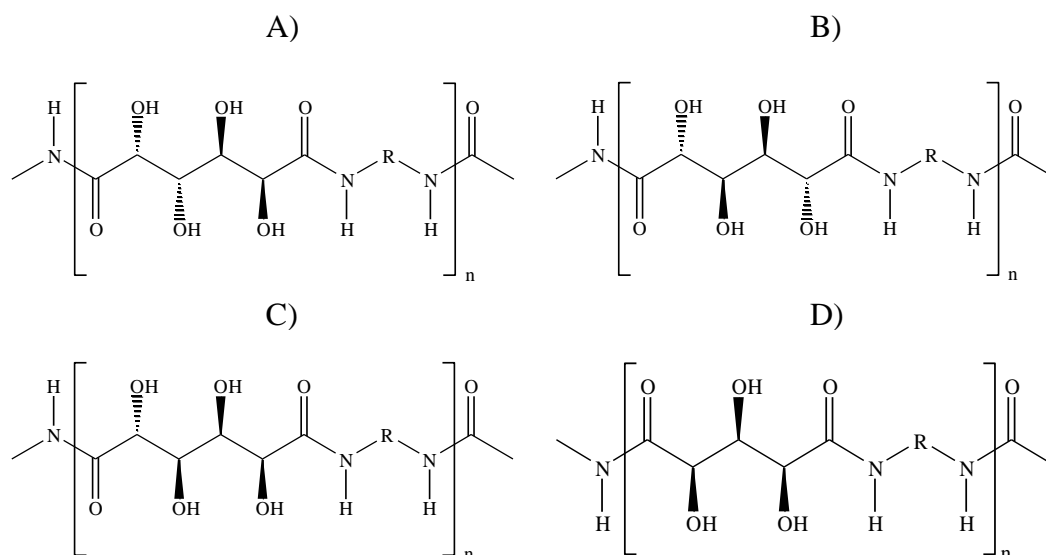


Figure 1.21: Range of PHPA based on A) galactaric acid, B) D-mannaric acid, C) D-glucaric, and D) xylaric acid

There are a variety of potential applications identified for PHPA. For example the polymer shown in Figure 1.22 has been shown to have possible applications as a nitrogen fertilizer and a biodegradable adhesive [4, 50].

1.5.3 Techniques used for Molecular Weight Determination

Kiely and colleagues have employed a wide variety of techniques to measure the molecular weights of PHPA polymer samples. Techniques such as ^1H NMR spectral integration end-group analysis, size exclusion chromatography (SEC) and light scattering have all been utilized to calculate molecular weights [45]. During their earlier investigations, random poly(hexamethylene-D-glucaramide) polymers were used as a control to verify the M_n for each of the aforementioned methods [45].

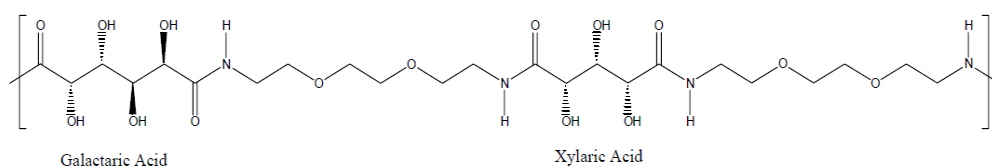


Figure 1.22: A block copolymer PHPA with galactaric acid, xylaric acid and 2,6-dioxaoctane-1,8-diamine, this has shown to have good film forming ability (Jarmen, 2008[4])

The first and most commonly used technique by Kiely *et. al* was to calculate PHPA molecular weights using ^1H NMR spectral integration end-group analysis. This involves a comparison of the integration value of the methylene protons on the carbons bonded to the internal amido-nitrogens (also known as the non-terminal methylene protons adjacent to the amido-nitrogens) to the integrated value for the methylene protons (end group) on the carbon bonded to the terminal amine nitrogen (also known as the terminal methylene protons adjacent to the amine nitrogen) [45-49]. The corresponding terminal and non-terminal methylene protons are illustrated in Figure 1.23. The signals generated by NMR for the poly(hexamethylene-D-galactaramide) groups are shown in Figure 1.23.

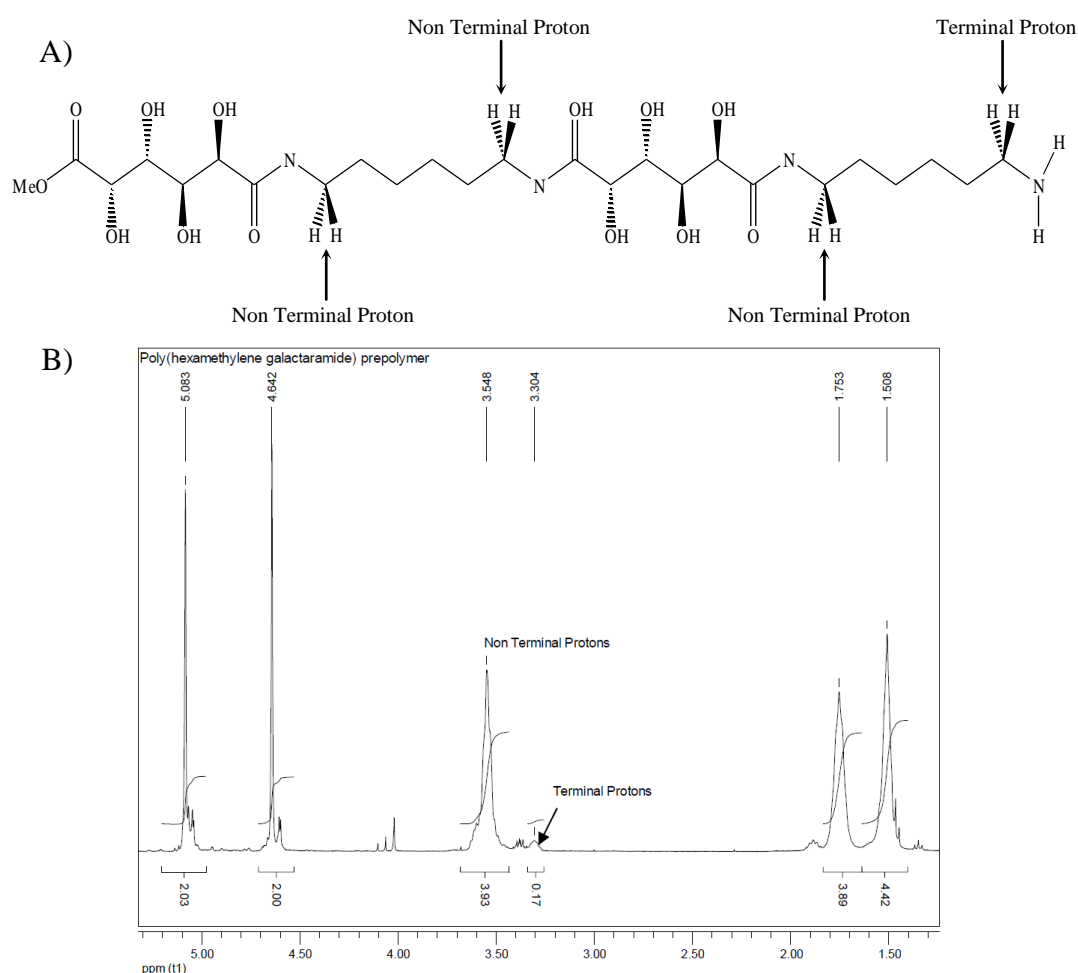


Figure 1.23: A) Poly(hexamethylene D-galactaramide) showing two terminal CH_2 protons and six non terminal CH_2 protons next to the amide and B) ^1H NMR spectra of poly(hexamethylene D-galactaramide) in TFA-d_1 showing the terminal CH_2 protons and the non terminal CH_2 protons next to the amides (Jarman, 2008 [4])

In recent years, a formula developed by Jarman to calculate a polymer's DP [4, 48] has been adopted by Kiely *et. al* to calculate PHPA M_n from ^1H NMR end-group analysis. Jarman's formula is based on the ratio of the integrated non-terminal and terminal methylene protons. To determine the formula, a range of terminal and non-terminal methylene protons (e.g. 1-15) was used to calculate theoretical DP values of poly(tetramethylene D-galactaramide). These values are then used to determine a ratio [4]. Plotting this ratio against DP, a straight line is obtained [4]. Rearranging the equation for this straight line an equation to calculate DP using the ratio of the terminal and non-terminal methylene protons is found that can be used routinely and easily used to calculate DP for each PHPA sample.

A major drawback of this method is that it is unsuitable for PHPA with very long chains. This is because at these sizes the terminal proton signals are very weak and unobservable. Furthermore, M_n calculations via this method are not applicable for polymers with molecular weights above 20,000 [2, 8, 39].

Another technique utilised by Kiely *et al.* was size exclusion chromatography (SEC). Prior to analysis by SEC, each PHPA sample was subjected to derivatisation [45]. Each PHPA sample was subjected to per-0-trimethylsilylation in hexamethyldisilazane, chlorotrimethylsilane, and pyridine solution at room temperature for 7 days [45]. Each sample was then compared to polystyrene to determine M_n . It was observed that the molecular weights obtained using this SEC method were reasonably consistent with those found via ^1H NMR end-group analysis (Table 1.3).

This SEC setup was extended to incorporate a multiple detectors. A molecular weight sensitive online light scattering along with a viscometric detector were used in series [47]. However, the molecular weights that were calculated using this setup were considerably higher than that calculated via end-group analysis (Table 1.3) [47]. For example, the M_n calculated for a random poly(hexamethylene-D-glucaramide) via light scattering was ~4800, compared to ~2400 as calculated by ^1H NMR end-group analysis [52].

| Glu/ HMDA | yield (%) | M_n (NMR) | (η_{rel}) | M_n (GPC) | M_w (GPC) | M_w/M_n (GPC) |
|--------------|--------------|-------------|----------------|-------------|-------------|-----------------|
| 1.00/1.00 | 79.8 | 2116 | 1.226 | 1785 | 3812 | 2.14 |
| 1.00/1.02 | 80.5 | 2375 | 1.233 | 1813 | 3842 | 2.12 |
| 1.00/1.05 | 81.9 | 2491 | 1.228 | 1678 | 3549 | 2.12 |
| 1.00/1.10 | 86.2 | 1772 | 1.208 | 1642 | 3545 | 2.16 |

Table 1.3: Molecular weights calculated by ^1H NMR end-group analysis and GPC (Kiely et al, 2000 [45])

The SEC method proposed used expensive solvents such as hexafluoroisopropanol [48] and tetrahydrofuran solution [45] as eluents for the PHPA. This is not a method that can be used extensively or routinely. Alternative SEC method using relatively less expensive solvents has yet to be established [48]. Therefore, further investigations are still required to determine such methods.

1.6 Aim of Research

The purpose of this study was to determine the molecular weight of a variety of PHPA samples. Firstly SEC was used to fractionate the polymer samples into narrower molecular weight fractions. From this each fraction was analysed by MALDI-TOF spectrometry to determine the molecular weight of the polymer sample. These results were then be compared to M_n determinations from ^1H NMR end group analysis.

2 Experimental

2.1 Materials

The polyhydroxypolyamides polymers were prepared by Dr Tyler N. Smith and Dr Michael R. Hinton at the Shafizadeh Rocky Mountain Centre for Wood and Carbohydrate Chemistry, University of Montana, Missoula, MT, USA. Dextran standards were kindly donated from SCION.

2.2 Instrumental

2.2.1 Matrix-assisted Laser Desorption Ionisation Time of Flight (MALDI-TOF)

An Auto Flex™ (Bruker Daltonics) operated using Flex Control (Bruker Daltonics) was used to obtain MALDI-TOF spectra. The spectrometer is equipped with a nitrogen laser (337nm) and two detectors. The first detector works when the reflectron device is off and allows the detection of ions in the linear mode, whereas the second detector is placed at the end of the second flight tube and allows the detection of ions in the reflectron mode.

2',4',6'-trihydroxyacetophenone (THAP) and 2,5-dihydroxybenzoic acid (sDHB) was used as the matrix. For THAP a ratio of 9:1 acetonitrile and water was used as the solvent. Deionised water (D.I) was used as the solvent for sDHB. No cationisation agents were added. Preparation of samples was done using a 3:1 ratio of polymer sample to matrix. Dry droplet technique was used to prepare sample on a aluminium MALDI target (Bruker Daltonic's).

Spiking solutions of KCl, and NaCl were prepared with D.I water to a concentration of 2 mM. A 1:1 ratio of polymer sample and spiking solution was prepared and prepared on a aluminium MALDI target plate using dry droplet technique with a ratio of 3:1, spiked polymer sample and matrix (Bruker Daltonics).

2.2.2 Size Exclusion Chromatography (SEC)

Samples were prepared in DI water. Injections of 50 μ L of sample were made. Separation was performed on Shodex SUGAR columns, KS-800 series (300mm x 7.8mm i.d); each column was held at 50°C. A SUGAR KS-G pre-column was used. The solvent delivery system was a Waters model 515 HPLC pump, and the eluent was D.I water. A Waters 2414 refractive index was used as the detector and held at 30°C. The mobile phase was pumped at 1.0mL/min of DI water.

2.2.3 Nuclear Magnetic Resonance (NMR)

NMR spectra were recorded using two spectrometers. A Bruker Avance AC-300 Fourier Transform NMR spectrometer with a 5mm inverse probe (300.1 3MHz for ^1H and 74.48MHz for ^{13}C) operating at 300K (27°C) was used for ^1H NMR end group analysis. A Bruker DRX400 400MHz spectrometer with a 5mm inverse probe (400.13MHz for ^1H and 100.62MHz ^{13}C) operating at 300K (27°C) was used for ^1H NMR end group analysis, T_1 and T_2 relaxation rate measurements.

All samples for ^1H NMR end group analysis, T_1 and T_2 relaxation rate measurements were prepared in D_2O with tertiary-butyl alcohol (1.240 ppm) as the reference. All NMR spectra were processed with TOPSPIN version 1.3 software.

T_1 relaxation rate measurements were done using the Bruker inversion recovery pulse program. T_2 relaxation rate measurements were done using the Carr-Purcell-Meiboom-Gill sequence pulse program. See Appendix 5.9 and 5.10 for

explanation of the pulse programs used by TOPSPIN software and some parameters used for measurements.

Different probe ^1H NMR end group analysis experiments for each unfractionated PHPA sample were carried out on a 300 MHz Bruker NMR spectrometer and a 400 MHz Bruker NMR spectrometer, four different probes were used. For the 300 MHz Bruker NMR spectrometer, a 5mm QNP and a Dual probes were used. For the 400 MHz Bruker NMR spectrometer, 5mm inverse and dual probes were used.

3 Results and Discussion

3.1 Dextrans as Models for Polyhydroxypolyamides

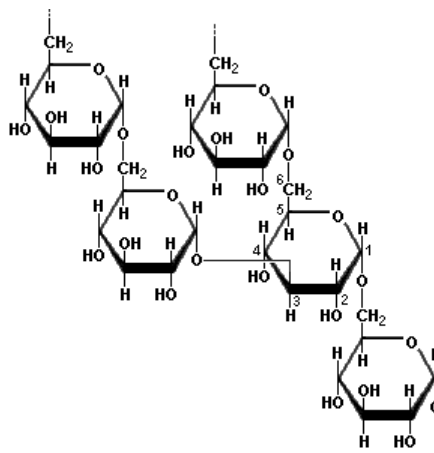


Figure 3.1 – Partial Structure of Dextran

Dextrans are glucans (glucose polymers) that are synthesized from sucrose by certain lactic-acid bacteria. The best-known bacteria used in this process, are 1) *Leuconostoc mesenteroides* and 2) *Streptococcus mutans*. Like polyhydroxypolyamide (PHPA) polymers, dextrans are water soluble. These dextrans will be used to model PHPA for SEC, MALDI-TOF spectrometry and NMR spectroscopy. The general structure of a dextran, illustrated in Figure 3.1, is many D-glucopyranose molecules in chains of varying lengths linked through α -1,6-glycosidic linkages. Attached to the glucose chains, are short side chains of D-glucopyranose attached via α -1,3-glycosidic linkages. The molecular weight of crude dextran is highly polydispersed and hence unsuitable for MALDI-TOF MS. But fractionated dextrans of narrower molecular weight range are available commercially.

It should be noted that dextrans are not entirely suitable as a model for PHPA as they contain two structural differences to PHPA. 1) dextrans contain glucopyranose rings whereas PHPA polymers have open chain aldaric acids and 2) the structure of dextran lacks the hydrocarbon unit which is present in PHPA

polymers. However other polymer standards such as polystyrene are even more unsuitable as they are not soluble in water.

3.2 Hydrolysis of Polyhydroxypolyamides

An issue associated with PHPA is the possibility of hydrolysis, whereby the polymer can disintegrate into smaller fragments. This could have the effect of significantly lowering the M_n when analysing by ^1H NMR end group analysis, or by any other technique. Polymer hydrolysis can occur if the polymer is left too long in solution, or when the polymer solutions is subjected to prolonged heat. With regards to our analysis, this could occur either at room temperature during the polymer preparation process, or due to the elevated temperature at which the HPLC experiment is performed ($\sim 50^\circ\text{C}$) or at which NMR spectra are acquired.

To ascertain the level of polymer hydrolysis, ^1H NMR degradation experiments were performed at room temperature and 50°C ; conditions that each polymer is expected to be subjected to before and during an HPLC run. From this analysis it should be possible to conclude whether hydrolysis is occurring either during the polymer sample preparation process prior to injection into the HPLC, or when the polymers are passing through the columns.

The results for ^1H NMR degradation experiments at room temperature (D_2O , 27°C , 400Hz NMR) demonstrated that the DP of each PHPA sample remained stable throughout the entire experiment (4 hours, 25 mins). An example of this is shown in Figure 3.2A for poly(tetramethylene D-glucaramide) post-polymer. This result suggests that each PHPA sample is quite stable in aqueous solution at room temperature for extended periods of time. Consequently, the likelihood of the PHPA sample hydrolyzing prior to the HPLC injection phase (~ 5 mins) is highly unlikely.

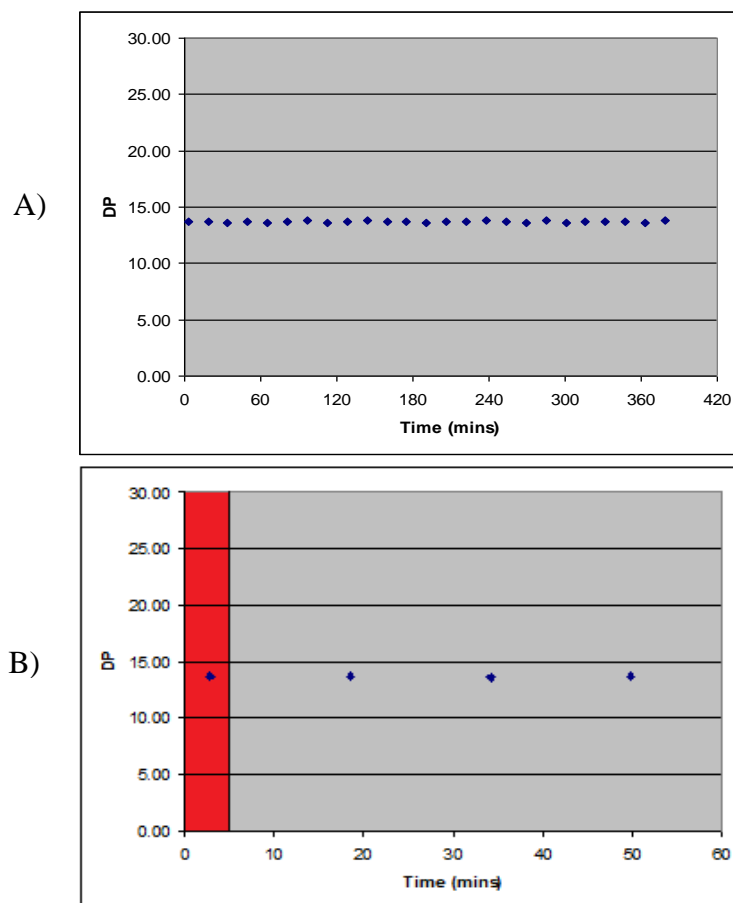


Figure 3.2: A) Change in DP determined by end-group analysis of Poly(tetramethylene D-glucaramide) post-polymer at room temperature B) Change in DP determined by end-group analysis of Poly(tetramethylene D-glucaramide) post-polymer at room temperature, red region is estimated time period taken to prepare sample for the HPLC.

Figure 3.2B illustrates the estimated time period from when the poly(tetramethylene D-glucaramide) post-polymer was prepared, until the polymer itself enters the columns. This result illustrates that the time period required for poly(tetramethylene D-glucaramide) post-polymer hydrolysis (at room temperature) is significantly longer than it would take to prepare a sample and inject it into the HPLC.

For the experiments performed at temperatures which simulated HPLC and NMR experimental conditions (i.e., 50°C), the DP was observed to be approximately 2

DP higher for each PHPA sample than that recorded at room temperature; for example for poly(tetramethylene D-glucaramide) post-polymer at 50°C the DP was 17 whereas at room temperature it was 15 (Figure 3.3). This discrepancy is most likely due to changes in relaxation times of the higher molecular weight fractions in the PHPA samples (this is explained in more depth in section 3.6.1.4). At this temperature, for each PHPA, DP was observed to decrease at a steady rate. This is illustrated for poly(tetramethylene D-glucaramide) post-polymer whereby over the entire experimental time period, the DP was reduced by ~23% (Figure 3.3).

Figure 3.4 illustrates the estimated time period that the Poly(tetramethylene D-glucaramide) post-polymer is subjected to elevated temperature within the columns under simulated experimental conditions. These results show that the PHPA samples are not subjected to elevated temperature conditions for a long enough period of time whilst within the columns to cause significant polymer hydrolysis.

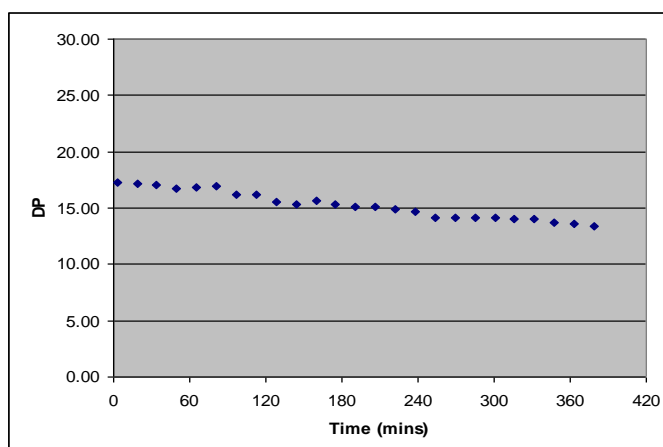


Figure 3.3: Change in DP determined by end-group analysis of Poly(tetramethylene D-glucaramide) post-polymer at 50°C

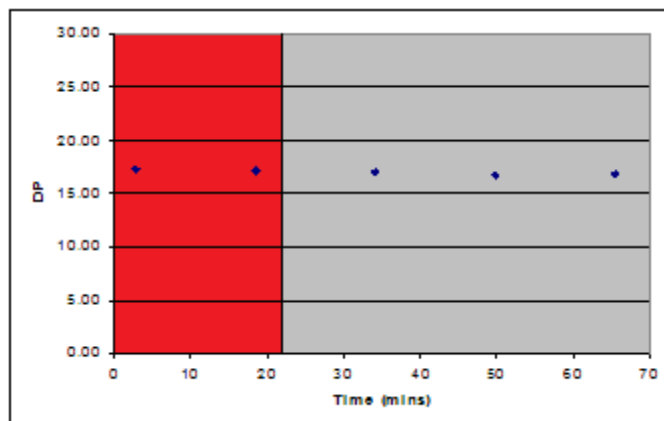


Figure 3.4: Change in DP determined by end-group analysis of Poly(tetramethylene D-glucaramide) post-polymer at 50 °C red region is estimated time period polymer spent in column

Taken together, these results suggest that the likelihood of any PHPA hydrolysis occurring during preparation or during an HPLC run is minor. Therefore, the smaller mass peaks that are observed in the HPLC are probably not due to polymer hydrolysis. A more likely explanation is that these peaks are due to smaller mass polymer molecules actually formed during the synthesis.

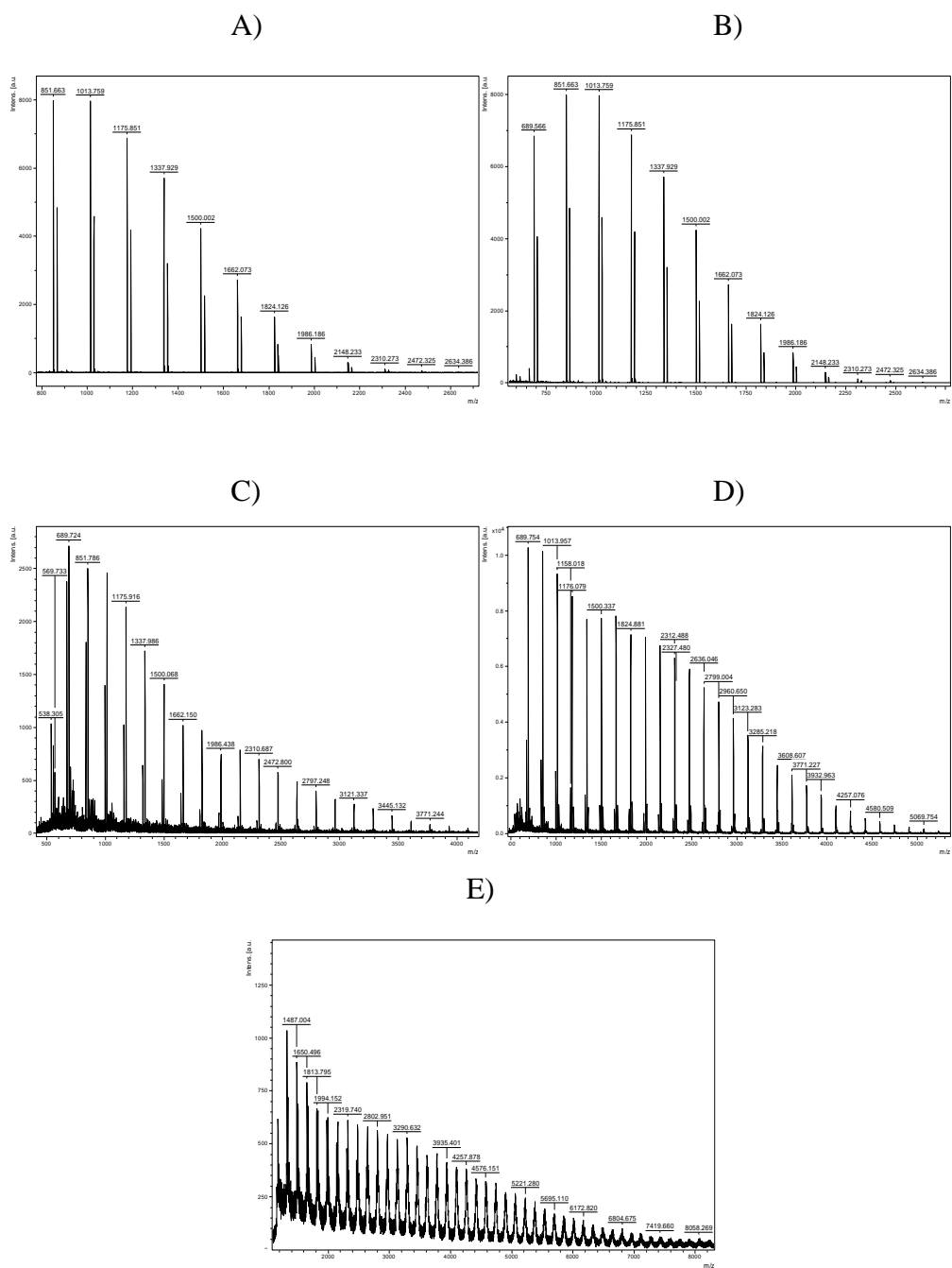
3.3 MALDI-TOF Spectrometry of Dextrans and Unfractionated Polyhydroxypolyamides

3.3.1 MALDI-TOF Spectra of Dextrans

Fractionated dextrans were used to determine the optimal conditions for MALDI-TOF spectrometry of the polyhydroxypolyamide PHPA samples. For this analysis, two matrices were used for each dextran fraction, 2',4',6'-trihydroxyacetophenone (THAP) and 2,5-dihydroxybenzoic acid, which is also referred to as super DHB (sDHB).

Results from the Dextran 1200 showed that the compound ionised well both in sDHB and THAP (see Figure 3.5). The mass distributions observed in both matrices were very similar and dispersed around 1200 m/z, although there was a slight asymmetry in both mass distributions (Table 3.1). The calculation of M_n by Polytools™, using the Peak Heights and Integral, gave a similar value to the manufacturer's M_n for Dextran 1200 (see Table 3.1).

For Dextran 4440, the detected mass distribution was well displaced towards the low mass region. Moreover, mass distributions detected in this region were found to be highly asymmetric. The results of the Polytools™ M_n calculations for Dextran 4440 differed significantly from that of the manufacturer's M_n (Table 3.1). The discrepancies of the displacement towards the low mass region and asymmetry of the distribution that was observed for sDHB became more apparent when THAP matrix was used. The displacement of the mass distribution was skewed even more to the lower mass region, hence exacerbating the asymmetry of the mass distribution. However, the highest positive ion peak reached for THAP was m/z ~5300, which is ~1500 mass units greater than that observed for the sDHB matrix (Figure 3.5, C & D) The Dextran 4440 Polytools™ M_n calculation, when using the peak height, was not significantly affected by matrix. however, when using peak integral in THAP, M_n was observed to be greater than that calculated for the sDHB matrix (Table 3.1). For both matrices M_n was underestimated compared to the manufacturer's M_n .



| Dextran | M_n in sDHB | | M_n in THAP | |
|---------|---------------|---------------|---------------|---------------|
| | Peak Height | Peak Integral | Peak Height | Peak Integral |
| 1200 | 1182.86 | 1341.33 | 1267.96 | 1278.93 |
| 4440 | 1414.63 | 1841.97 | 1475.90 | 2082.67 |
| 9890 | - | - | - | - |

Table 3.1: Polytools™ Calculations of M_n using Peak Height and Peak Integral for Dextrans 1200, 4440 and 9890.

Dextran 9890 in sDHB matrix failed to produce any positive ions. The analysis performed with the THAP matrix was capable of ionising Dextran 9890, however, detection was only possible in linear mode as no ions were observed in reflectron mode. The mass distribution produced by Dextran 9890 in the THAP matrix was displaced even further into the low mass region, and hence had greater asymmetry, than that observed for Dextran 4440. Such a result is consistent with previous research performed on dextrans using MALDI-TOF MS, whereby discrepancies of the mass distribution were observed to increase with the dextran molecular weight [53, 54].

As the MALDI-TOF ion detection for Dextran 9890 was only conducted in linear mode, a reliable Polytools™ M_n calculation was not possible. This is because the reflectron mode has greater resolution than linear mode, and hence is capable of determining mass with greater accuracy. A consequence of this is that the reflectron mode will produce a more consistent 162 m/z repeating unit between each positive ion peak. This is compared to the linear mode which, due to the lower resolution of this method, detects repeating units varying from 163-164 m/z. This phenomenon is illustrated in Figure 3.6.

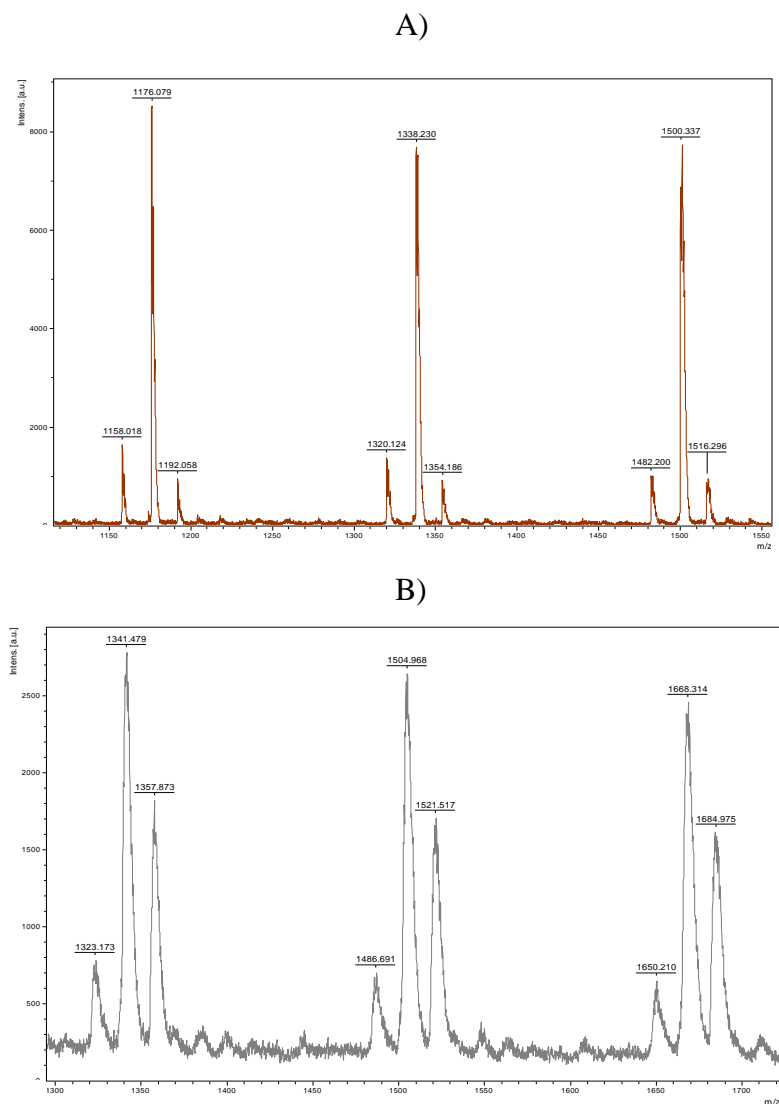


Figure 3.6: Dextran 4440 detected using A) Reflectron Mode, and B) Linear Mode.

It should be appreciated, however, that despite giving greater mass accuracy than the Linear Mode, the Reflectron mode has a greater bias towards the lower mass region. A corollary of this is that the M_n calculations of mass distributions detected in Reflectron Mode can potentially give results lower than that of the actual M_n .

The discrepancies in the molecular weights for the heavier dextran molecules, Dextran 4440 and 9890, in the MALDI-TOF are potentially due to two factors. Firstly, dextrans of low mass appear to be much easier to ionise than higher mass

dextrans. This was clearly observed for the sDHB matrix whereby Dextran 1200 was readily ionised and detected in the MALDI, whereas no positive ion peaks were detected for Dextran 9890. The second factor affecting mass discrepancy could be due to fragmentation of the higher mass dextrans in the MALDI-TOF. This is because the overall desorption/ionization efficiency for smaller dextran compounds would not be expected to be much higher than the larger ones in this mass region [53, 54]. It is therefore possible that fragmentation is the cause of the positive ion peaks observed in the lower mass region for both dextran 4440 and 9890.

In summary, dextrans are not entirely suitable as a standard for achieving good M_n data for PHPA's by MALDI-TOF spectrometry. This is based on the fact that neutral polarity dextrans either become harder to ionise above 3000m/z, or they suffer from fragmentation. This is opposed to PHPA polymers which have many amide groups present in their structure (see Figure 3.7) which might be ionised more readily. This increased ionisation should result in a more consistent mass distribution, hence overcoming the mass discrepancies observed for the higher molecular weight dextrans.

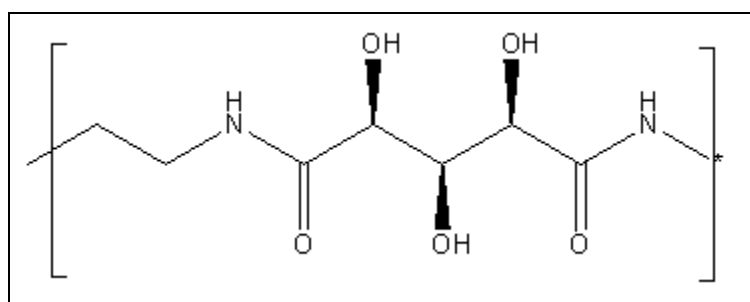


Figure 3.7: Repeating Unit of Poly(ethylene xylaramide).

3.3.2 MALDI-TOF Spectra of Spiked Dextrans

Ions that are generated in MALDI-TOF spectrometry can be formed with a variety of different cation adducts. Examples of cation adducts where this phenomenon has been observed are H^+ , K^+ , Na^+ and Li^+ . However, determining which cation adduct is resulting in certain ions can be problematic especially for polysaccharide based polymers. Previous research on these types of polymers have found that the polydispersity of polysaccharides gives rise to relatively poor mass accuracy. This often makes it difficult to identify the types of pseudomolecular ions that are produced by a specific adduct (i.e., K^+ , Na^+ etc.) in a MALDI-TOF spectrum. The difference between cation adduct masses potentially introduces problems when deciphering which structure is being observed for any particular ion in the spectrum. Therefore, if a structure is unknown before analysis, it can be difficult to confidently assign structures to ion peaks. This introduces the possibility of several possible structures being potentially concluded from the analysis.

The reason multiple structures could potentially be assigned is due to the mass differences between two specific cation adducts. These differences correspond to the mass of structural pieces that may or may not be a part of the overall structure, depending on which adduct is forming. In order to determine which structure belongs to the ion in question, it is necessary to determine which cation is involved. For instance, K^+ (Mass = 39 Da) and Na^+ (Mass = 23 Da) have a mass difference of 16 Da, which corresponds to the mass of oxygen. By spiking the sample using one of the respective adducts salts (i.e., KCl, NaCl etc.), it is possible to distinguish which adduct is forming ions. From this, a conclusion on which structure is being observed can be made about a specific ion.

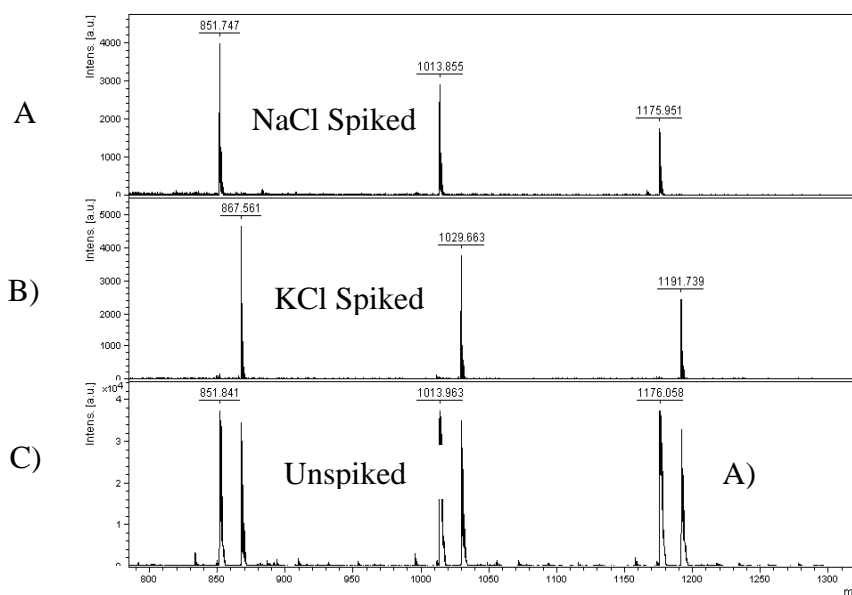


Figure 3.8: MALDI-TOF mass Spectra for A) Dextran 1200 spiked with 2mM of NaCl B) Dextran 1200 spiked with 2mM of KCl THAP C) Unspiked Dextran 1200.

These problems are observed in the analysis of fractionated and unfractionated PHPA samples. The mass accuracy of the ions generated in the MALDI is poor because of the relatively high polydispersity of PHPA polymers. The discrepancy between the suggested structure mass and the observed mass from the MALDI is usually around ± 1 -2Da, but can be as large as ± 5 Da.

To verify whether spiking conditions are suitable for use with PHPAs, Dextran 1200, was used. Dextran 1200 was readily ionised and detected in the MALDI-TOF spectrometer and produced more accurate results than the higher mass dextrans (see Figure 3.5, A & B; see also Section 3.3.1). It should be appreciated that, for this specific analysis, the Dextran 1200 polymer type mass distribution is not of importance, but rather the individual pseudomolecular ions generated.

In order to analyse the spiked Dextran 1200 samples, the sDHB matrix was utilised. An unspiked sample of Dextran 1200 was also run simultaneously. Comparing the resulting from the resultant spectra, an area was selected (Figure 3.8C) from which the observed masses were used to generate hypothesised

structures (Table 3.2). One set of ions corresponds to the sodium adducts ($[\text{H}-(\text{Glu})_n\text{-OH}] + \text{Na}^+$) and the other is the potassium adducts ($[\text{H}-(\text{Glu})_n\text{-OH}] + \text{K}^+$).

The spectrum of Dextran 1200, in the presence of NaCl, showed only ions at m/z 851, 1013 and 1175 (Figure 3.8A). The ions at 867, 1029 and 1191 were no longer present. For the analysis in which Dextran 1200 was combined with KCl, signals were observed at m/z 867, 1029 and 1191 (Figure 3.8B), and the remaining signals were no longer present (Figure 3.8C). This confirms that the hypothesised structures in Table 3.2 are correct.

From these results it can be concluded that the process of using either Na^+/K^+ salts to spike a sample might also be applied to PHPA samples. However, it should be appreciated that the types of results observed for Dextran 1200 may not necessarily produce the same observations for spiked PHPA samples. The reason for this is that each PHPA sample contains impurities in the form of inorganic material. This is illustrated by the ICP-MS data (Table 3.3) which shows that there remains Na^+ and K^+ contamination in each of the samples.

Dextran 1200 is a relatively clean sample, so the Na/K spiked sample produces a significant change in the observed mass. However, as the PHPA sample still contains inorganic impurities, this method will only produce a limited change in the peak intensity.

| n | $[\text{H}-(\text{Glu})_n\text{-OH}] + \text{Na}^+$ | $[\text{H}-(\text{Glu})_n\text{-OH}] + \text{K}^+$ |
|----------|---|--|
| 5 | 851m/z | 867m/z |
| 6 | 1013m/z | 1029m/z |
| 7 | 1175m/z | 1191m/z |

Table 3.2: Hypothesised structures between 800m/z and 1250m/z.

| Sample | ²³ Na | ³⁹ K |
|--|------------------|-----------------|
| Calibration Blank | 0.83 | -4.50 |
| Poly(tetramethylene D-glucaramide) post-polymer | 740.98 | 12.02 |
| Poly(tetramethylene D-glucaramide) pre-polymer | 7555.18 | 107.14 |
| Poly(3',6'-dioxaoctamethylene D-glucaramide) pre-polymer | 10447.46 | 145.99 |
| Poly(ethylene D-glucaramide) post-polymer | 2663.67 | 141.56 |
| Poly(ethylene xylaramide) pre-polymer (A) | 97.77 | -9.42 |
| Poly(ethylene xylaramide) pre-polymer (B) | 3753.62 | -5.04 |

Table 3.3: ICP-MS data of the Concentration (ppb) of Sodium and Potassium in each PHPA samples.

3.3.3 MALDI-TOF Spectra of Unfractionated Polyhydroxypolyamides

MALDI-TOF spectrometry of the unfractionated PHPA sample demonstrated that the compound ionized better in the THAP matrix (Figure 3.9) than in sDHB. This was concluded because the ions produced in the THAP matrix were of a higher intensity, and produced a more polymer like mass distribution, compared to the results for the sDHB matrix.

The spectrum of each unfractionated PHPA sample, showed that the mass distribution was well displaced towards the low mass region. Furthermore the mass distributions detected for each sample was observed to be asymmetric. These discrepancies of the displacement towards the low mass region and the asymmetry of the mass distributions were more prominent for unfractionated poly(3',6'-dioxaoctamethylene D-glucaramide) pre-polymer, poly(ethylene D-glucaramide) post-polymer, poly(ethylene xylaramide) pre-polymers (A) and (B) than for the poly(tetramethylene D-glucaramide) pre and post-polymers (Figure 3.9). This may indicate that the latter two are somewhat lower in molecular weight or less polydisperse than the former.

Because of these discrepancies the M_n calculations for each PHPA samples (Table 3.4) differed from that observed from that of the ^1H NMR end group analysis performed at the University of Waikato. These results obtained for the unfractionated PHPA samples are similar to what was observed for the fractionated dextrans (see Section 3.3.1). For the dextran samples a possible hypothesis for what is occurring in the MALDI mass spectra is that fragmentation was occurring. This hypothesis could also explain what is being observed in the MALDI-TOF mass spectra for unfractionated PHPA samples and why lower than expected results for the Polytools M_n calculations are being obtained.

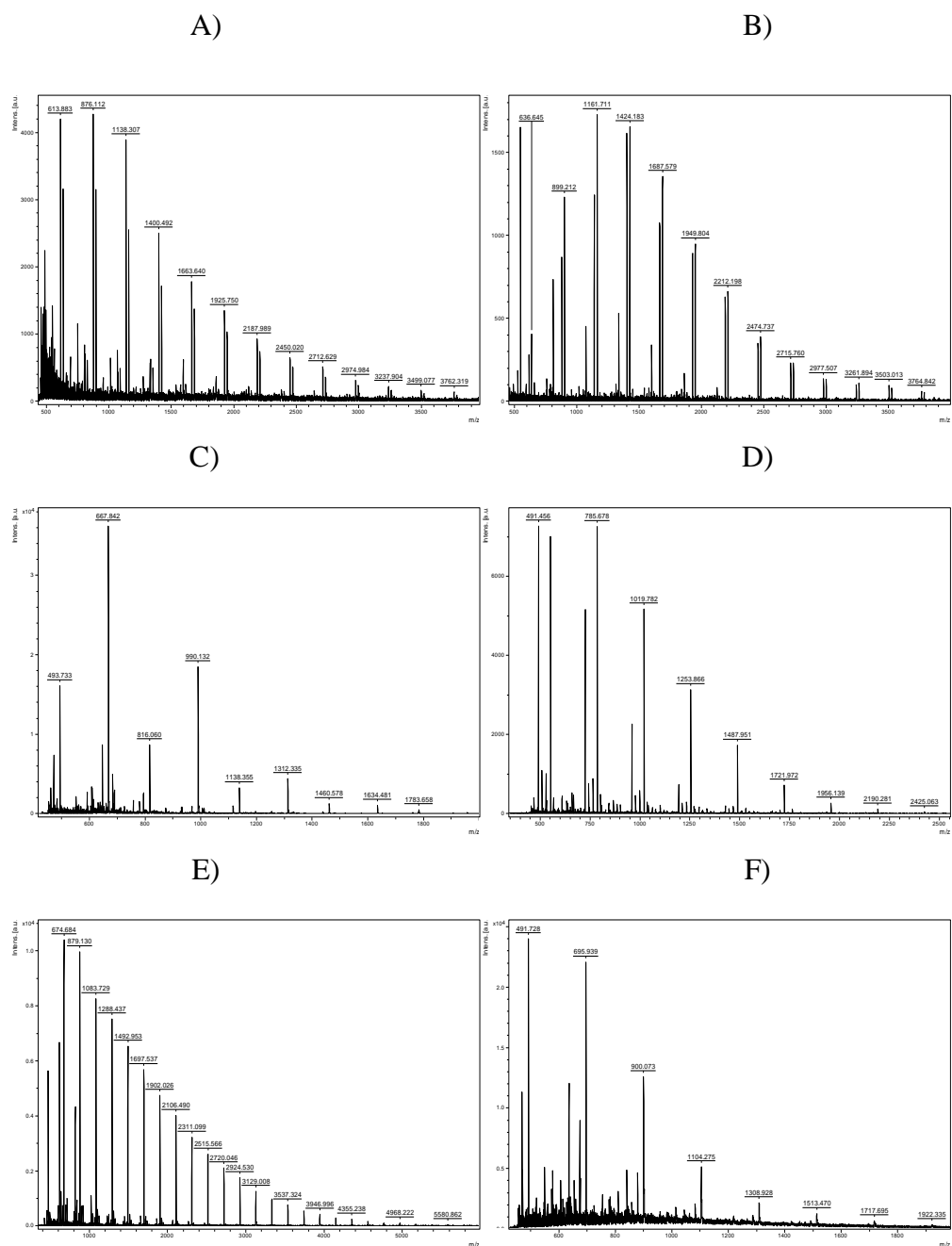


Figure 3.9: MALDI-TOF Mass Spectra of Unfractionated A) Poly(tetramethylene D-glucaramide) Post-polymer, B) poly(tetramethylene-D-glucaramide pre-polymer, C) Poly(3',6'-dioxaoctamethylene D-glucaramide) pre-polymer, D) poly(ethylene D-glucaramide) Post-polymer, E) Poly(ethylene xylaramide) pre-polymer (A), and F) Poly(ethylene xylaramide) pre-polymer (B) in THAP Matrix.

| Un-fractionated PHPA sample | Polytools™ calculations from the MALDI-TOF spectrum | | | ¹ H NMR end group analysis M _n |
|--|---|----------------|----------------|--|
| | M _n | M _w | Polydispersity | |
| Poly(tetramethylene D-glucaramide) Pre-polymer | 1735 | 1924 | 1.11 | 2438 |
| Poly(tetramethylene D-glucaramide) Post-polymer | - | - | - | 7958 |
| Poly(3',6'-dioxaoctamethylene D-glucaramide) pre-polymer | - | - | - | 3564 |
| Poly(ethylene D-glucaramide) post-polymer | 1407 | 1523 | 1.08 | 2000 |
| Poly(ethylene xylaramide) pre-polymer (A) | 3688 | 3801 | 1.03 | 3646 |
| Poly(ethylene xylaramide) pre-polymer (B) | 2904 | 3009 | 1.04 | 2925 |

Table 3.4: Polytools™ Calculations of M_n using Peak Height and Peak Integral and ¹H End Group Calculations of M_n for each unfractionated PHPA sample.

However the discrepancies observed for the unfractionated PHPA samples appear to be somewhat alleviated upon fractionation; MALDI-TOF mass spectrometry of fractionated PHPA's will be dealt with in subsequent sections (see Section 3.6).

3.4 SEC of Dextran and Polyhydroxypolyamides

3.4.1 Characteristics of SEC Columns Used

Fractionation of each PHPA sample was undertaken on Shodex KS sugar columns (KS800 series). These are analytical columns that are used *inter alia* for SEC of saccharides and polysaccharides. Prior to use the columns were characterised with saccharide standards; the void volume (V_o) was determined for KS801-804 (Table 3.5) using 2M Dextran ($M_n = 2,000,000$ Da). However this dextran was unsuitable for KS805 and 806 columns as the exclusion limit for these columns was much greater than 2,000,000, therefore this dextran was included on these columns. Since no other suitable saccharide standard was available to be used to find V_o for these columns, the manufactures exclusion limit was used as an indicator of molecular size. Glucose was used to indicate the elution time of a monosaccharide sugar.

Preliminary experiments showed that the combination of columns KS804 and 805 in series would be best for fractionation of PHPA samples. This setup produced peaks which were of a greater resolution relative to analysing with each column separately or other combinations of columns in series. Results of the SEC fractionation of each PHPA sample will be dealt with in subsequent sections (Section 3.7).

| Column | Exclusion Limit | Retention Time (mins) of 2M Dextran | Retention Time (mins) of glucose |
|--------|-----------------|--|-------------------------------------|
| KS-801 | 1000 | 5.342 | 8.322 |
| KS-802 | 10,000 | 5.428 | 9.813 |
| KS-803 | 100,000 | 6.508 | 10.207 |
| KS-804 | 400,000 | 6.684 | 11.597 |
| KS-805 | 5,000,000 | 6.833* | 12.237 |
| KS-806 | 50,000,000 | 7.950* | 12.446 |

* – The Exclusion Limit is Larger than 2M Dextran so these Retention Times do not correspond to V_0

Table 3.5: Manufacturers' Exclusion Limit and Retention Time of 2M Dextran and Glucose of each Shodex KS series SEC column.

3.4.2 SEC of Unfractionated Polyhydroxypolyamides

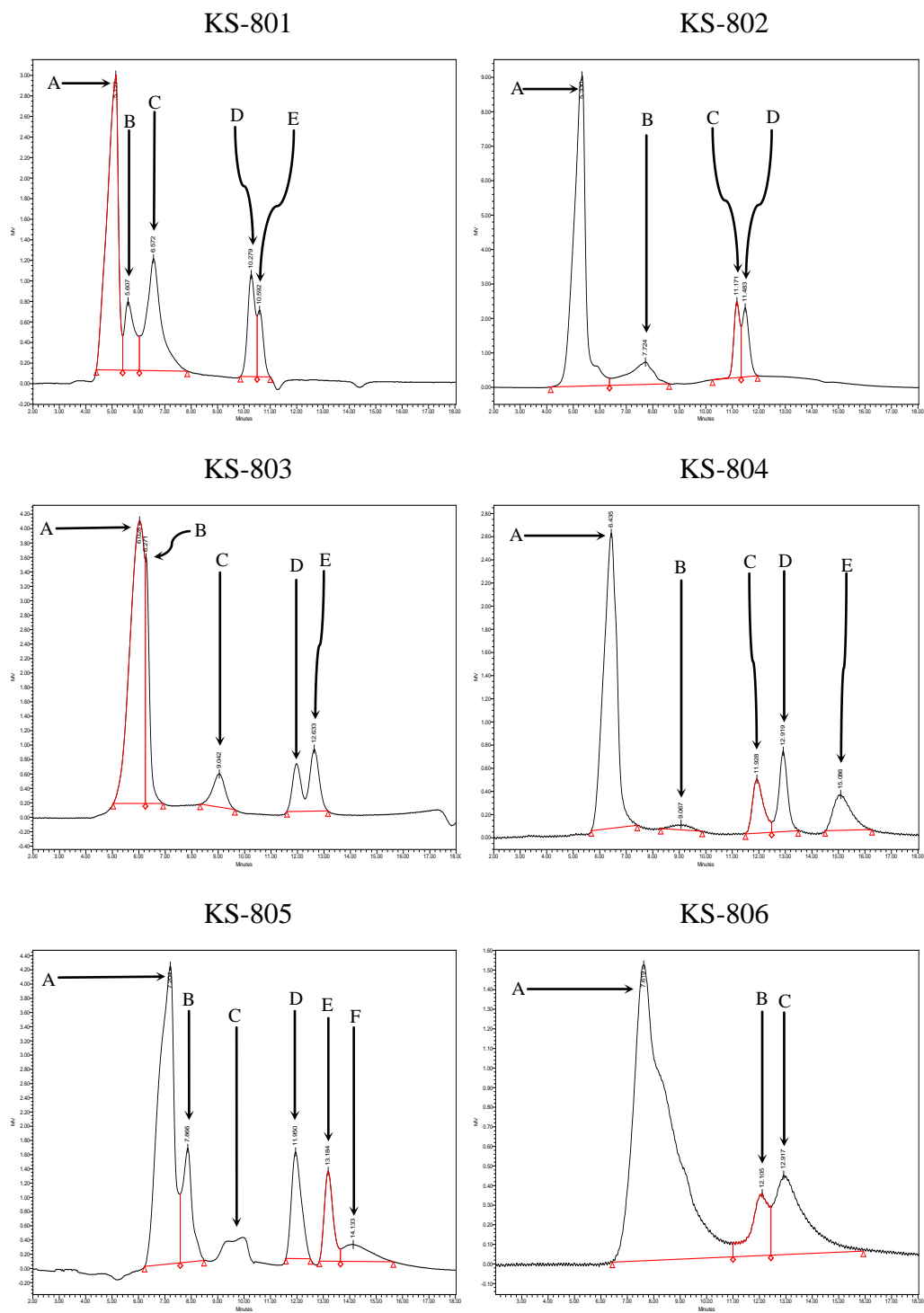
Poly(tetramethylene-D-glucaramide) post-polymer:

Figure 3.10: SEC Chromatograms of Poly(tetramethylene D-glucaramide) Post-polymer on each individual KS columns.

| Peak | KS-801 | KS-802 | KS-803 | KS-804 | KS-805 | KS-806 |
|------|--------|--------|--------|--------|--------|--------|
| A | 47.85 | 70.57 | 63.03 | 65.34 | 57.05 | 80.18 |
| B | 11.57 | 11.08 | 14.58 | 4.23 | 14.32 | 4.83 |
| C | 25.19 | 10.14 | 6.39 | 19.34 | 2.42 | 14.99 |
| D | 10.33 | 8.21 | 6.81 | 11.08 | 3.38 | - |
| E | 5.06 | - | 9.20 | - | 14.56 | - |
| F | - | - | - | - | 8.27 | - |

Table 3.6: Integrated Areas of labelled peaks in SEC chromatograms of unfractionated poly(tetramethylene-D-glucaramide post-polymer on the KS series SEC columns.

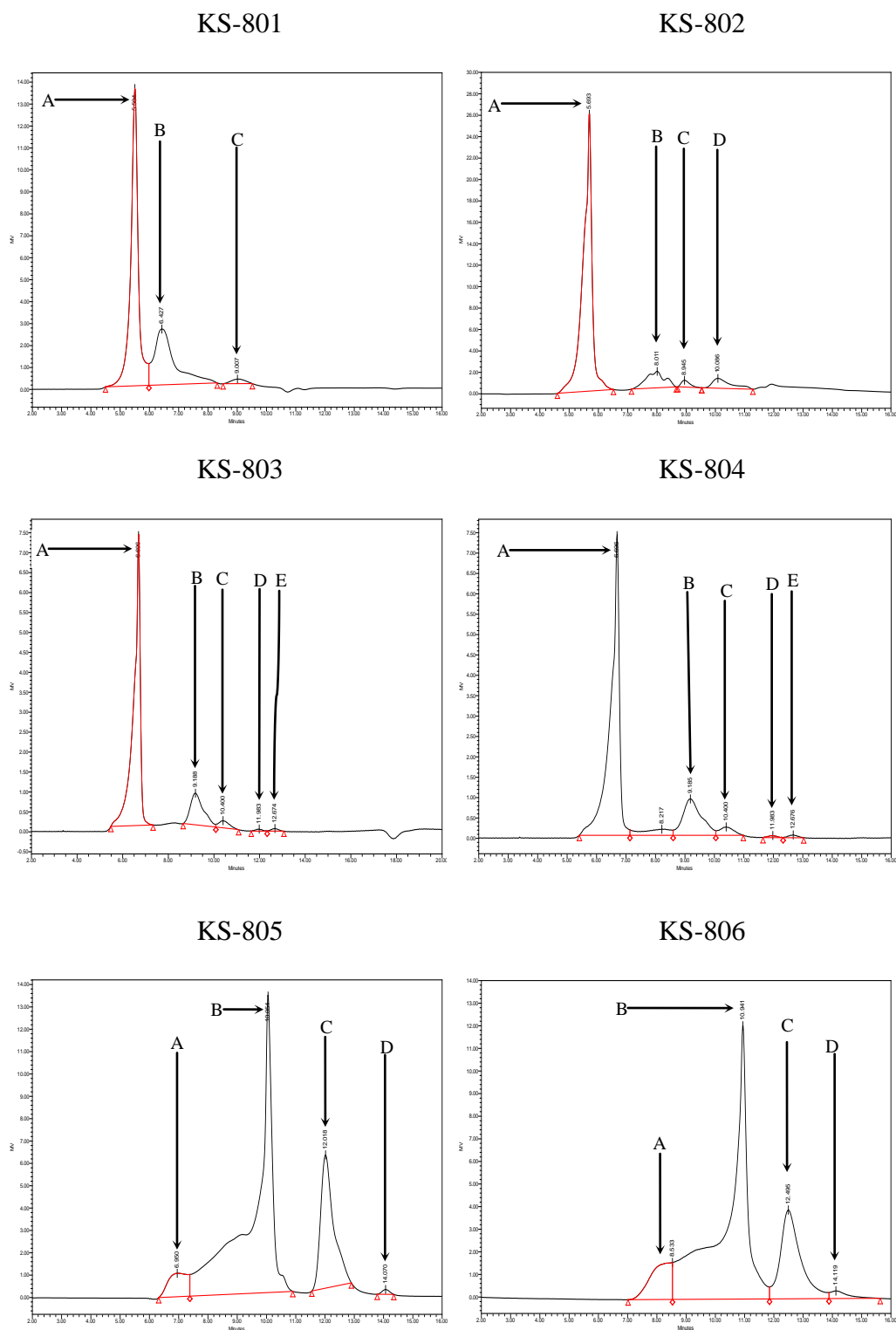
Poly(tetramethylene-D-glucaramide) pre-polymer:

Figure 3.11: SEC Chromatograms of Poly(tetramethylene D-glucaramide) Pre-polymer on each individual KS columns.

| Peak | KS-801 | KS-802 | KS-803 | KS-804 | KS-805 | KS-806 |
|------|--------|--------|--------|--------|--------|--------|
| A | 63.58 | 84.33 | 82.10 | 35.88 | 6.32 | 9.78 |
| B | 34.36 | 3.78 | 15.22 | 28.05 | 66.98 | 71.21 |
| C | 2.06 | 10.06 | 1.80 | 8.77 | 25.99 | 18.69 |
| D | - | 1.82 | 0.45 | 23.17 | 0.72 | 0.32 |
| E | - | - | 0.44 | 4.13 | - | - |

Table 3.7: Integrated Areas of labelled peaks in SEC chromatograms of unfractionated poly(tetramethylene-D-glucaramide pre-polymer on the KS series SEC columns.

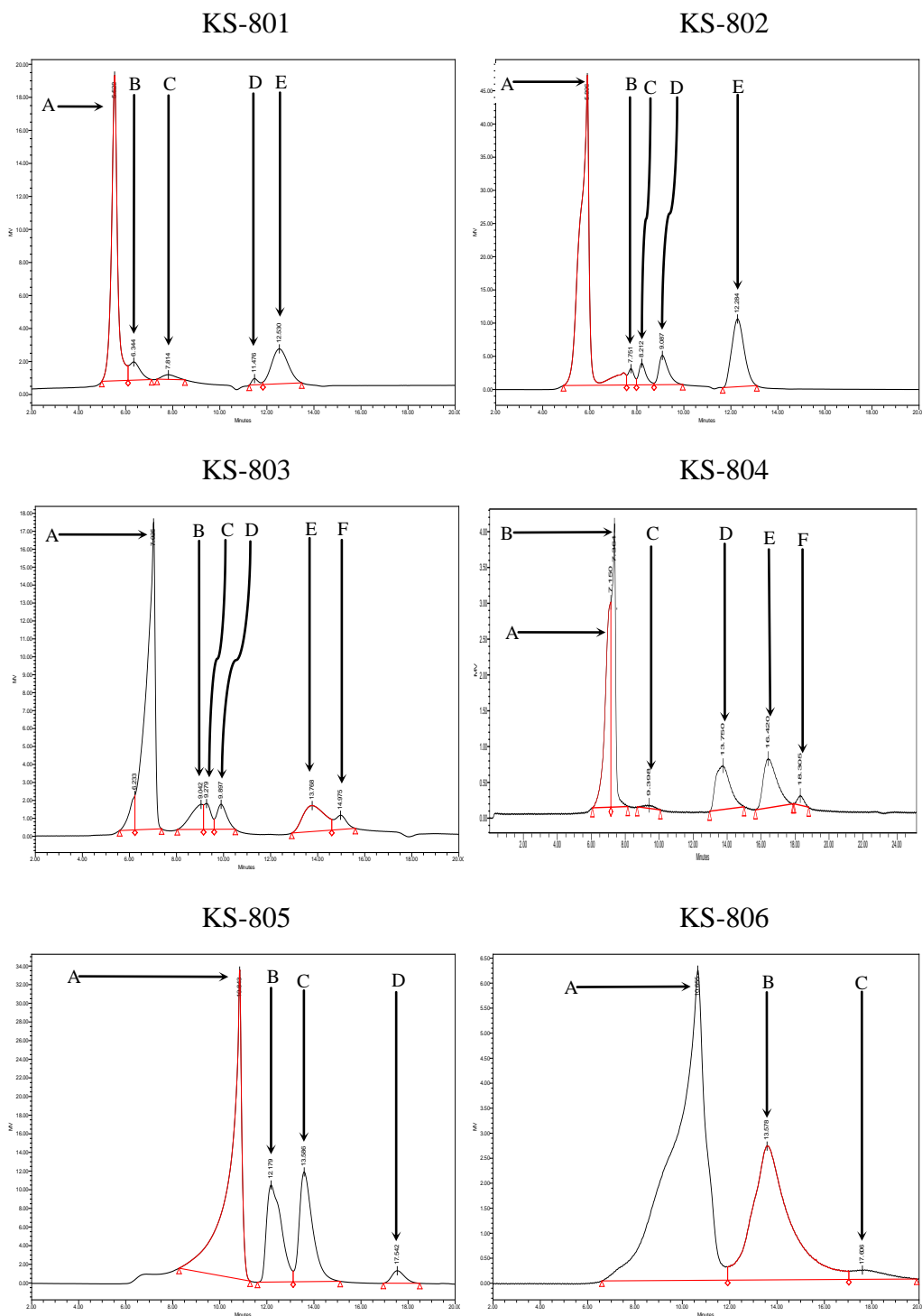
Poly(3',6'-dioxaoctamethylene D-glucaramide) pre-polymer:

Figure 3.12: SEC Chromatograms of Poly(3',6'-dioxaoctamethylene D-glucaramide) pre-polymer on each individual KS columns.

| Peak | KS-801 | KS-802 | KS-803 | KS-804 | KS-805 | KS-806 |
|------|--------|--------|--------|--------|--------|--------|
| A | 61.43 | 61.08 | 63.94 | 31.01 | 57.82 | 65.95 |
| B | 9.38 | 4.71 | 7.21 | 30.52 | 20.39 | 32.84 |
| C | 7.32 | 2.45 | 5.14 | 0.88 | 20.23 | 1.21 |
| D | 1.63 | 3.80 | 7.43 | 17.54 | 1.57 | - |
| E | 20.24 | 7.69 | 13.08 | 18.41 | - | - |
| F | - | 20.26 | 3.19 | 1.64 | - | - |

Table 3.8: Integrated Areas of labelled peaks in SEC chromatograms of unfractionated poly Poly(3',6'-dioxaoctamethylene D-glucaramide) pre-polymer on the KS series SEC columns.

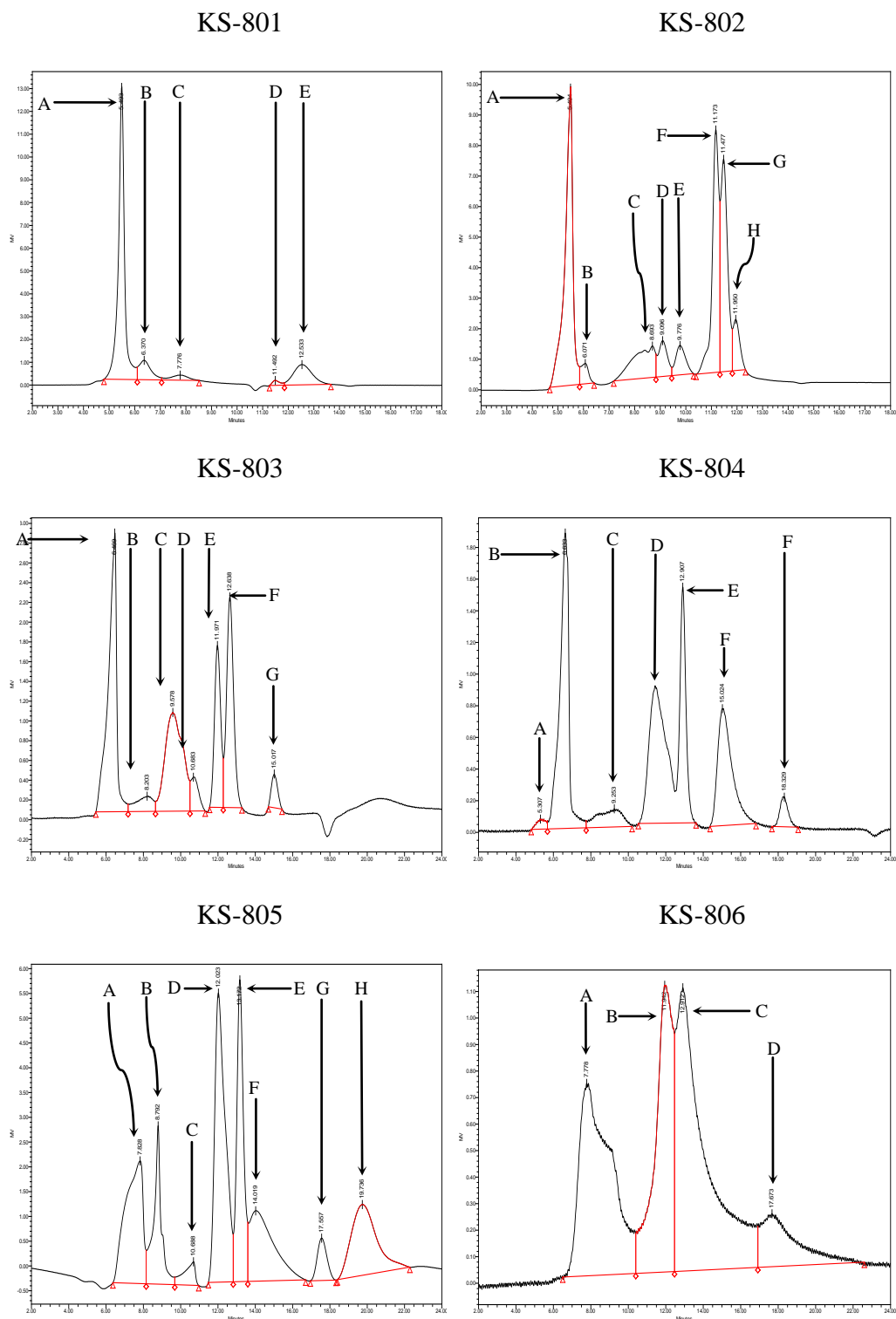
Poly(ethylene D-glucaramide) post-polymer:

Figure 3.13: SEC Chromatograms of Poly(ethylene D-glucaramide) Post-polymer on each individual KS columns.

| Peak | KS-801 | KS-802 | KS-803 | KS-804 | KS-805 | KS-806 |
|------|--------|--------|--------|--------|--------|--------|
| A | 75.15 | 29.91 | 30.98 | 1.13 | 17.77 | 35.98 |
| B | 8.79 | 2.02 | 4.31 | 30.78 | 9.76 | 22.71 |
| C | 1.45 | 10.90 | 23.65 | 5.16 | 2.05 | 35.33 |
| D | 14.61 | 4.78 | 3.81 | 26.57 | 25.52 | 5.98 |
| E | - | 5.04 | 13.25 | 16.10 | 17.32 | - |
| F | - | 22.23 | 20.13 | 17.67 | 13.29 | - |
| G | - | 19.65 | 3.87 | 2.58 | 2.56 | - |
| H | - | 5.47 | - | - | 11.75 | - |

Table 3.9: Integrated Areas of labelled peaks in SEC chromatograms of unfractionated poly(ethylene D-glucaramide) Post-polymer on the KS series SEC columns.

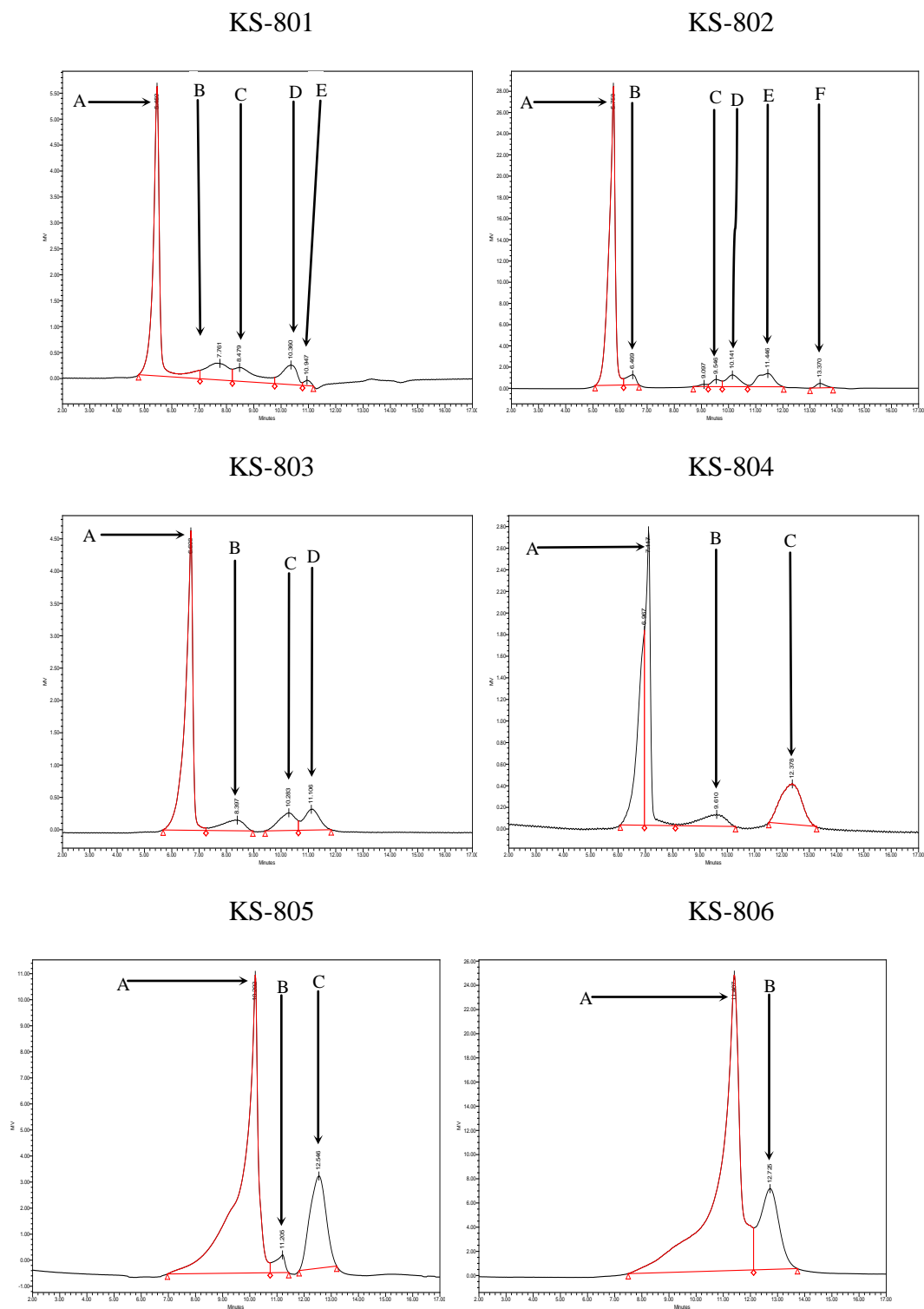
Poly(ethylene xylaramide) pre-polymer (A):

Figure 3.14: SEC Chromatograms of Poly(ethylene xylaramide) pre-polymer (A) on each individual KS columns.

| Peak | KS-801 | KS-802 | KS-803 | KS-804 | KS-805 | KS-806 |
|------|--------|--------|--------|--------|--------|--------|
| A | 13.67 | 20.07 | 22.87 | 1.94 | 6.07 | 15.48 |
| B | 3.50 | 7.14 | 4.32 | 17.50 | 8.10 | 84.52 |
| C | 20.41 | 6.77 | 36.04 | 8.08 | 0.86 | - |
| D | 18.42 | 12.48 | 36.77 | 1.10 | 1.97 | - |
| E | 17.32 | 14.16 | - | 71.38 | 83.00 | - |
| F | 24.85 | 39.38 | - | - | - | - |
| G | 1.83 | - | - | - | - | - |

Table 3.10: Integrated Areas of labelled peaks in SEC chromatograms of unfractionated poly(ethylene xylaramide) pre-polymer (A) on the KS series SEC columns.

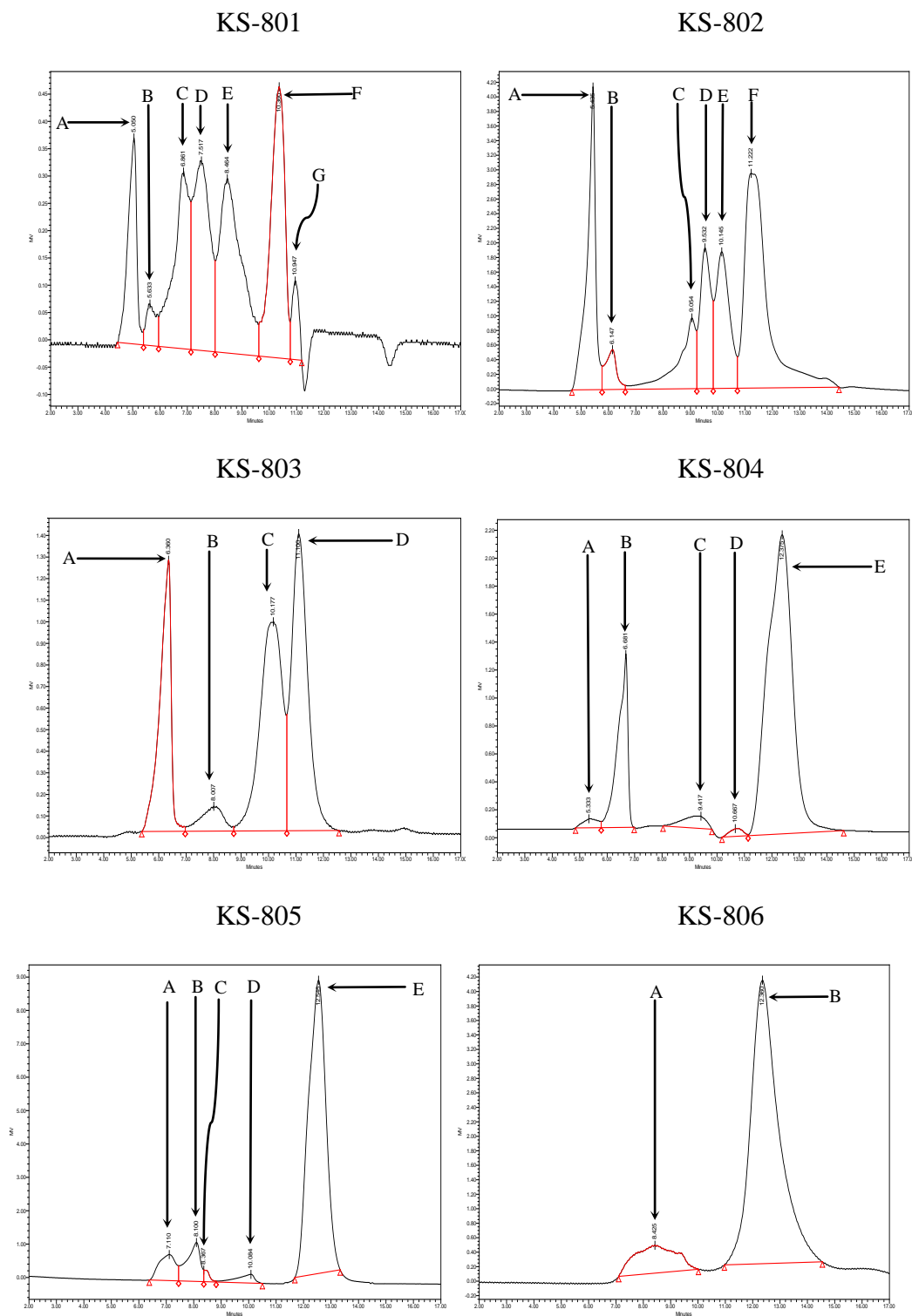
Poly(ethylene xylaramide) pre-polymer (B):

Figure 3.15: SEC Chromatograms of Poly(ethylene xylaramide) pre-polymer (B) on each individual KS columns.

| Peak | KS-801 | KS-802 | KS-803 | KS-804 | KS-805 | KS-806 |
|------|--------|--------|--------|--------|--------|--------|
| A | 57.80 | 76.26 | 71.40 | 66.68 | 71.10 | 79.15 |
| B | 17.49 | 6.00 | 8.55 | 9.01 | 3.27 | 20.85 |
| C | 9.11 | 1.95 | 10.01 | 24.31 | 25.63 | - |
| D | 13.42 | 5.67 | 10.04 | - | - | - |
| E | 2.18 | 8.39 | - | - | - | - |
| F | - | 1.74 | - | - | - | - |

Table 3.11: Integrated Areas of labelled peaks in SEC chromatograms of unfractionated poly(ethylene xylaramide) pre-polymer (B) on the KS series SEC columns.

| Retention Time (mins) of 2M Dextran | Retention Time (mins) of Glucose |
|--|-------------------------------------|
| 12.650 | 22.858 |

Table 3.12: Retention Time of 2M Dextran and Glucose of Shodex KS-804 and 805 SEC column in series.

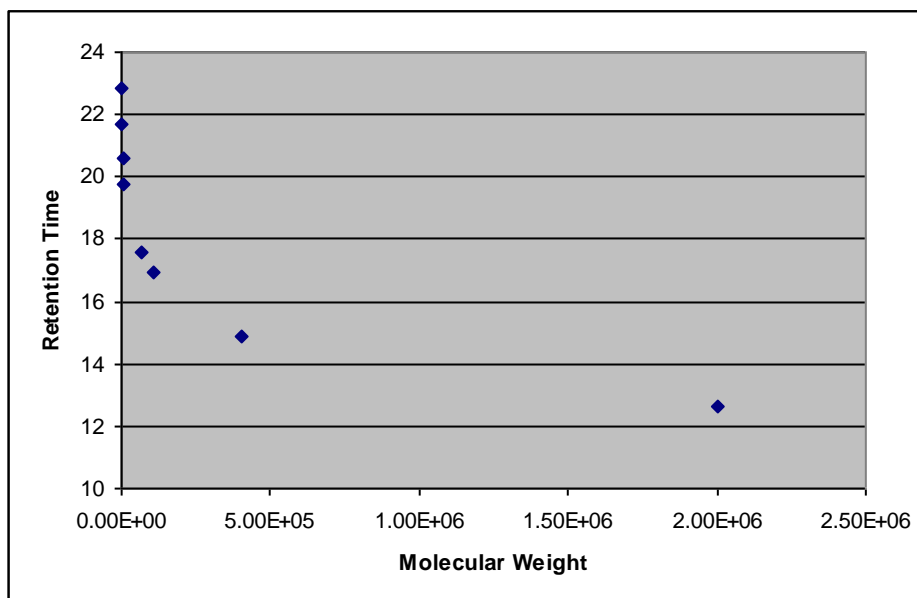
The SEC chromatograms showed that some lower molecular weight, peaks were resolved on KS-801, but the resolution of these peaks decreased with increasing exclusion limits. Conversely, there appears to be a large V_0 peak from columns KS-801 to KS-804, however for columns KS-805 and KS-806 this was partially included. This possibly means that these latter peaks may be due to extremely large polymers, certainly larger than the exclusion limit of the 804 column (400,000). There is a slight possibility that the apparently extremely large material preceding the big peak on the 805 and 806 columns is ionic but ICP-MS analysis of each PHPA sample (Table 3.3) confirmed that this is not due to inorganic contamination of the polymer sample and so, if ionic material is present, it is organic ionic material. If the peaks observed are indeed organic ionic material, they should ionize well in the MALDI analyses however this is not the case (see Section 3.6.1.3 below) and so we conclude that the PHPA samples contain very large polymer molecules.

3.4.3 Calibration Curves for SEC Columns KS-804 and 805 in series

The combination of columns KS-804 and 805 in series was chosen to fractionate the un-fractionated PHPA sample. Fractionated dextrans of known molecular weights were to construct a calibration curve of molecular weight vs. retention time. From Table 3.12 it can be observed that glucose is eluting quicker than the smaller molecular weight peaks for PHPA. This difference can be attributed to the difference in their hydrodynamic behaviour. The curve provides a rough guide to molecular size but because of the difference in chemical structures of the

standards versus the PHPAs data obtained from the curve is unlikely to be extremely accurate; indeed the retention times of the smaller PHPA materials are much larger than any of the dextrans.

A)



B)

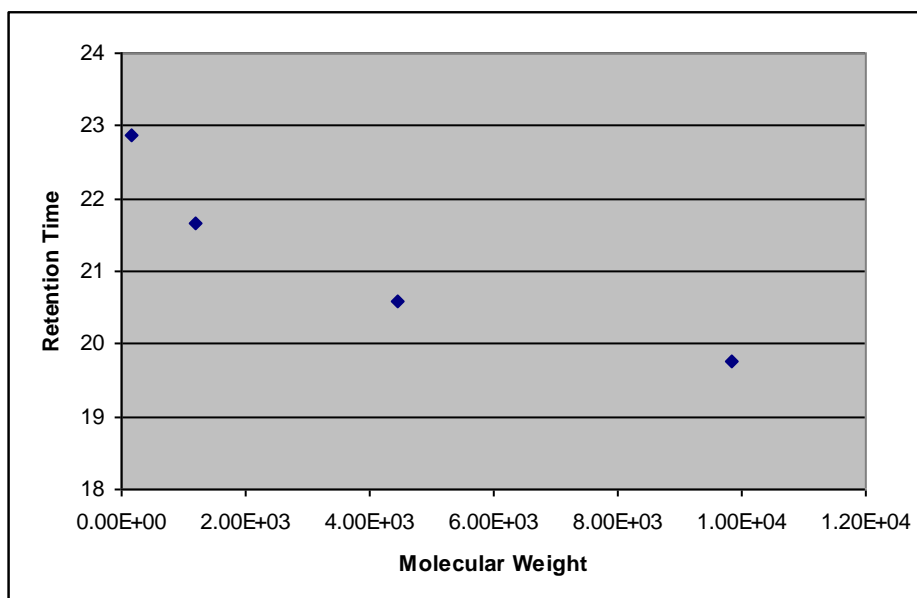


Figure 3.16: Calibration curve of Dextrans Molecular Weight versus their Retention Time on KS-804 and 805 SEC columns in series.

3.5 Measurements of NMR Relaxation Times

In the NMR, polymers exhibit certain characteristics that are unique to polymers. One of these characteristics is the well-studied effect that molecular weight has on relaxation measurements. Understanding what is occurring and why different molecular weight polymers affect relaxation times of mixtures has been previously explained in depth (see Section 1.4).

Using results and conclusions obtained in other polymer studies, this technique can be used to determine whether fractions obtained near the V_0 region are extremely high molecular weight polymer fractions. It is important to note that this method is not able to accurately determine molecular weight for these PHPA fractions as there is no data available for relaxation times of known molecular weights for PHPA fractions. It is also not possible to use a calibration curve created using polymer standards of known molecular weights (i.e., fractionated dextrans). This is because the chemical environment for the signal used for relaxation measurements for the polymer standard is unique to that polymer and will be different to the polymer being studied.

Relaxation measurements of each individual PHPA fractions were only measured for poly(tetramethylene D-glucaramide) post-polymer and poly(3',6'-dioxaoctamethylene D-glucaramide) pre-polymer fractions. The conclusions that will be made from this relaxation study can be extended to what is observed for all the other PHPA samples.

To achieve accurate measurements of relaxation times it is necessary to choose a signal that does not overlap with other signals and for this study, we have selected the H-2 signal for poly(tetramethylene D-glucaramide) post-polymer and the H-3 signal for poly(3',6'-dioxaoctamethylene D-glucaramide) pre-polymer. This is because it was found that, this signal provided the most consistent results compared to the other signals. Furthermore, the T_1 relaxation measurement for this signal showed greater variation between high molecular weight fractions,

where motion is more restricted, and lower molecular weight fractions, which can move faster.

3.6 Analysis of Fractionated PHPAs

Before each PHPA sample was fractionated the M_n values were recalculated at the Chemistry Department, University of Waikato, NZ (400Hz NMR) using ^1H NMR end group analysis in D_2O , with *t*-butanol used as the reference standard (see Table 3.13). The only significant disparity was in the results for the two xylaramide pre-polymers. This may reflect the fact that the PHPA analysis from Montana was conducted by different operators.

However when determining the M_n for each unfractionated PHPA sample using two different NMR instruments it can be observed that there is a difference in the M_n calculated (see Table 3.13). This same effect can also be observed when using different probes in each respective NMR (Table 3.14). It is thought that possibly in Montana a 600MHz NMR was used to measure the xylaramides whereas a 400MHz NMR was used to measure the D-glucaramides, this might explain the differences in the M_n values calculated at Montana and Waikato for the xylaramides.

| Name of Polymer | Waikato ^a Calculated M _n | Montana ^b Calculated M _n |
|--|---|---|
| Poly(tetramethylene D-glucaramide) pre-polymer | 2438 | 2443 |
| Poly(tetramethylene D-glucaramide) post-polymer | 3591 | 3608 |
| Poly(3',6'-dioxaoctamethylene D-glucaramide) pre-polymer | 2801 | 2844 |
| Poly(ethylene D-glucaramide) post-polymer | 1620 | 1750 |
| Poly(ethylene xylaramide) pre-polymer (A) ^c | 1831 | 3735 |
| Poly(ethylene xylaramide) pre-polymer (B) ^c | 948 | 1603 |

^a - Measured at the Chemistry Department of the University of Waikato, Hamilton, New Zealand using a 400 MHz Bruker NMR spectrometer.

^b - Measured at The Shafizadeh Rocky Mountain Centre for Wood and Carbohydrate Chemistry, university of Montana, Missoula, MT, USA using a 400 MHz Varian NMR spectrometer.

^c - See note in text

Table 3.13: M_n Calculations by ¹H NMR end group analysis of each PHPA sample Prior to fractionation by SEC

| Name of Polymer | 400Hz | | 300Hz | |
|--|--------------|------|-------|------|
| | Inverse Dual | Dual | QMP | Dual |
| Poly(tetramethylene D-glucaramide) pre-polymer | 2438 | 3105 | 1915 | 2653 |
| Poly(tetramethylene D-glucaramide) post-polymer | 3591 | 4394 | 1514 | 1897 |
| Poly(3',6'-dioxaoctamethylene D-glucaramide) pre-polymer | 2801 | 6376 | 2799 | 1683 |
| Poly(ethylene D-glucaramide) post-polymer | 1620 | 1800 | 1537 | 1224 |
| Poly(ethylene xylaramide) pre-polymer (A) | 1831 | 2136 | 1576 | 1916 |
| Poly(ethylene xylaramide) pre-polymer (B) | 948 | 1133 | 835 | 601 |

Table 3.14 – M_n Calculations by 1H NMR end group analysis of each unfractionated PHPA sample on a 300 MHz Bruker NMR spectrometer using a QMP and Dual probe and on a 400 MHz Bruker NMR spectrometer using a Inverse Dual and Dual probe

3.6.1 Poly(tetramethylene D-glucaramide) Post-polymer

3.6.1.1 Introduction

Poly(tetramethylene D-glucaramide) post-polymer is a C4 poly(alkylene D-glucaramide) resulting from the polymerisation of poly(tetramethylene D-glucaramide) pre-polymer. The repeating unit structure of this polymer is illustrated in Figure 3.17A. M_n calculated by ^1H NMR end group analysis for the poly(tetramethylene D-glucaramide) post-polymer at UoW was very similar to that calculated at UoM (Table 3.13).

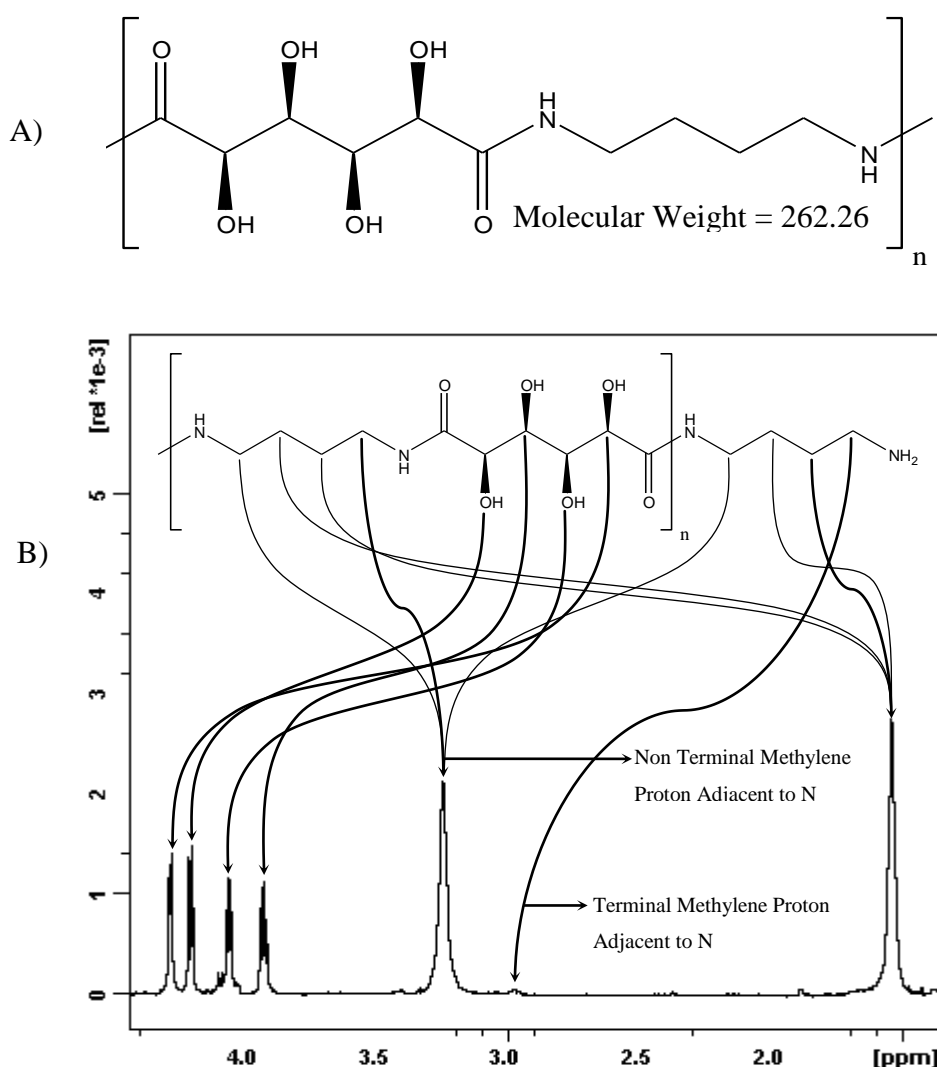


Figure 3.17: A) Structure of the Poly(tetramethylene d-glucaramide) post-polymer repeating unit. B) Fully Labeled ^1H NMR Spectrum of Poly(tetramethylene d-glucaramide) Post-polymer.

3.6.1.2 Fractionation by SEC

From the resulting SEC chromatogram, five major peaks were resolved (Figure 3.18). Note from Figure 3.18 the smaller, less resolved peaks that are detected between the retention times of 16-21 minutes. Due to the fact that these peaks are small, this whole region was collected as one fraction (see phase C from Figure 3.18).

The two predominant peaks in the chromatogram, Peak A and Peak B are observed around the V_0 region. Assuming that the refractive index responses are all approximately equal, the percentage peak areas show that these peaks make up the majority (~60%) of the unfractionated poly(tetramethylene D-glucaramide) post-polymer sample (Table 3.15), assuming that the refractive index responses are all approximately equal. As previously mentioned, the peaks observed in this region are due to extremely high molecular weight polymers (see Section 3.4.2), which was confirmed by the fact that all fractions exhibited similar ^1H NMR spectra (Figure 3.20).

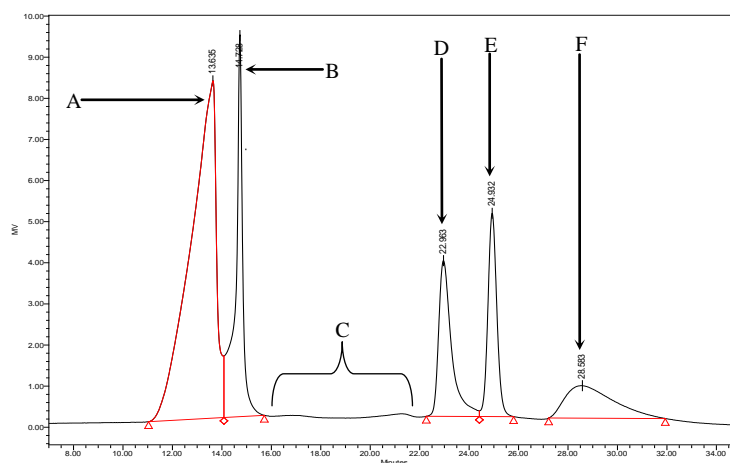


Figure 3.18: SEC Chromatogram of Poly(tetramethylene D-glucaramide) Post-polymer on columns KS-804 and KS-805 in series.

| Fraction | Retention Time (mins) | Area | Area (%) |
|----------|-----------------------|--------|----------|
| A | 13.575 | 548634 | 44.90 |
| B | 14.683 | 192863 | 15.78 |
| C | 16.051 - 20.973 | 41525 | 3.42 |
| D | 23.003 | 135586 | 11.10 |
| E | 24.933 | 141205 | 11.56 |
| F | 28.504 | 161829 | 13.24 |

Table 3.15: Integrated Areas of labelled peaks in SEC chromatogram of unfractionated poly(tetramethylene-D-glucaramide post-polymer on KS-804 and 805 SEC columns in series.

3.6.1.3 Maldi-TOF of Fractions

Results from the MALDI-TOF performed on each fraction gave varying information about the molecular weights. The resulting mass spectra obtained for fractions A-C gave little information about the possible M_n of these fractions. Peaks A and B were collected near the V_0 region; the region where it is expected that higher mass molecules would elute (Figure 3.18). The exclusion limits of KS-804 and KS-805 (see Table 3.5) well exceed the M_n calculated by ^1H NMR end group analysis of unfractionated poly(tetramethylene D-glucaramide) post-polymer. However, all of the ion peaks observed are produced in the low mass region ($<1500\text{m/z}$).

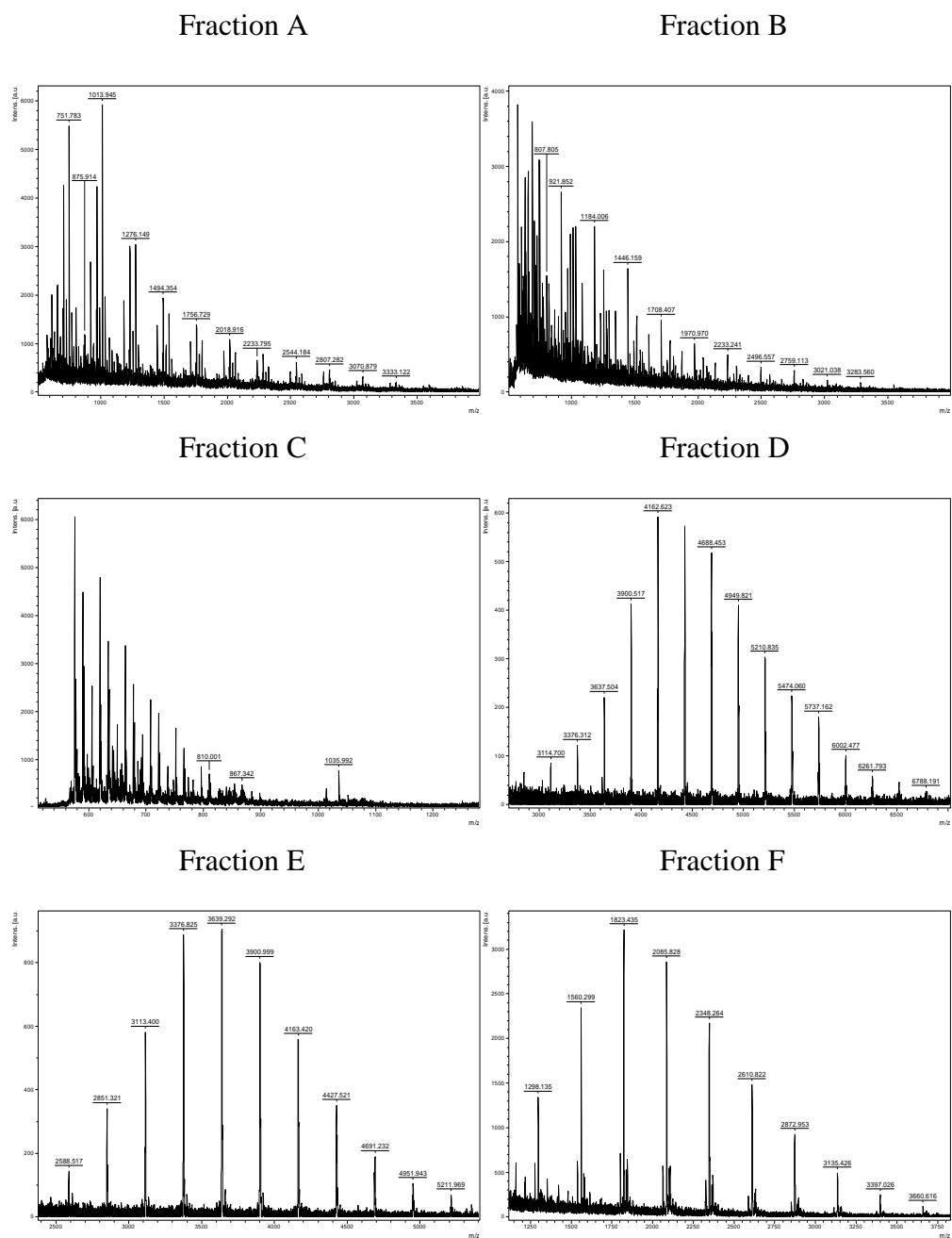


Figure 3.19: Mass Spectra of Poly(tetramethylene D-glucaramide) Post-polymer Fractions from SEC (see also Figure 3.18)

| Poly(tetramethylene D-glucaramide) Post-polymer | Laser Power |
|---|-------------|
| Unfractionated | 55% |
| Fraction A | 65% |
| Fraction B | 60% |
| Fraction C | 60% |
| Fraction D | 45% |
| Fraction E | 40% |
| Fraction F | 40% |

Table 3.16: MALDI-TOF Laser Power used to ionise the Poly(tetramethylene D-glucaramide) Post-polymer Fractions.

One of the possible explanations for the intense peaks produced around V_0 on these columns is that poly(tetramethylene D-glucaramide) post-polymer could contain ionised organic material (see also Section 3.4). If organic material was ionising in these fractions, then this suggests that these peaks should fly well in the MALDI. A consequence of this is that a relatively low laser power is required to produce an acceptable MALDI-TOF mass spectrum.

However, this scenario seems unlikely because the laser power used to produce ions for fractions A and B is much higher than one would expect if ionic material was present (Table 3.16). A more likely scenario is that the ions observed in the low mass region ($<1500m/z$) could be due to fragmentation of extremely high molecular weight poly(tetramethylene D-glucaramide) post-polymer. This is because the higher laser power needed to ionise these large polymer molecules could in fact be causing the polymer itself to fragment into smaller ions.

It should also be appreciated that, besides the issues associated with producing ions stated above, the spectrometer is only capable of detecting up to 1 million Daltons. However, this issue is not necessarily significant. This is because a review of the literature shows that there have been no reports of MALDI-TOF measurements of linear non-derivatised polysaccharides that have molecular weights exceeding 7000 Da [53, 54]. Note also that the conclusions drawn for fractions A and B can also be extended to fraction C.

The MALDI-TOF spectra of fractions D-F show a more polymer-like mass distribution (Table 3.17, D-F). The discrepancies observed for the unfractionated polymer sample are not observed for these fractions (see Section 3.3.3). The polydispersity of the mass distribution for fractions D and E are symmetrical and are found within the 3000 – 5000Da region (Figure 3.19, D & E); which is the expected molecular weight range for these fractions, based on the SEC results. The mass distribution of Peak F is slightly asymmetric, but not to the degree that was observed for the dextrans and for the unfractionated sample. The mass distribution for peak F was observed around the 1800Da region (Figure 3.19F).

Polytools™ M_n calculations for each of fractions D-F gave results that were very similar to that obtained from ^1H NMR end group analysis (see Table 3.17). The M_n for fraction 5 is similar to that calculated from the ^1H NMR end group analysis of the unfractionated poly(tetramethylene D-glucaramide) post-polymer. The M_n values of fractions 4 and 6 were, respectively, ~1000 greater and ~1700 less than the ^1H NMR end group analysis of the unfractionated polymer.

These results highlight the issues associated with utilising ^1H NMR end group analysis as a tool for determining molecular weight. This is because the SEC results (Table 3.15) for poly(tetramethylene D-glucaramide) post-polymer indicate >60% of the material has extremely high molecular weight fractions. This is further confirmed by the high laser power that was required to produce ions in the MALDI-TOF experiment (Table 3.16). However, the molecular weight, as calculated by end group analysis, is strongly biased toward the lower molecular weight fractions.

| Poly(tetramethylene D-glucaramide) Post-polymer | Polytools™ calculations from the MALDI-TOF spectrum | | | ¹ H NMR end group analysis M _n |
|---|---|----------------|----------------|--|
| | M _n | M _w | Polydispersity | |
| Unfractionated | 1518 | 1805 | 1.19 | 3591 |
| Fraction A | - | - | - | 15,000 |
| Fraction B | - | - | - | 8000 |
| Fraction C | - | - | - | 524 |
| Fraction D | 4575 | 4705 | 1.03 | 4512 |
| Fraction E | 3547 | 3691 | 1.04 | 3668 |
| Fraction F | 2082 | 2210 | 1.06 | 2059 |

* – M_n Calculated using THAP as the Matrix

** – M_n Calculated at Waikato University

Table 3.17: Polytools™ Calculations of M_n using Peak Height and Peak Integral and ¹H End Group Calculations of M_n for each Poly(tetramethylene D-glucaramide) Post-polymer Fraction.

3.6.1.4 NMR Spectroscopy

To confirm that fractions A and B are extremely higher molecular weight polymer fractions, NMR Spectroscopy can be utilised. Such a confirmation can be drawn from the fact that high molecular weight polymers with long chain lengths are more difficult to observe in the NMR than lower molecular weight material. This is due to the extended time that is needed for protons in higher molecular weight polymers to relax to thermal equilibrium. This has the effect of reducing the T_2 relaxation time which, in turn, makes the proton signals broader (because T_2 is inversely proportional to signal linewidth). Such a broadening of the signal can reach the point where the signals produced by some polymers are lost in the baseline.

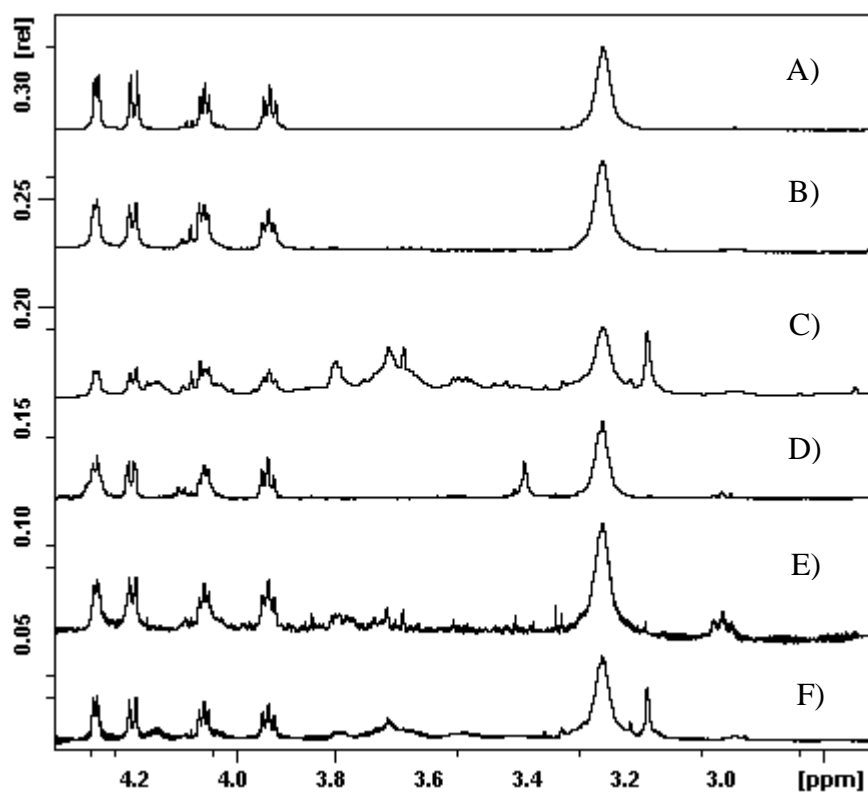


Figure 3.22

Figure 3.20: NMR of A) Fraction A 128 scans, B) Fraction B 129 scans, C) Fraction C 1000 scans, D) Fraction D 1000 scans, E) Fraction E 4000 scans and F) Fraction F 1000 scans.

This is the origin of the bias in the end-group analysis; the contribution to the internal methylene signal from very large molecules is so broadened that it has little effect on signal area, hence the sharper signals from smaller molecules make the largest contribution to this signal. Initial ^1H NMR analysis performed on each fraction showed that the resulting ^1H NMR spectra were all very similar. Furthermore, the resulting spectra was similar to that observed for the unfractionated poly(tetramethylene D-glucaramide) post-polymer (Figure 3.20).

Since polymer molecular chains are thermally active, elevation of temperature can cause the relaxation times to decrease. This should cause an increase in T_2 , thus allowing the proton signals in larger molecules to be observed hence increasing the spectrum resolution. A consequence of this is that the higher molecular weight polymers will have an increased contribution to the end-group analysis.

To test this assumption the experimental temperature was increased from room temperature (27°C) to 70°C . Note that this analysis is similar to the degradation experiments that were performed on the poly(tetramethylene D-glucaramide) post-polymer, which produced an increase of 2 DP (see Section 3.2). Figure 3.21 shows the effect that temperature has upon the DP calculations from the post-polymer ^1H spectrum. DP was observed to increase with elevated temperatures, with the highest DP of ~ 18 being detected at 70°C . This is well below what would be expected for fractions A and B. However, despite the increase in DP, raising the temperature increases the potential for hydrolysis of poly(tetramethylene D-glucaramide) post-polymer. Therefore, high temperature experiments have limited potential.

T_1 and T_2 relaxations times were determined for all of the fractionated peaks at room temperature, with the exception of fraction C and T_2 for fraction E. The reason for this is because the signal amplitude collected during the timeframe was negligible. Despite this, enough T_1 and T_2 measurements for the SEC peaks could be obtained to establish an observable trend (see Table 3.18).

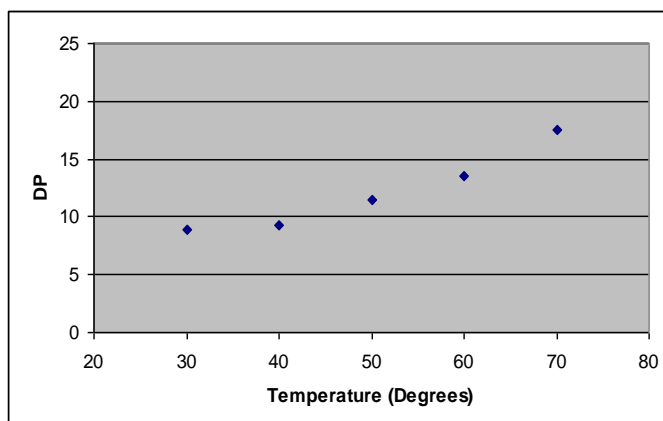


Figure 3.21: Effect upon DP calculated by End-group analysis of varying the temperature of the ^1H NMR experiment for unfractionated poly(tetramethylene D-glucaramide) post-polymer.

From these results it can be observed that the T_1 and T_2 relaxation rates for fractions A and B are significantly lower than that for fractions D-F. Taking into consideration the previous results observed for SEC, MALDI and ICP-MS, this result further suggests that fractions A and B are of extremely high molecular weight. These results are also similar to other polymer studies in which relaxation analysis was applied to polymers of known molecular weight [42].

It should be appreciated that ^1H NMR end group analysis is only applicable for polymers with molecular weights less than 20,000 [2, 8, 39]. The MALDI-TOF results for fractions D-F show that the M_n calculated for these fractions are well below this limit (see Table 3.17). Therefore, the ^1H NMR end group analysis is applicable to these fractions, with the resulting M_n calculated from this analysis being in agreement with the Polytools™ M_n calculated from the MALDI-TOF analysis.

| Poly(tetramethylene D-glucaramide) Post-polymer | T_1 Relaxation Rate (sec ⁻¹) | T_2 Relaxation Rate (sec ⁻¹) |
|---|--|--|
| Unfractionated | 1.290 | 160.83 |
| Fraction A | 1.155 | 147.69 |
| Fraction B | 1.158 | 144.74 |
| Fraction C | - | - |
| Fraction D | 1.312 | 173.80 |
| Fraction E | 1.356* | - |
| Fraction F | 1.513 | 200.45 |

* – T_1 Calculated Manually[41]

Table 3.18: T_1 and T_2 relaxation time measurements for each individual poly(tetramethylene D-glucaramide) post-polymer fraction.

3.6.1.5 Conclusions

The results obtained from the SEC (Section 3.6.1.2), MALDI-TOF (Section 3.6.1.3) and ¹H NMR relaxation measurements (Section 3.6.1.4) suggest that the fractions A and B observed around the V_0 region (Figure 3.18) is Poly(tetramethylene D-glucaramide) of extremely high molecular weights. Conservative use of the dextran calibration curve (see Section 3.4.3) shows that both peaks A and B have molecular weights that are well in excess of 100,000 (Fraction A ~1,000,000, Fraction B ~400,000). At these molecular weights, the use of ¹H NMR end group analysis and MALDI-TOF to determine the molecular weights for these fractions is not applicable. Conversely, fractions D–F have much lower molecular weights meaning both ¹H NMR end group analysis and MALDI-TOF are well suited to determine the molecular weights of these fractions. This is confirmed from the results of both analysis which show the calculated M_n values being in agreement (see Table 3.17).

Based on these results, an understanding of what is occurring in the MALDI-TOF for the un-fractionated Poly(tetramethylene D-glucaramide) post-polymer can be hypothesised. From the SEC results, it is observed that the majority of the unfractionated Poly(tetramethylene D-glucaramide) post-polymer is made up of fractions A and B. From this, it was concluded that fragmentation was occurring for these fractions in the MALDI-TOF (see Section 3.6.1.3). Therefore, the observed spectrum from the MALDI-TOF for the un-fractionated Poly(tetramethylene D-glucaramide) post-polymer is actually the fragmented remains of fractions A and B.

3.6.2 Poly(tetramethylene D-glucaramide) Pre-polymer

3.6.2.1 Introduction

Poly(tetramethylene D-glucaramide) pre-polymer is used in polymerisation to give the higher molecular weight post-polymer. Like poly(tetramethylene D-glucaramide) post-polymer, poly(tetramethylene D-glucaramide) pre-polymer is a C4 poly(alkylene D-glucaramide). The repeating unit structure of poly(tetramethylene D-glucaramide) pre-polymer (Figure 3.22) also has the same repeating unit structure as poly(tetramethylene D-glucaramide) post-polymer (Figure 3.17). M_n calculated by ^1H NMR end group analysis for the poly(tetramethylene D-glucaramide) pre-polymer at UoW were very similar to that calculated at UoM (Table 3.13).

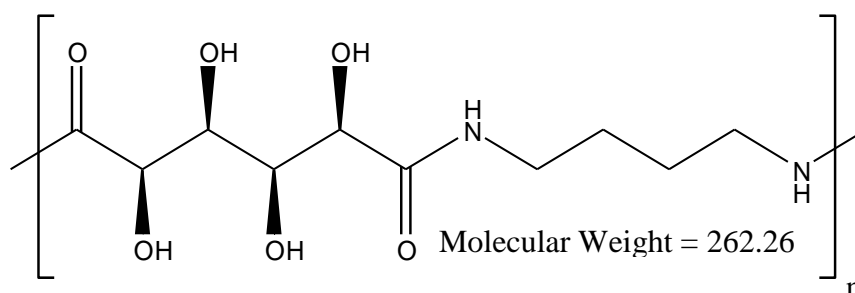


Figure 3.22: Structure of the Poly(tetramethylene D-glucaramide) pre-polymer repeating unit

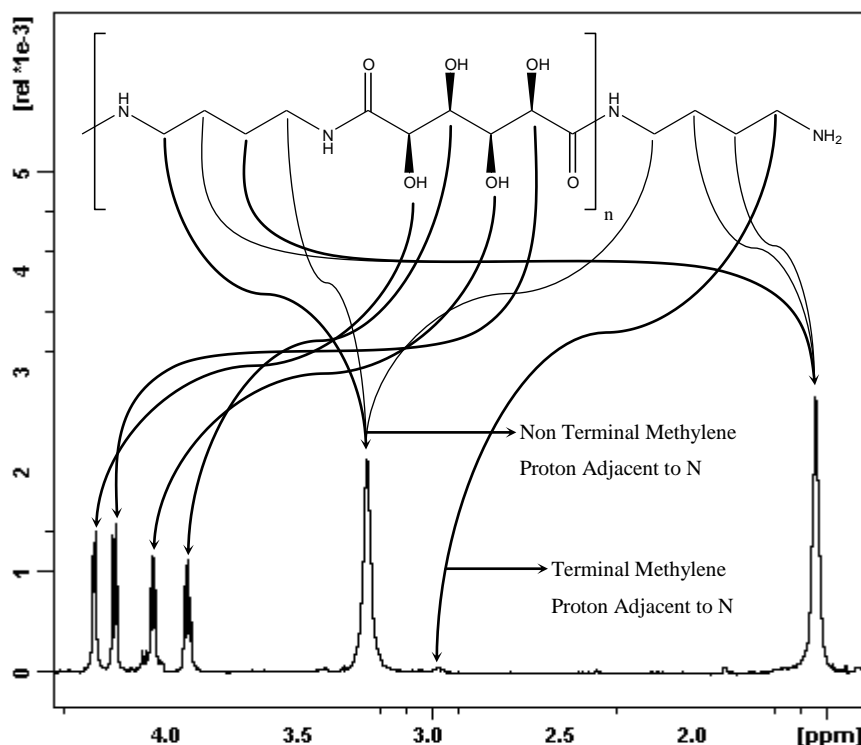


Figure 3.23: Fully Labeled ^1H NMR Spectrum of Poly(tetramethylene D-glucaramide) Pre-polymer

3.6.2.2 Fractionation by SEC

The resulting SEC chromatogram detected for the pre-polymer (Figure 3.24) is quite different to that observed for the post-polymer (Figure 3.18). However, the retention times of the four peaks detected for the pre-polymer are very similar to that detected for the post-polymer. In the poly(tetramethylene D-glucaramide) pre-polymer SEC spectra, it can be observed that there are four prominent peaks. Note also that there are less resolved peaks that are detected between the retention times 18-22.5 minute. Due to the peak amplitudes in this region being small, this whole region was again collected as one fraction. Assuming that the refractive index responses are all approximately equal, the majority of poly(tetramethylene D-glucaramide) pre-polymer is made up of Peaks A and B (~72%). This proportion is significantly higher compared to what was observed for the post-polymer (~60%, see also Table 3.15).

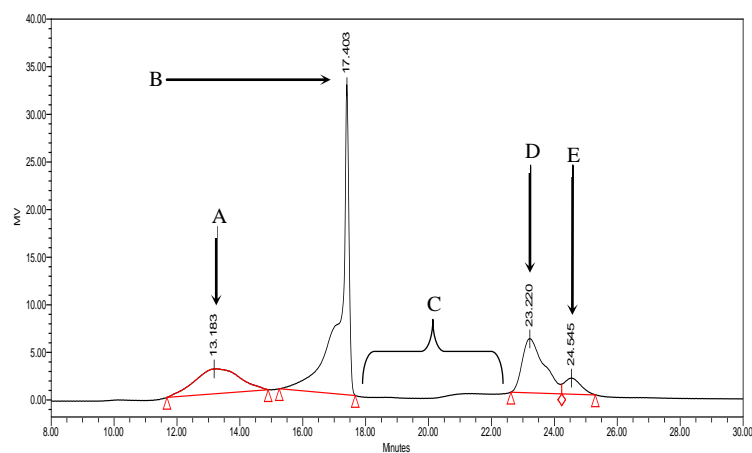


Figure 3.24 : SEC Chromatogram of Poly(tetramethylene D-glucaramide) Pre-polymer on columns KS-804.

| Fraction | Retention Time (mins) | Area | Area (%) |
|----------|-----------------------|--------|----------|
| A | 13.183 | 259736 | 20.83 |
| B | 17.403 | 633989 | 50.85 |
| C | 18.000 – 22.500 | 15804 | 1.27 |
| D | 23.220 | 275689 | 22.11 |
| E | 24.545 | 61543 | 4.94 |

Table 3.19: Integrated areas of labelled peaks in SEC chromatogram of unfractionated poly(tetramethylene-D-glucaramide Pre-polymer on KS-804 and 805 SEC columns in series.

3.6.2.3 MALDI-TOF of Fractions

The results from the MALDI-TOF gave varying information about the molecular weights of each of the polymer fractions. The MALDI mass spectra for fractions A and B (Figure 3.25, A & B) are very similar to the results obtained for poly(tetramethylene D-glucaramide) post-polymer (Figure 3.19, A & B). Conclusions drawn from the study of the poly(tetramethylene D-glucaramide) post-polymer fractions were that these fractions are high molecular weight polymers that are fragmenting in the MALDI. Due to the similar spectra, these same conclusions can be extended to the corresponding fractions for the pre-polymer (see Section 3.6.1). Furthermore, the conclusions drawn above for fractions A and B can also be extended to the mass spectra observed for fraction C.

The mass spectra for fractions D and E produced polymer-like mass distributions. The PolytoolsTM M_n calculation for these fractions gave results that were similar to ^1H NMR end group analysis. Of the fractions end group analysis of the unfractionated material gave a result smaller than either of these fractions.

| Poly(tetramethylene D-glucaramide) Post-polymer | Laser Power |
|--|-------------|
| Unfractionated | 55% |
| Fraction A | 65% |
| Fraction B | 60% |
| Fraction C | 60% |
| Fraction D | 45% |
| Fraction E | 40% |

Table 3.20: MALDI-TOF Laser Power used to ionise Poly(tetramethylene D-glucaramide) Pre-polymer Fractions.

| Poly(tetramethylene D-glucaramide) Pre-polymer | Polytools™ calculations from the MALDI-TOF spectrum | | | ¹ H NMR end group analysis M_n |
|--|---|-------|----------------|---|
| | M_n | M_w | Polydispersity | |
| Un-fractionated | 1735 | 1924 | 1.11 | 2438 |
| Peak A | - | - | - | 7958 |
| Peak B | - | - | - | 3564 |
| Peak C | 1407 | 1523 | 1.08 | 2000 |
| Peak D | 3688 | 3801 | 1.03 | 3646 |
| Peak E | 2904 | 3009 | 1.04 | 2925 |

Table 3.21: Polytools™ Calculations of M_n using Peak Height and Peak Integral and ¹H End Group Calculations of M_n for each Poly(tetramethylene D-glucaramide) Pre-polymer Fraction.

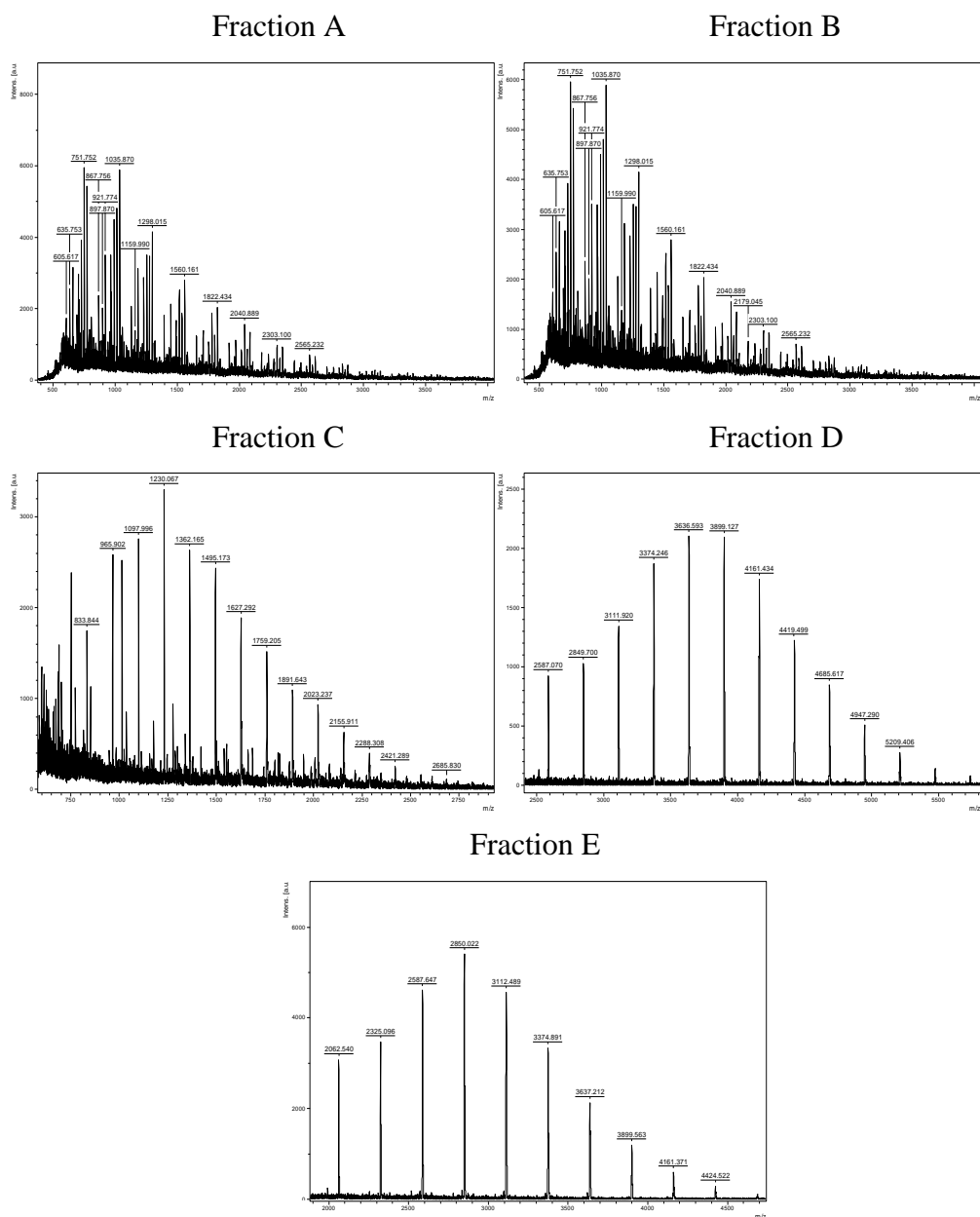


Figure 3.25: Mass Spectra of Poly(tetramethylene D-glucaramide) Pre-polymer Fractions from SEC (see also Figure 3.24)

3.6.2.4 NMR Spectroscopy

Initial ^1H NMR analysis performed on each of the fractions showed that the resulting spectra are very similar to that are for the un-fractionated poly(tetramethylene D-glucaramide) pre-polymer (Figure 3.26). Moreover, the ^1H NMR for each fraction is very similar to poly(tetramethylene D-glucaramide) post-polymer. For fractions D and E, there observed traces of smaller non polymer organic material (Figure 3.26 D and E). However, these traces are small and consequently do not influence the resulting spectrum significantly.

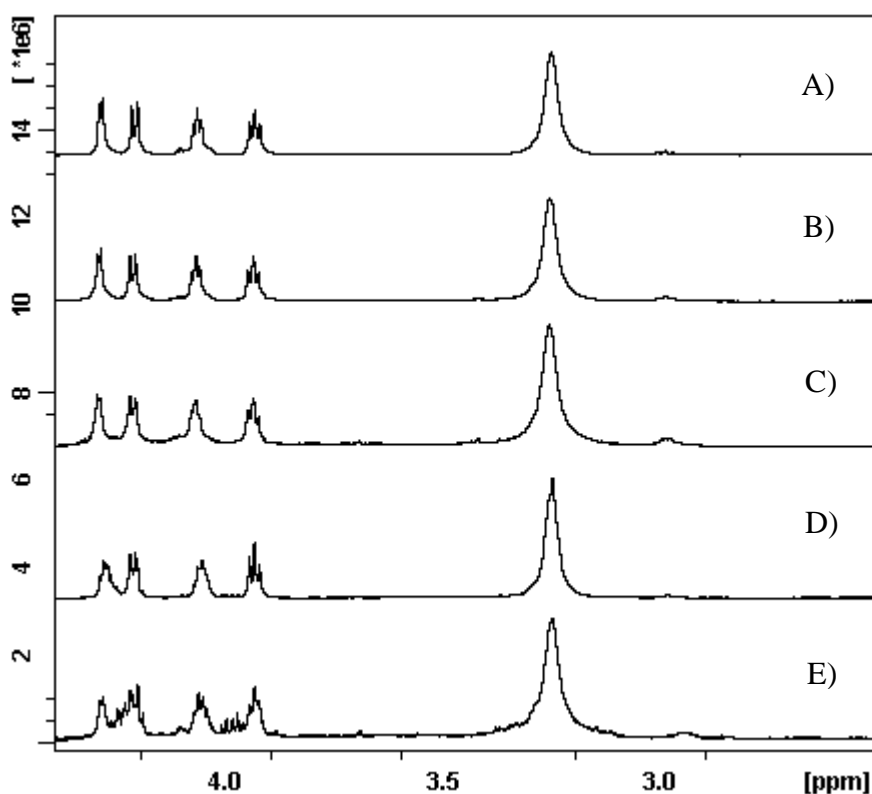


Figure 3.26: NMR of A) Fraction A 1000 scans, B) Fraction B 1000 scans, C) Fraction C 2000 scans, D) Fraction D 1000 scans and E) Fraction E 1500 scans

3.6.2.5 Conclusions

Previous work on fractions collected in the V_0 region in the SEC for Poly(tetramethylene D-glucaramide) post-polymer showed that these fractions are extremely high molecular weight polymers. These same conclusion are extended to fractions A-B for Poly(tetramethylene D-glucaramide) pre-polymer. Conservative use of the dextran calibration curve (see Section 3.4.3) for fractions A it shows that the molecular weight is around 1,000,000, with fraction B having a molecular weight around 200,000.

With the majority of the unfractionated poly poly(tetramethylene D-glucaramide) pre-polymer sample being comprised of high molecular weight polymers the same conclusion that was suggested for unfractionated poly(tetramethylene D-glucaramide) post-polymer can be used to describe what is occurring for unfractionated poly(tetramethylene D-glucaramide) pre-polymer during MALDI-TOF spectrometry (see Section 3.6.1.5).

3.6.3 Poly(3',6'-dioxaoctamethylene D-glucaramide) Pre-polymer

3.6.3.1 Introduction

Poly(3',6'-dioxaoctamethylene D-glucaramide) pre-polymer differs to that of other PHPA samples polymer because it is a poly (oxaalkylene aldaramide), not a poly (alkylene aldaramide) (Figure 3.27).

The M_n calculated by ^1H NMR end group analysis for the poly(3',6'-dioxaoctamethylene D-glucaramide) pre-polymer at UoW was very similar to that calculated at UoM (Table 3.13). A structural advantage of poly(3',6'-dioxaoctamethylene D-glucaramide) pre-polymer is that its comprised of 3',6'-dioxaocta groups (Figure 3.27). The presence of these groups within the structure provides more regions for poly(3',6'-dioxaoctamethylene D-glucaramide) pre-polymer to be ionised in the MALDI-TOF relative to the other PHPA samples. Consequently, it was expected that this pre-polymer would ionise more readily because of these extra oxygens to ionise in the MALDI compare to the other PHPA samples.

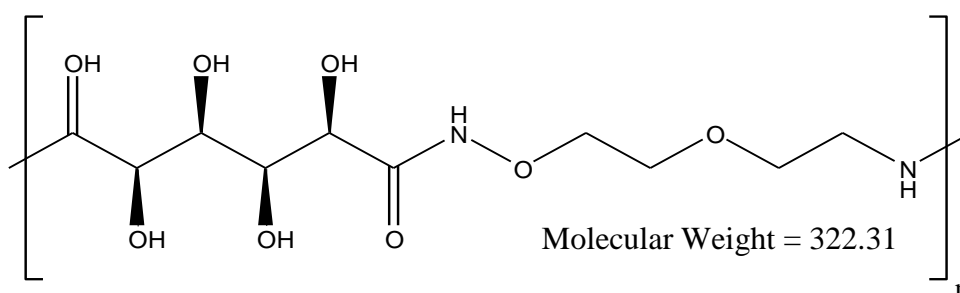


Figure 3.27: Structure of the Poly(3',6'-dioxaoctamethylene D-glucaramide) Pre-polymer repeating unit.

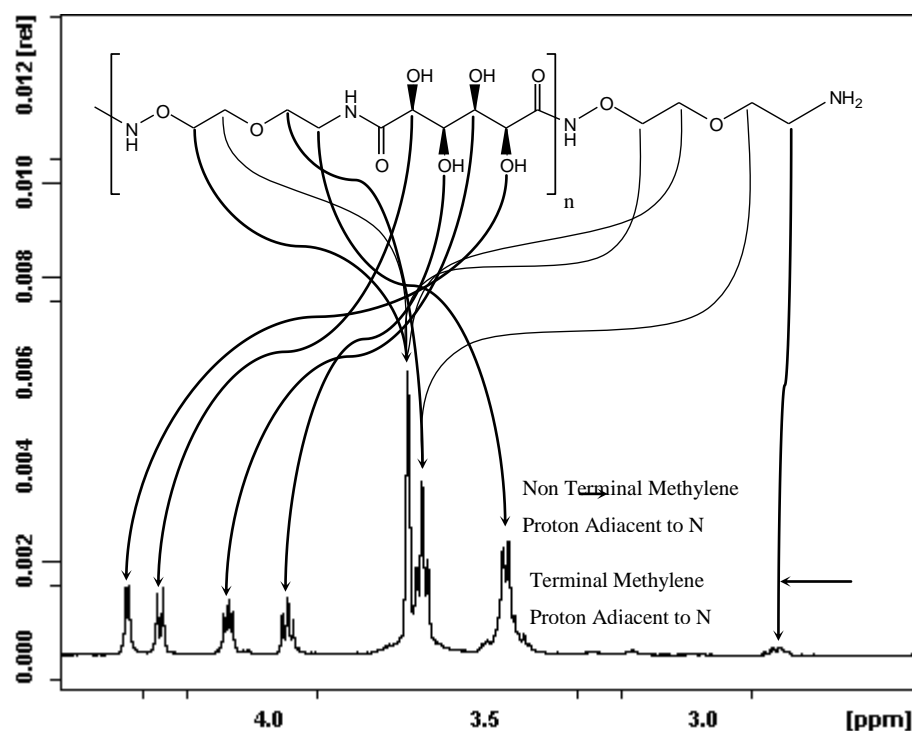


Figure 3.28: Fully Labelled ^1H NMR Spectrum of Poly(3',6'-dioxaoctamethylene D-glucaramide) Pre-polymer.

3.6.3.2 Fractionation by SEC

From the resulting SEC chromatogram, six major peaks of interest were resolved (Figure 3.20). A seventh, albeit less resolved, peak was also detected between the retention times of 19-22.5 minutes. From the chromatogram, the predominant peak observed is Peak B which is observed around the V_0 region. Assuming that the refractive index responses are all approximately equal, the proportional peak areas show that peak B comprises the majority (~53%) of the unfractionated poly(3',6'-dioxaoctamethylene D-glucaramide) pre-polymer sample (Table 3.22). Note also that, similar to the poly(tetramethylene D-glucaramide) pre- and post-polymer (see Sections 3.6.1.2 & 3.6.2.2), the majority (~59%) of the unfractionated poly(3',6'-dioxaoctamethylene D-glucaramide) pre-polymer sample is comprised of the peaks that are in the V_0 region.

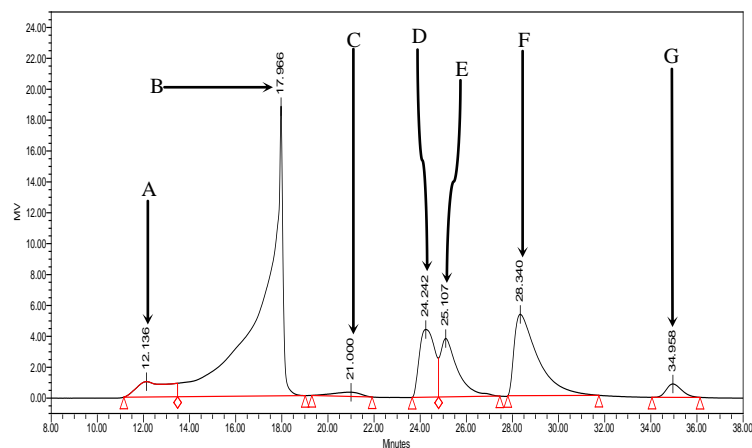


Figure 3.29: SEC Chromatogram of Poly(3',6'-dioxaoctamethylene D-glucaramide) Pre-polymer on columns KS-804 and KS-805 in series.

| Fraction | Retention Time (mins) | Area | Area (%) |
|----------|-----------------------|--------|----------|
| A | 12.136 | 98884 | 5.76 |
| B | 17.966 | 908585 | 52.91 |
| C | 21.000 | 1730 | 1.03 |
| D | 24.242 | 166874 | 9.72 |
| E | 25.107 | 182217 | 10.61 |
| F | 28.340 | 312860 | 18.22 |
| G | 34.958 | 30320 | 1.77 |

Table 3.22: Integrated Areas of labelled peaks in SEC chromatogram of unfractionated Poly(3',6'-dioxaoctamethylene D-glucaramide) Pre-polymer on KS-804 and 805 SEC columns in series.

3.6.3.3 MALDI-TOF of Fractions

From the results of the MALDI-TOF performed, a series of ions separated by the repeating unit mass was obtained for each of the seven fractions. These results are markedly different to that observed for the other PHPA samples, particularly for fractions collected around the V_0 region. For other PHPA fractions collected in this region, the MALDI mass spectra for these fractions a polymer like distribution is not obtained.

Fractions A and B for poly(3',6'-dioxaoctamethylene D-glucaramide) pre-polymer, a polymer-like mass distribution was detected (Figure 3.30A & B). Comparing the calculated PolytoolsTM M_n (Table 3.24) to both the region these fractions were collected in the SEC (Figure 3.29) together with the laser power used to ionise these fractions (Table 3.23), this suggests that the mass spectra for these fractions is due to fragmentation (see also previous results and conclusions from Section 3.6.1). These same conclusions for fractions A and B can be extended to fraction C.

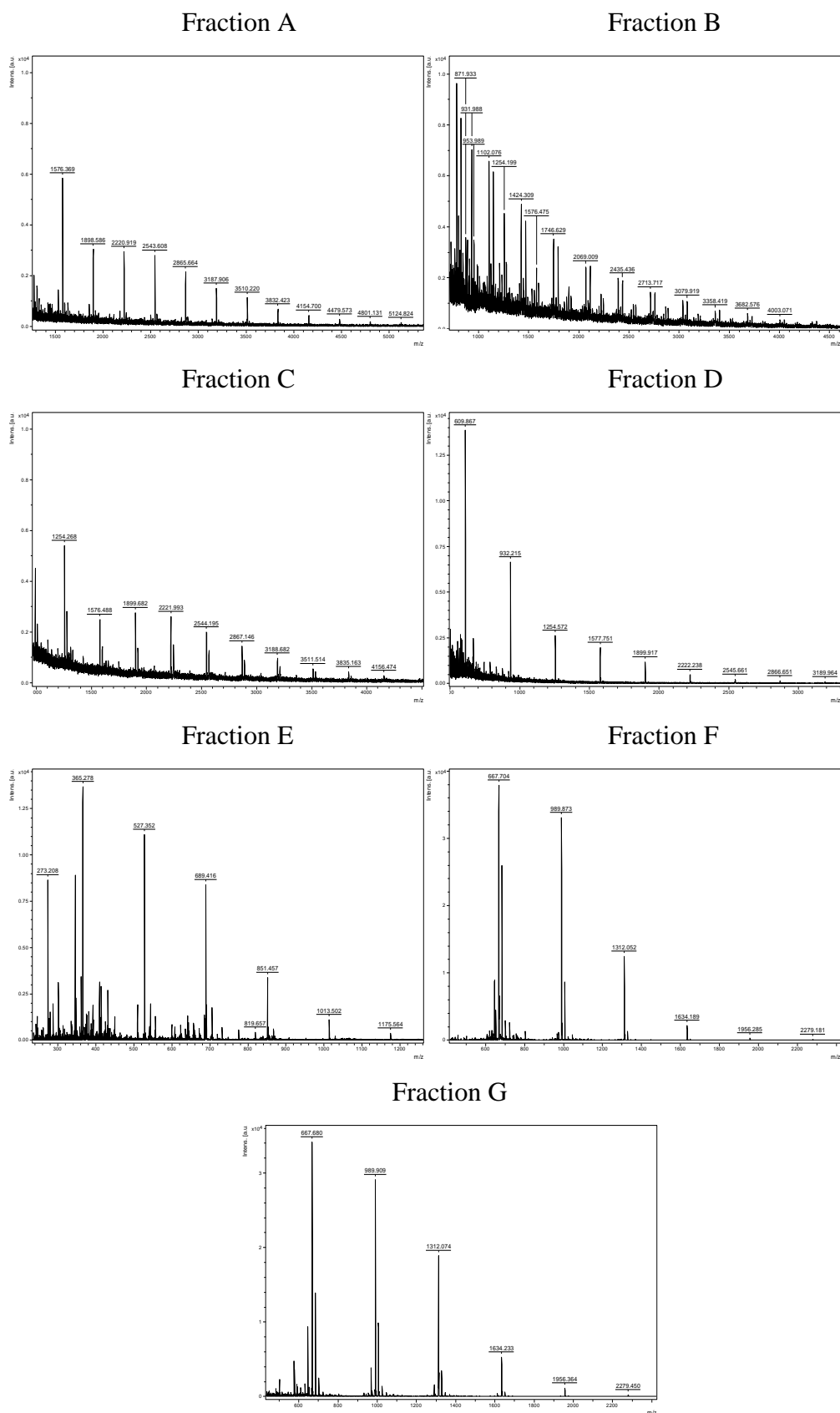


Figure 3.30: Mass Spectra of Poly(3',6'-dioxaoctamethylene D-glucaramide) Pre-polymer Fractions from SEC (see Figure 3.29).

| Poly(3',6'-dioxaoctamethylene D-glucaramide) Post-polymer | Laser Power |
|---|-------------|
| unfractionated | 52.5% |
| Fraction A | 62.5% |
| Fraction B | 65% |
| Fraction C | 60% |
| Fraction D | 50% |
| Fraction E | 50% |
| Fraction F | 45% |
| Fraction G | 40% |

Table 3.23: MALDI-TOF Laser Power used to Ionise Poly(3',6'-dioxaoctamethylene D-glucaramide) Post-polymer Fractions.

Observations from the MALDI-TOF spectra of fractions D and E showed a series of ions separated by the repeating unit mass was obtained for each. Note that only a moderate laser power was required to ionise these fractions (Table 3.23), however, the laser power used may still be sufficient to cause polymer fragmentation. Despite this, high molecular weight fractions are not expected for these fractions because of the region they were collected in the SEC (from 24-26mins). Comparing the calculated M_n from PolytoolsTM and ¹H NMR end-group analysis for both fractions D and E shows that the calculated M_n differ by ~3000 (Table 3.24). Based on the SEC results, the M_n calculated from ¹H NMR end-group analysis for these fractions is the more expected molecular weight range. Moreover, the M_n calculated by ¹H NMR end-group analysis for these fractions is similar in magnitude to that calculated for unfractionated poly(3',6'-dioxaoctamethylene D-glucaramide) post-polymer (Table 3.24).

However it should be appreciated that these results for fractions D and E could be also due to polydispersity effects. If fractions D and E have a polydispersity greater than 1.2 it is well known that this would cause their respective mass distribution to be skewed towards the lower mass region. As previously mentioned polymer peaks at polydispersity >1.2 , there are a number of factors which contribute to this affect (see Section 1.4.2). This however is probably not the cause of the mass distributions observed in fractions D and E as the two fractions overlapped each other and both peaks are not that broad (Figure 3.29).

The MALDI-TOF spectra of fractions F and G produced mass distributions that was truncated in the low mass regions. Comparison of the Polytools M_n for fractions F and G to that obtained by ^1H NMR end group analysis (Table 3.24) shows that both values are in agreement. Therefore, despite the discrepancies observed for each fraction's MALDI mass distribution, these discrepancies have little influence on the Polytools M_n calculation.

An explanation for this could be that because the M_n for each fraction is so low, the mass distribution that would be obtained for these fractions in the MALDI will be observed in the low mass region. This is where sDHB (located around 350Da) matrix signals are well known to be found. A consequence of this is that some of the mass distributions for these fractions will be cut off by the threshold used to remove matrix signals the matrix signals.

| Poly(3',6'-dioxaoctamethylene D-glucaramide) Post-polymer | Polytools™ calculations from the MALDI-TOF spectrum | | | ¹ H NMR end group analysis M_n |
|---|---|-------|----------------|---|
| | M_n | M_w | Polydispersity | |
| Unfractionated | 831 | 897 | 1.08 | 2801 |
| Fraction A | 2129 | 2390 | 1.12 | 2502 |
| Fraction B | - | - | - | 2987 |
| Fraction C | 2063 | 2355 | 1.14 | 805 |
| Fraction D | 942 | 1177 | 1.25 | 4005 |
| Fraction E | 510 | 646 | 1.13 | 3719 |
| Fraction F | 987 | 1091 | 1.10 | 986 |
| Fraction G | 916 | 994 | 1.08 | 598 |

Table 3.24: Polytools™ Calculations of M_n using Peak Height and Peak Integral and ¹H End Group Calculations of M_n for each Poly(3',6'-dioxaoctamethylene D-glucaramide) Pre-polymer Fraction.

3.6.3.4 NMR Spectroscopy

Initial ^1H NMR analysis performed on each fraction, showed that the resulting spectra for fractions A-E are very similar to that observed for the un-fractionated poly(3',6'-dioxaoctamethylene D-glucaramide) post-polymer (Figure 3.28).

For fractions F and G, weak signals corresponding to poly(3',6'-dioxaoctamethylene D-glucaramide) pre-polymer were present in the ^1H NMR (Figure 3.31, F & G). However, the MALDI results for these fractions show the presence of a polymer. The possible origin of these signals could be due to smaller organic mass material that are used in the synthesis of poly(3',6'-dioxaoctamethylene D-glucaramide) pre-polymer which is still present after completion of synthesis.

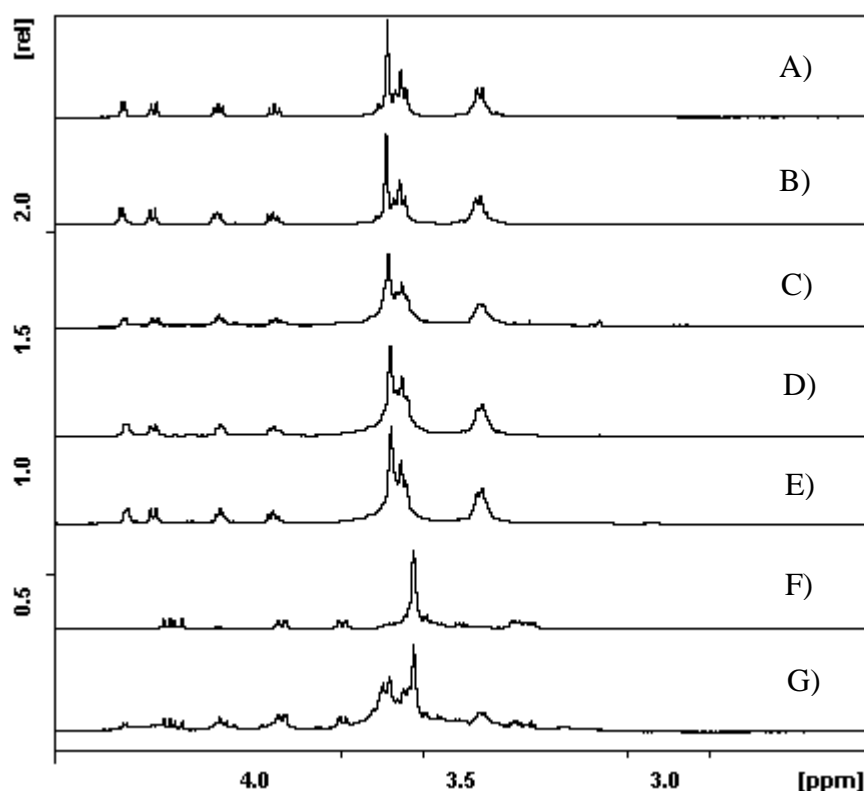


Figure 3.31: NMR of A) Fraction A 500 scans, B) Fraction B 500 scans, C) Fraction C 4500 scans, D) Fraction D 1000 scans, E) Fraction E 1000 scans F) Fraction F 500 scans and Fraction G 10 000 scans.

Lower molecular weight peaks are resolved in the chromatograms on KS-801 and 802 (Figure 3.1) However, with the higher exclusion limit columns of KS-804 and KS-805, which are used in series to collect each fraction, these peaks are no longer resolved into separate peaks (Figure 3.29). Therefore, when fractions F and G are collected, smaller mass material is also collected together with the polymer of interest, hence explaining the extraneous material visible in the ^1H NMR.

Coupling the results from both the ^1H NMR and SEC chromatograms of columns KS-801 and KS-802 for these fractions an understanding of the possible composition of these fractions can be understood. Both results suggest that there are more smaller non polymer organic material in these fractions and in the poly(3',6'-dioxaoctamethylene D-glucaramide) pre-polymer itself.

| Poly(3',6'-dioxaoctamethylene D-glucaramide) pre-polymer | T_2 Relaxation Rate (sec^{-1}) |
|--|---|
| Unfractionated | 209.00 |
| Fraction A | 191.8 |
| Fraction B | 194.7 |
| Fraction C | 209.1 |
| Fraction D | 219.4 |
| Fraction E | 227.8 |
| Fraction F | - |
| Fraction G | - |

Table 3.25: T_1 and T_2 relaxation time measurements for each individual poly(3',6'-dioxaoctamethylene D-glucaramide) pre-polymer fraction.

The T_2 relaxation times were determined for all of the fractionated peaks, excepts for fractions F and G which produced negligible signal amplitude during the collection timeframe. Despite this, Table 3.25 shows that the other T_2 measurements for the SEC peaks establish an observable trend. The T_2 relaxation rate results for these fractions are very similar to those results obtained for poly(tetramethylene D-glucaramide) post-polymer (Section 3.6.1.4). Moreover, the relaxation rates for poly(3',6'-dioxaoctamethylene D-glucaramide) pre-polymer are in agreement with results from previous polymer studies [42]. From these studies, it was concluded from the T_2 relaxation rates calculated for Poly(tetramethylene D-glucaramide) post-polymer that the peaks observed around the V_0 region were due to extremely high molecular weight polymers. The resulting T_2 relaxation rates for poly(3',6'-dioxaoctamethylene D-glucaramide) pre-polymer adds weight to this argument for fractions collected near V_0 .

3.6.3.5 Conclusions

Combining the results obtained from the SEC, MALDI-TOF and ^1H NMR relaxation measurements for fractions A and B strongly suggests that these fractions are indeed poly(3',6'-dioxaoctamethylene D-glucaramide) post-polymer of extremely high molecular weights. Conservative use of the dextran calibration curve (see Section 3.4.3) for fractions A shows that the molecular weight is in excess of 2,000,000, with fraction B having a molecular weight around 70,000.

With regards to Fractions D and F, accurately determining the molecular weights of these fractions using MALDI is not possible. This is because fragmentation is occurring due to the moderate laser power used to ionise these fractions. However, based on the region that these fractions were collected in the SEC, the ^1H NMR end-group analysis of the fractions gives accurate estimate M_n .

For Fractions F and G, comparison of the M_n values calculated via ^1H NMR end group analysis and MALDI-TOF shows that the weights are in agreement. However, results from the ^1H NMR for these fractions suggest that the in-series

column setup of KS-804 and KS-805 is not appropriate for collecting fractions of poly(3',6'-dioxaoctamethylene D-glucaramide) pre-polymer that have small molecular weights (i.e., <1000). This is because signals from smaller non polymer organic material could still be present in the unfractionated sample of poly(3',6'-dioxaoctamethylene D-glucaramide) post-polymer from synthesis. These results provide a preliminary understanding of the fraction's composition. For both fractions F and G, results from the SEC Chromatograms of columns KS-801 and KS-802 and ¹H NMR suggest that smaller non polymer organic material comprises the majority of the fractions. However, in order to determine more accurately the relative composition of smaller non polymer organic material to that of the smaller molecular weight poly(3',6'-dioxaoctamethylene D-glucaramide) pre-polymer fraction, fractionation of the unfractionated poly(3',6'-dioxaoctamethylene D-glucaramide) pre-polymer sample should be undertaken on columns KS-801 and KS-802.

With the majority of the unfractionated poly(3',6'-dioxaoctamethylene D-glucaramide) pre-polymer sample being comprised of high molecular weight polymers, this suggests that fragmentation was occurring for these fractions (A & B) in the MALDI-TOF. Consequently, observations from the MALDI-TOF for other unfractionated poly(3',6'-dioxaoctamethylene D-glucaramide) pre-polymer could be due to the fragmented remains of the high molecular weight fragments described above.

3.6.4 Poly(ethylene D-glucaramide) Post-polymer

3.6.4.1 Introduction

The smallest of the poly(alkylene D-glucaramide), poly(ethylene D-glucaramide) post-polymer, is a C2 poly D-glucaramides (Figure 3.32). The M_n calculated by ^1H NMR end group analysis for the poly(ethylene D-glucaramide) post-polymer at UoW was very similar to that calculated at UoM (Table 3.13).

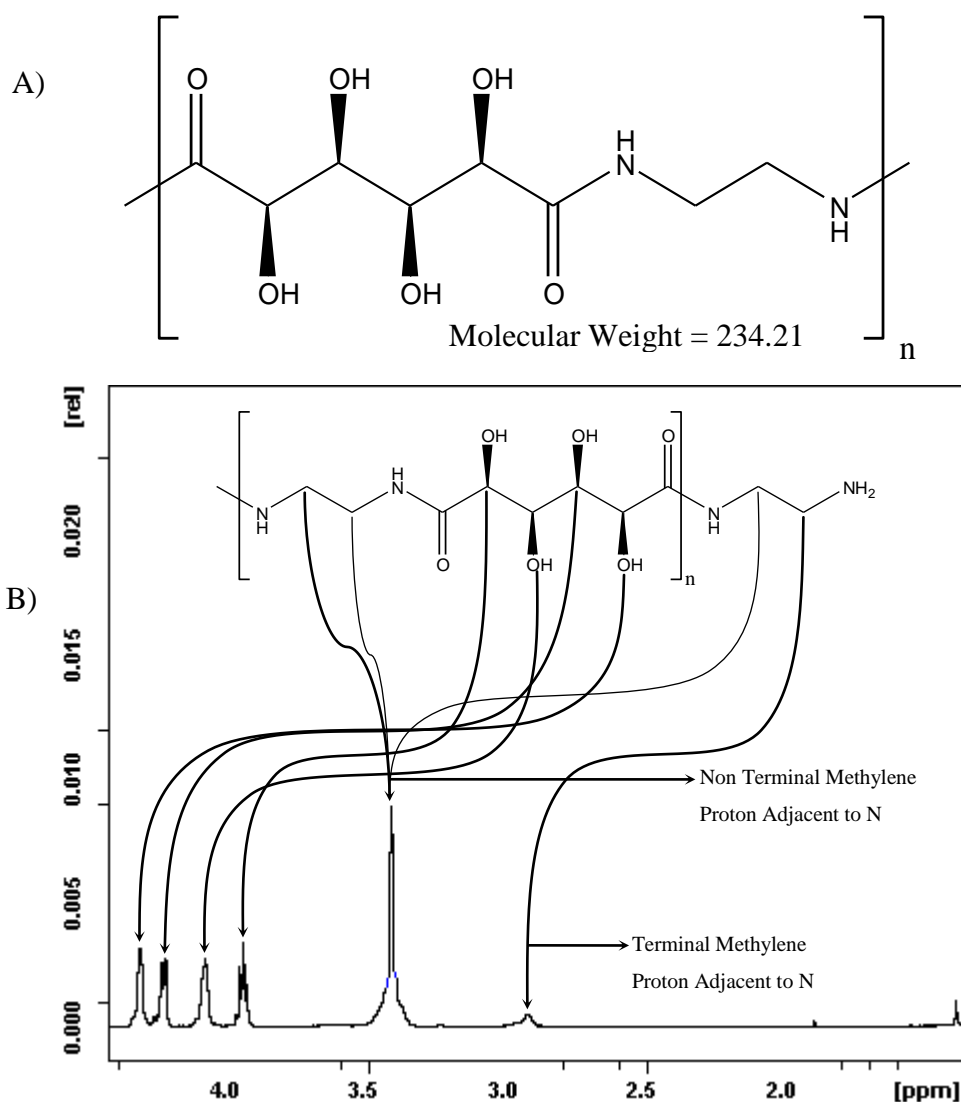


Figure 3.32: A) Structure of the Poly(ethylene D-glucaramide) post-polymer repeating unit. B) Fully Labeled ^1H NMR Spectrum of Poly(ethylene D-glucaramide) Post-polymer.

3.6.4.2 Fractionation by SEC

From the resulting SEC chromatogram, six major peaks were resolved (Figure 3.33). Note that the chromatogram detected for poly(ethylene D-glucaramide) post-polymer is similar to that for the poly(tetramethylene D-glucaramide) post- and pre-polymers (Figure 3.18 and Figure 3.24). The two predominant peaks in the chromatogram, Peaks A and B, are observed around the V_0 region. Assuming that the refractive index responses are all approximately equal, the percentage peak areas for these fractions comprise the majority (~62%) of the unfractionated poly(ethylene D-glucaramide) post-polymer sample (Table 3.26). Previous results have shown that these peaks are likely to correspond to extremely high molecular weight polymers (see Section 3.6.1).

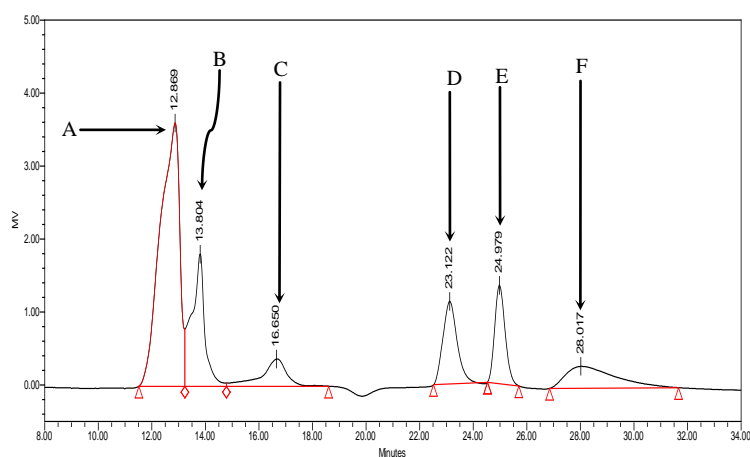


Figure 3.33: SEC Chromatogram of Poly(ethylene D-glucaramide) Post-polymer on columns KS-804 and KS-805 in series.

| Fraction | Retention Time (mins) | Area | Area (%) |
|----------|-----------------------|--------|----------|
| A | 12.869 | 184066 | 46.05 |
| B | 13.804 | 64053 | 16.03 |
| C | 16.650 | 32187 | 8.05 |
| D | 23.122 | 40372 | 10.10 |
| E | 24.979 | 37192 | 9.30 |
| F | 28.017 | 41828 | 10.46 |

Table 3.26: Integrated Areas of labelled peaks in SEC chromatogram of unfractionated Poly(ethylene D-glucaramide) Post-polymer on KS-804 and 805 SEC columns in series.

3.6.4.3 MALDI-TOF of Fractions

Similar to the results obtained for the other D-glucaramide PHPA's, only the lower molecular weight poly(ethylene D-glucaramide) post-polymer fractions produced satisfactory MALDI-TOF results that could be used for M_n calculation. From the other PHPA studies (see Section 3.6.1 and 3.6.3) it was demonstrated that the fractions collected around the V_0 region in the SEC are likely to be extremely high molecular weight fractions. Therefore, similar conclusions can be extended to the mass spectra of fractions A-C for poly(ethylene D-glucaramide) post-polymer.

The MALDI-TOF spectra of fraction D show a series of ions separated by the repeating unit mass which is skewed to the lower mass region (Figure 3.34). The observed MALDI mass spectra, and the laser power used to ionise this fraction (Table 3.27) are very similar to that used for fractions D-E of poly(3',6'-dioxaoctamethylene D-glucaramide) pre-polymer (see Section 3.6.3.4). Consequently, similar conclusions made for fractions D-E MALDI mass spectra for poly(3',6'-dioxaoctamethylene D-glucaramide) pre-polymer can be extended to the MALDI mass spectra observed for this fraction.

For fraction E, the M_n calculated from ^1H NMR end-group analysis is within the expected molecular weight range, based on the SEC results. Furthermore, the M_n calculated by ^1H NMR end-group analysis for fraction E is similar in magnitude to that calculated for unfractionated poly(ethylene D-glucaramide) post-polymer via ^1H NMR end-group analysis (Table 3.28).

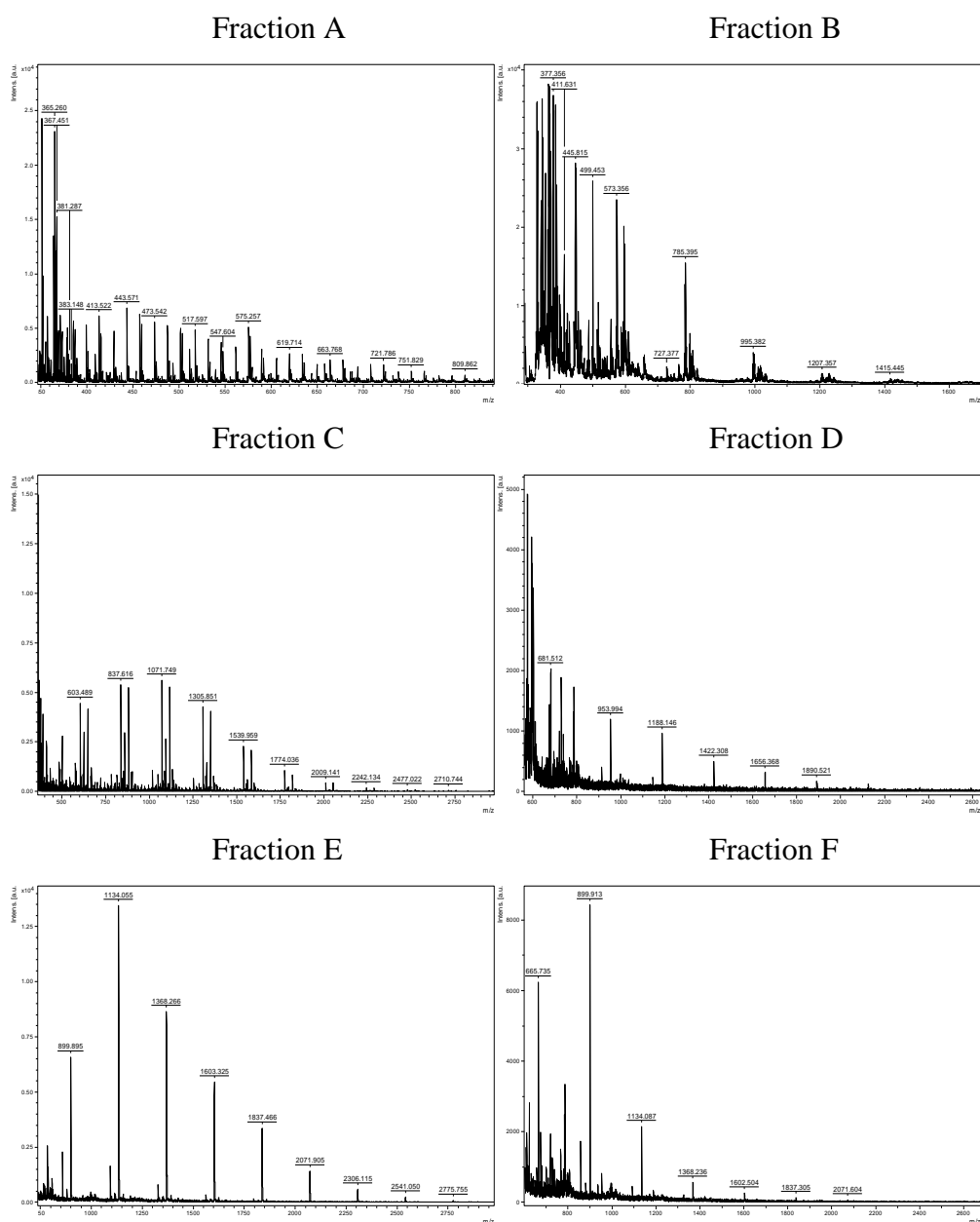


Figure 3.34: Mass Spectra of Poly(ethylene D-glucaramide) Post-polymer Fractions from SEC (see Figure Figure 3.33).

The resulting MALDI-TOF spectrum for fraction E produced a similar mass distribution to that observed for unfractionated poly(ethylene D-glucaramide) post-polymer (Figure 3.9D) with the detected mass distribution being asymmetric and well displaced towards the low mass region. The value for M_n calculated from the MALDI spectrum was similar to the value given by ^1H NMR end group analysis (Table 3.28), it can be observed that the values for each fraction are in agreement. Therefore, despite the discrepancies observed in the MALDI mass distribution for fraction E, these discrepancies have little influence on the Polytools M_n calculation.

The mass distribution produced for fraction F was truncated in the low mass regions with greater asymmetry than fraction E. The PolytoolsTM M_n calculation was able to be obtained for this fraction (see Table 3.28). Note that this M_n value could not be compared to that calculated via ^1H NMR end-group analysis as calculation by via this analysis could not be achieved (see Section 0 below for further explanation).

| Poly(ethylene D-glucaramide) Post-polymer | Laser Power |
|---|-------------|
| Unfractionated | 57.5% |
| Fraction A | 62.5% |
| Fraction B | 60% |
| Fraction C | 57.5% |
| Fraction D | 55% |
| Fraction E | 45% |
| Fraction F | 42.5% |

Table 3.27: MALDI-TOF Laser Power used to Ionise Poly(ethylene D-glucaramide)Post-polymer Fractions.

| Poly(ethylene D-glucaramide) post-polymer | Polytools™ calculations from the MALDI-TOF spectrum | | | ¹ H NMR end group analysis M _n |
|--|--|----------------|----------------|---|
| | M _n | M _w | Polydispersity | |
| Unfractionated | 986 | 1134 | 1.15 | 1620 |
| Fraction A | - | - | - | 558 |
| Fraction B | - | - | - | - |
| Fraction C | 1085 | 1221 | 1.12 | 506 |
| Fraction D | 1270 | 1365 | 1.08 | 4446 |
| Fraction E | 1132 | 1424 | 1.07 | 1404 |
| Fraction F | 881 | 938 | 1.06 | - |

Table 3.28: Polytools™ Calculations of M_n using Peak Height and Peak Integral and ¹H End Group Calculations of M_n for each Poly(ethylene D-glucaramide) Post-polymer Fraction.

3.6.4.4 NMR Spectroscopy

^1H NMR analysis performed on each fraction showed that the resulting ^1H NMR spectra for fractions A-D are not only similar to each other, but are also very similar to that observed for the unfractionated poly(ethylene D-glucaramide) post-polymer (Figure 3.32B).

For fraction E, only small traces of signals corresponding to the polymer of interest were able to be located. Signals from the smaller non polymer organic material are again similar to what is observed for poly(3',6'-dioxaoctamethylene D-glucaramide) pre-polymer (see Section 3.6.3.4). However, despite these signals being present in greater amounts than the polymer signals of interest, there was still sufficient signal from the lower molecular weight poly(ethylene D-glucaramide) post-polymer fraction for ^1H NMR end-group analysis to be performed. The resulting M_n from end-group analysis was in agreement with the PolytoolsTM M_n calculation from the MALDI-TOF analysis.

From the resulting ^1H NMR spectrum obtained for fraction F, no traces of signals corresponding to the polymer of interest were located (Figure 3.35F). However, the MALDI-TOF results for this fraction clearly indicate that the polymer of interest is indeed part of the fraction (Figure 3.34F). This means that the majority of this fraction is comprised of smaller non polymer organic material. Consequently, both the terminal and non-terminal methylene protons could not be located and, hence, M_n calculation via ^1H NMR end-group analysis is not possible.

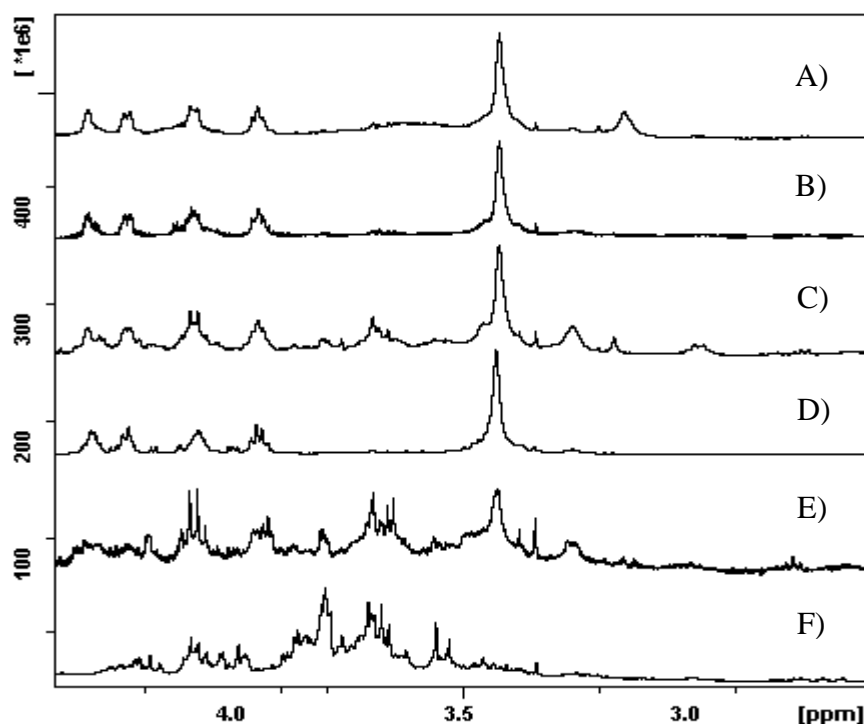


Figure 3.35: NMR of A) Fraction A 4000 scans, B) Fraction B 4500 scans, C) Fraction C 6000 scans, D) Fraction D 4000 scans, E) Fraction E 4000 scans and F) Fraction F 7560 scans.

3.6.4.5 Conclusions

Previous work on fractions collected in the V_0 region in the SEC for other D-glucaramide PHPA's has shown that these fractions are indeed high molecular weight polymers (see Section 3.6.1 & 3.6.3). Therefore, the same conclusions can be extended to fractions A-C. Conservative use of the dextran calibration curve (see Section 3.4.3) shows that the molecular weights for fractions A-C is approximately 1,800,000, 1,500,000, and 200,000 respectively.

For fraction E, comparison of the calculated M_n values from the ^1H NMR end group analysis and MALDI-TOF shows that the molecular weights are in agreement. However, results from the ^1H NMR for these fractions suggest that the in-series column setup of KS-804 and KS-805 is not appropriate for collecting fractions of poly(ethylene D-glucaramide) post-polymer that have small molecular weights (i.e., <1000). Furthermore, the abundance of signals from the smaller non

polymer organic material present in the ^1H NMR suggests that this material comprises the majority of this fraction.

With regards to fraction F, only the PolytoolsTM M_n could be calculated due to the issues associated with the ^1H NMR for this fraction (see Section 0). A corollary of this is that the smaller non polymer organic material comprises the majority of fraction F, rather than the polymer of interest. In order to accurately determine the composition of smaller non polymer organic material relative to that of the smaller molecular weight poly(ethylene D-glucaramide) post-polymer for fractions E and F, fractionation of the unfractionated poly(ethylene D-glucaramide) post-polymer sample should be undertaken on columns KS-801 and KS-802.

These results provide evidence, similar to that observed for the other D-glucaramide polymers, that the majority of the unfractionated poly(ethylene D-glucaramide) post-polymer sample is comprised of high molecular weight polymers. Previous results have suggested that fragmentation is occurring for these fractions (A & B) with in the MALDI-TOF. Therefore, the MALDI-TOF mass spectra observed for the unfractionated poly(3',6'-dioxaoctamethylene D-glucaramide) pre-polymer could be the result of fragmented remains of the high molecular weight fragments described above (see Section 3.6.3.3).

3.6.5 Poly(ethylene xylaramide) Pre-polymer (A)

3.6.5.1 Introduction

Poly(ethylene xylaramide) pre-polymer (A) is one of two poly(ethylene xylaramide) pre-polymers used in this study; pre-polymer (B) being the other (see Section 3.6.6 below). Despite being structurally identical, the only difference between the two polymers is the methods by which they are synthesised. For poly(ethylene xylaramide) pre-polymer (A), the polymer was prepared through the diammonium salt method using NaOMe and triethylamine (TEA) [46].

The M_n calculated by ^1H NMR end group analysis for the poly(ethylene xylaramide) pre-polymer (A) at UoW was observed to be approximately half of the value that was calculated at UoM (Table 3.13). The reason for this significant discrepancy will be covered in the sections below.

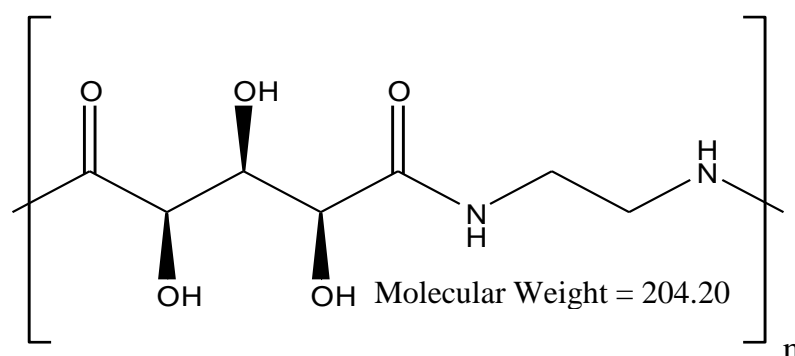


Figure 3.36: Structure of the Poly(ethylene xylaramide) Pre-polymer (A) repeating unit.

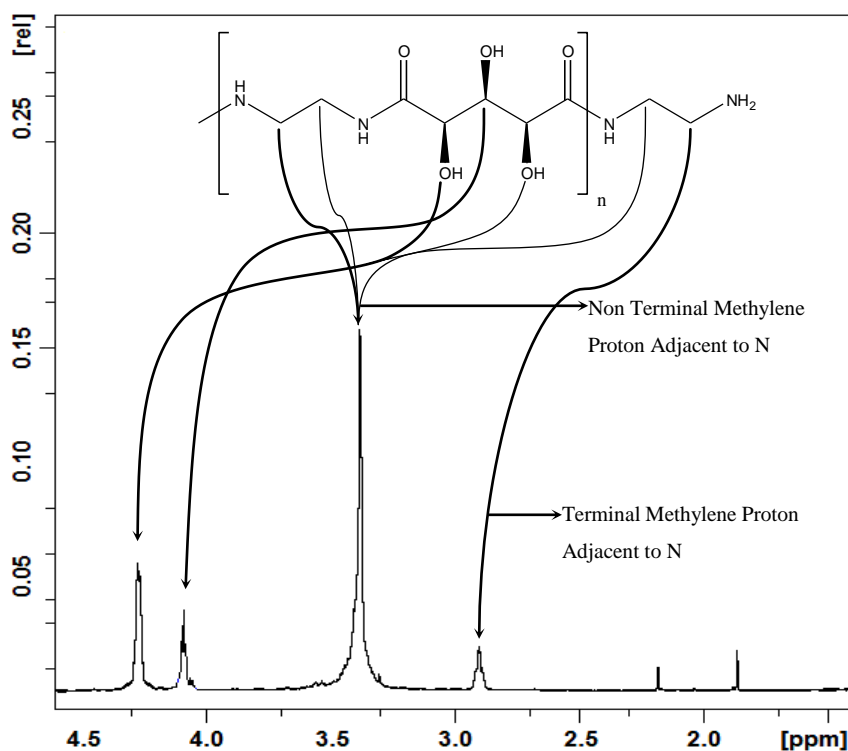


Figure 3.37: Fully Labelled ^1H NMR Spectrum of Poly(ethylene xylaramide) Pre-polymer (A).

3.6.5.2 Fractionation by SEC

From the resulting SEC chromatogram for poly(ethylene xylaramide) pre-polymer (A), four predominant peaks were resolved (Figure 3.38). Assuming that the refractive index responses are all approximately equal, peaks around the V_0 are likely to region make up the majority (~69%) of the proportional peak areas of the unfractionated poly(tetramethylene D-glucaramide) post-polymer sample (Table 3.29). From the studies performed on the D-glucaramide polymers, the peaks collected in the V_0 region correspond to extremely high molecular weight polymers (see Section 3.6.1 and 3.6.3). Therefore, the same conclusions for these polymers can probably be extended to the peaks collected for poly(ethylene xylaramide) pre-polymer (A) within this region.

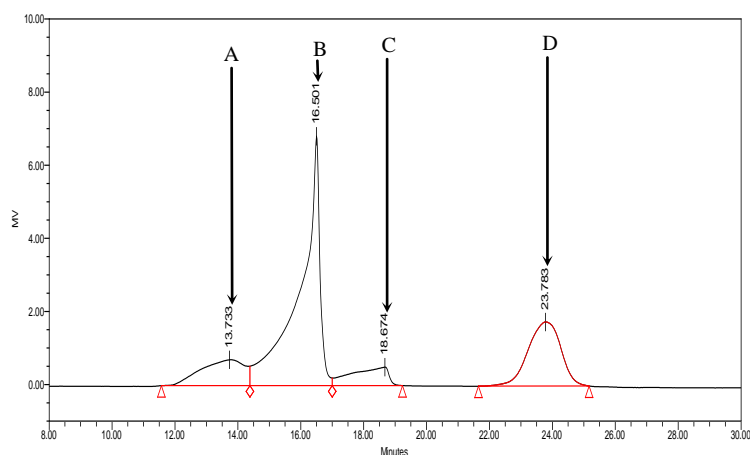


Figure 3.38: SEC Chromatogram of Poly(ethylene xylaramide) Pre-polymer (A) on columns KS-804 and KS-805 in series.

| Fraction | Retention Time (mins) | Area | Area (%) |
|----------|-----------------------|--------|----------|
| A | 13.733 | 66751 | 12.81 |
| B | 16.501 | 292754 | 56.20 |
| C | 18.674 | 38858 | 7.46 |
| D | 23.783 | 122564 | 23.53 |

Table 3.29: Integrated Areas of labelled peaks in SEC chromatogram of unfractionated Poly(ethylene xylaramide) Pre-polymer (A) on KS-804 and 805 SEC columns in series.

3.6.5.3 MALDI-TOF of Fractions

Results from the MALDI-TOF performed on each of the poly(ethylene xylaramide) pre-polymer (A) fractions gave varying information about their molecular weights. For fractions A-C, little information about the possible M_n could be obtained from the resulting MALDI mass spectra. For fractions A and B, ion peaks from the MALDI mass spectrum were only observed in the low mass region ($<1000m/z$). This result was not unexpected, even though these fractions

were collected near the V_0 region. As with previous MALDI results observed from the D-glucaramide polymer samples (see Sections 3.6.1.3, 3.6.2.3, 3.6.3.3 and 3.6.4.3), a higher laser power was required to ionise these samples. However, the higher laser power probably causes the extremely high molecular weight fractions of A and B to fragment in the MALDI.

The MALDI mass spectrum for fraction C gave, a polymer mass distribution different to that of poly(ethylene xylaramide) pre-polymer (A). This was a skew polymer mass distribution with a repeating unit of 44Da, with both Na^+ and K^+ adducts observed (Figure 3.39C), whereas the expected repeating unit for (ethylene xylaramide) pre-polymer (A) is ~204Da (see below).

| Poly(ethylene xylaramide) Pre-polymer (A) | Laser Power |
|--|-------------|
| Unfractionated | 55% |
| Fraction A | 62.5% |
| Fraction B | 65% |
| Fraction C | 60% |
| Fraction D | 45% |

Table 3.30: MALDI-TOF Laser Power used to Ionise Poly(ethylene xylaramide) Pre-polymer (A) Fractions.

The same discrepancies for the unfractionated poly(ethylene xylaramide) pre-polymer (A) were observed for fraction D in that the detected mass distribution was asymmetric and well displaced towards the low mass region. However, similar to the results obtained for the other PHPA fractions with lower M_n (see Section 3.6.1.3, 3.6.2.3, 3.6.3.3 and 3.6.4.3), the PolytoolsTM calculations are in agreement with the end-group analysis. Therefore, the discrepancies observed for the mass distribution are again having a minimal effect on the PolytoolsTM M_n calculations.

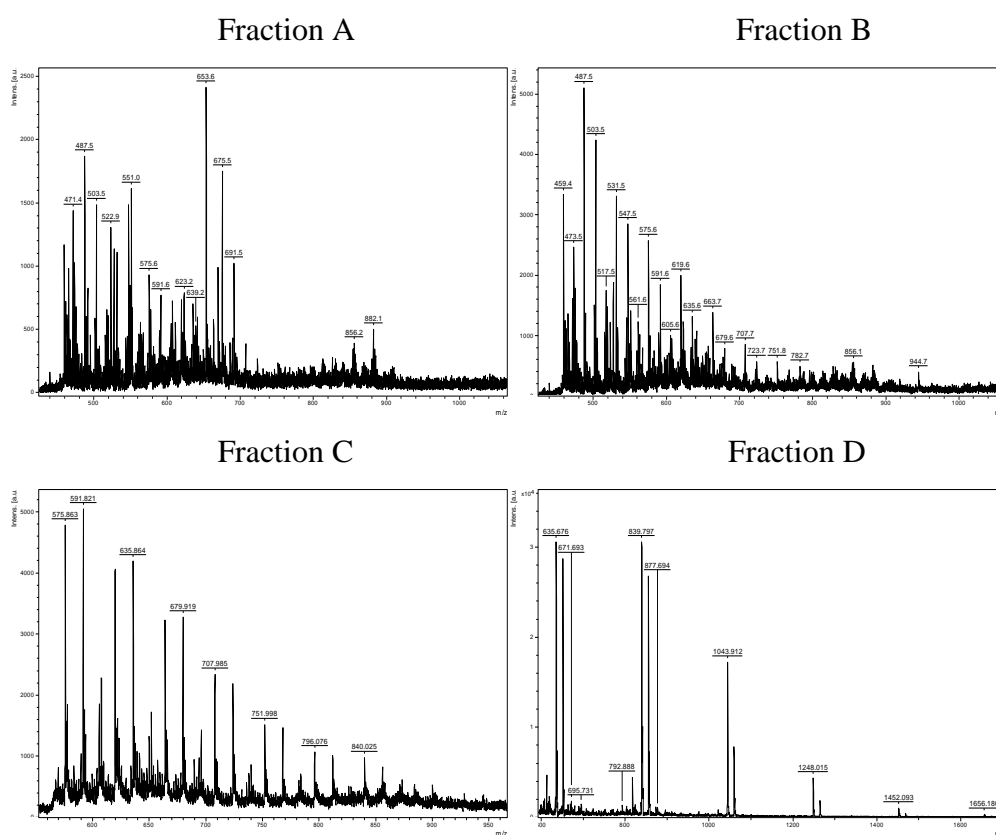


Figure 3.39: Mass Spectra of Poly(ethylene xylaramide) Pre-polymer (B) Fractions from SEC (see Figure Figure 3.38)

| Poly(ethylene xylaramide) pre-polymer (A) | Polytools™ calculations from the MALDI-TOF spectrum | | | ¹ H NMR end group analysis M _n |
|---|---|----------------|----------------|--|
| | M _n | M _w | Polydispersity | |
| Unfractionated | 1389 | 1731 | 1.25 | 948 |
| Fraction A | - | - | - | 1315 |
| Fraction B | - | - | - | 786 |
| Fraction C | - | - | - | - |
| Fraction D | 605 | 619 | 1.09 | 607 |

Table 3.31: Polytools™ Calculations of M_n using Peak Height and Peak Integral and ¹H End Group Calculations of M_n for each Poly(ethylene xylaramide) Pre-polymer (B) Fraction.

3.6.5.4 NMR Spectroscopy

^1H NMR analysis performed on fractions A and B show that the resulting spectra are not only similar to each other, but are also very similar to that observed for the unfractionated poly(ethylene xylaramide) pre-polymer (A) (Figure 3.37).

For fraction C, there is no trace of any signals corresponding to poly(ethylene xylaramide) pre-polymer (A). From the full ^1H NMR spectrum of fraction C (Figure 3.41A) it can be observed that there are only two prominent signals, a quartet around 4.1ppm and a doublet around 1.5ppm. ^{13}C NMR of this fraction (Figure 3.41B) also has two signals of interest; a signal around 20ppm, and the other signal around 68ppm.

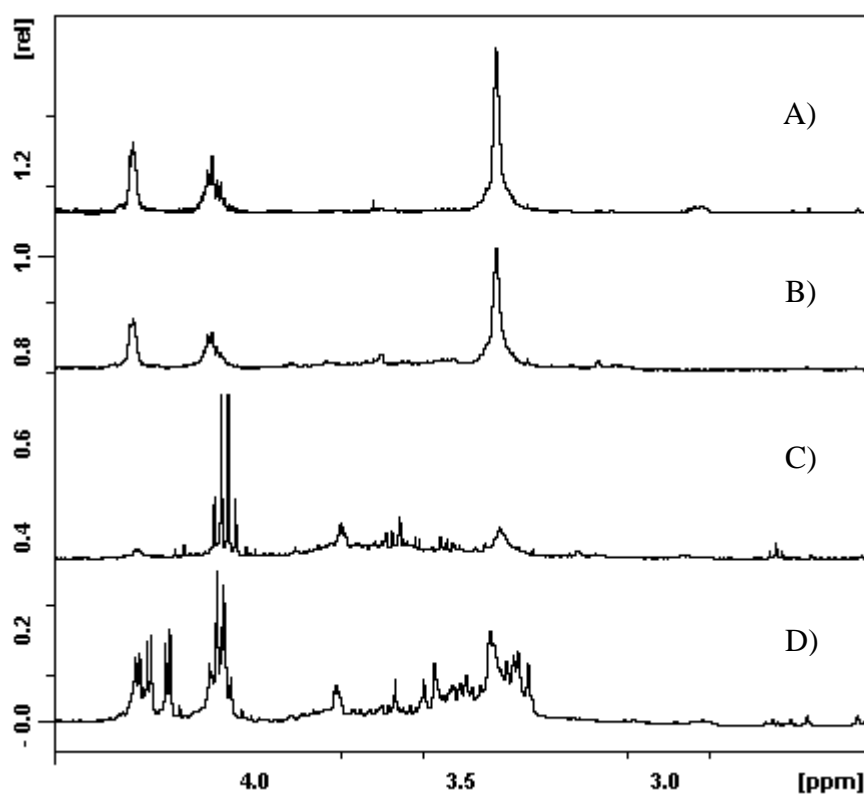


Figure 3.40: NMR of A) Fraction A 1000 scans, B) Fraction B 1000 scans, C) Fraction C 500 scan and D) Fraction D 1500 scans.

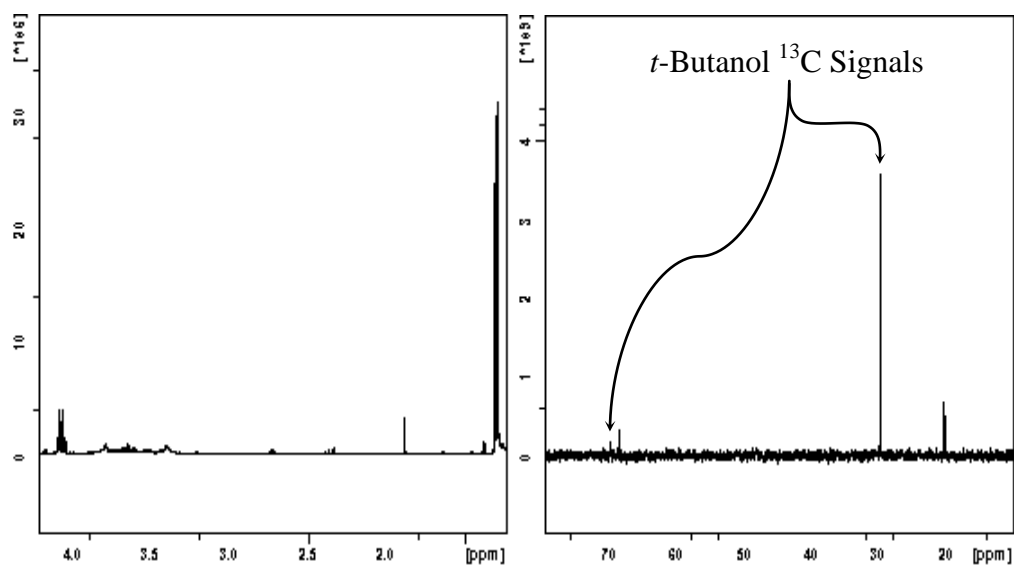


Figure 3.41: A) ^1H and B) ^{13}C NMR of Fraction C.

A possible structure for this fraction is polyethylene glycol (Figure 3.42). This structure has a repeating unit structure of 44Da, which is indeed observed in the MALDI. However, as the polyethylene glycol structure is symmetrical it would be expected that only one signal would be observed in both the ^1H and ^{13}C NMR. However, as two signals are observed for both NMR spectra, this also negates the possibility of polyethylene glycol being present in this fraction.

Figure 3.43 illustrates another possible structure for fraction C which fits the results obtained from the $^1\text{H}/^{13}\text{C}$ NMR and MALDI. This is because not only does it fit the repeating unit observed in the MALDI results for fraction C, but the expected $^1\text{H}/^{13}\text{C}$ NMR signals for this structure fit the respective result of $^1\text{H}/^{13}\text{C}$ NMR obtained for this fraction. However, understanding why and how this hypothesised structure is actually present in the unfractionated poly(ethylene xylaramide) pre-polymer (A) sample is beyond the scope of this investigation.

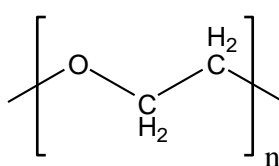


Figure 3.42: Repeating Unit of polyethylene glycol

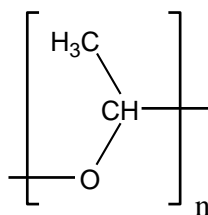


Figure 3.43: Hypothesised structure of the repeating unit possibly observed in Fraction C.

With regards to fraction D, small traces of the unidentified polymer that were observed in fraction C are again present in this fraction. In addition to the presence of this polymer, other smaller mass signals from other organic material are present in this fraction. However, despite the presence of these signals, it is still possible to perform ^1H NMR end-group analysis on this fraction. The resulting M_n calculated from end-group analysis was in agreement with the PolytoolsTM M_n calculation from the MALDI-TOF analysis.

3.6.5.5 Conclusions

As with previous results which concluded that peaks collected near V_0 are extremely high molecular weight polymers (see Sections 3.6.1 and 3.6.3), the same conclusions can be extended to unfractionated poly(ethylene xylaramide) pre-polymer (A). It can be observed from the SEC results that the majority of the PHPA sample composition is of extremely high molecular weight polymers. Conservative use of the dextran calibration curve (see Section 3.4.3) showed both peaks A and B have molecular weights that are well in excess of 100,000 (Fraction A $\sim 1,500,000$ and Fraction B $\sim 500,000$). Therefore, similar to the MALDI results for the unfractionated D-glucaramide sample (see Section 3.6.1.3, 3.6.2.3, 3.6.3.3 and 3.6.4.3), what is most likely being observed in the MALDI for the unfractionated poly(ethylene xylaramide) pre-polymer (A) is fragments of these fractions.

With regards to fraction C, from the resulting spectrum of MALDI, ^1H and ^{13}C NMR it can be concluded that there is another polymer present in the unfractionated poly(ethylene xylaramide) pre-polymer (A) sample. Figure 3.43 illustrates the hypothesised structure of this unknown polymer. The conclusions of what would be expected for this structure in a ^1H and ^{13}C NMR fits the subsequent results obtained this fraction. Furthermore, the repeating unit of this polymer structure also fits the results observed from the MALDI. However, comprehensive identification of this polymer is not possible because it is outside the scope of this investigation.

For fraction D, despite the presence of significant amounts of smaller non polymer organic material in this fraction, a molecular weight was able to be obtained via ^1H NMR end group analysis and MALDI. Comparison of the molecular weights from both analysis shows that the values are in agreement. Note that, similar to the poly(3',6'-dioxaoctamethylene D-glucaramide) post-polymer, in order to determine the relative composition of smaller non polymer organic material and smaller molecular weight poly(ethylene xylaramide) pre-polymer (A) fraction, further fractionation of unfractionated poly(ethylene xylaramide) pre-polymer (A) should be undertaken on columns KS-801 and KS-802.

3.6.6 Poly(ethylene xylaramide) pre-polymer (B)

3.6.6.1 Introduction

Poly(ethylene xylaramide) pre-polymer (B) is a C₂ xylaramide polymer which, as explained previously, is structurally identical to poly(ethylene xylaramide) pre-polymer (A) (Figure 3.44). However, poly(ethylene xylaramide) pre-polymer (B) was synthesized through the ester/amine method developed by Hinton [55].

M_n calculated by ¹H NMR end group analysis for the poly(ethylene xylaramide) pre-polymer (B) is significantly different to that calculated for poly(ethylene xylaramide) pre-polymer (A) (Table 3.13). Furthermore, the M_n calculated for poly(ethylene xylaramide) pre-polymer (B) at UoW was significantly different to that calculated at UoM (see Table 3.13). The reason for this for this discrepancy will be explained in subsequent sections.

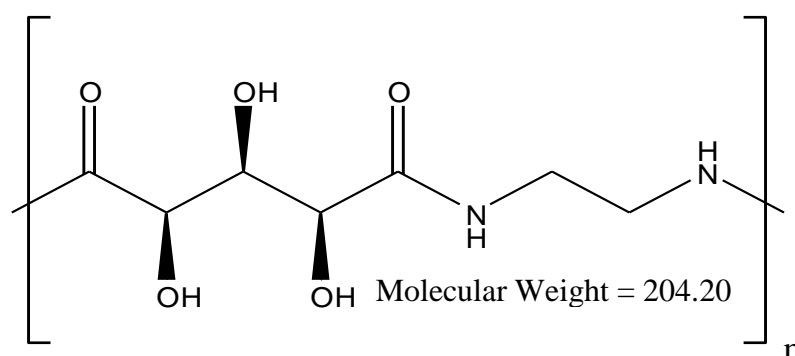


Figure 3.44: Structure of the Poly(ethylene xylaramide) Pre-polymer (B) repeating unit

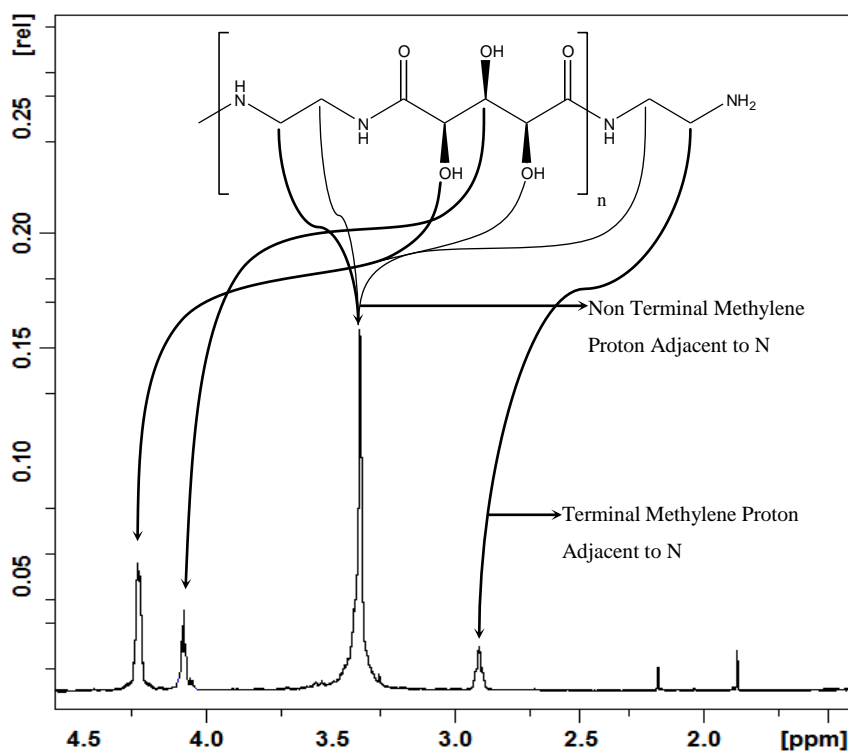


Figure 3.45: Fully Labelled ^1H NMR Spectrum of Poly(ethylene xylaramide) Pre-polymer (B).

3.6.6.2 Fractionation by SEC

The SEC chromatogram detected for poly(ethylene xylaramide) pre-polymer (B) produced four peaks (Figure 3.46), which is very similar to that observed for poly(ethylene xylaramide) pre-polymer (A). This result is expected because the both xylaramide polymers have very similar structure and properties. However, the major difference between the two xylaramide polymers is that peak D is the most prominent peak for poly(ethylene xylaramide) pre-polymer (B), compared to peak B for the poly(ethylene xylaramide) pre-polymer (A).

A possible explanation for the larger fraction D peak for poly(ethylene xylaramide) pre-polymer (B) is that there are greater amounts of smaller mass material present in the fraction collected. Comparing the resulting chromatograms of KS-801 and KS-802 for both the poly(ethylene xylaramide) pre-polymer (A) (Figure 3.14) and (B) (Figure 3.15) it can be observed that poly(ethylene xylaramide) pre-polymer (B)

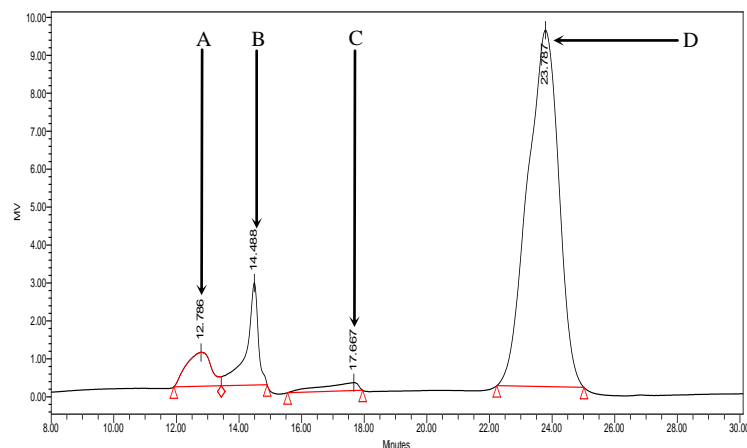


Figure 3.46: SEC Chromatogram of Poly(ethylene xylaramide) Pre-polymer (B) on columns KS-804 and KS-805 in series.

has more smaller mass peaks present on these columns. As previously mentioned for the poly(3',6'-dioxaoctamethylene D-glucaramide) pre-polymer (see Section 3.6.3), on these higher exclusion limit columns the lower mass peaks become less resolved.

Comparison of the retention times for fractions A and B of poly(ethylene xylaramide) pre-polymer (B) to pre-polymer (A) show that both fractions have a noticeably lower retention time for pre-polymer (B) (Figure 3.46). Therefore, because of the lower retention time, this suggests that the molecular weight of these fractions for poly(ethylene xylaramide) pre-polymer (B) are larger than that for poly(ethylene xylaramide) pre-polymer (A).

| Fraction | Retention Time (mins) | Area | Area (%) |
|----------|-----------------------|--------|----------|
| A | 12.814 | 56744 | 6.78 |
| B | 14.488 | 87114 | 10.40 |
| C | 17.667 | 20891 | 2.49 |
| D | 23.787 | 672797 | 80.33 |

Table 3.32: Integrated Areas of labelled peaks in SEC chromatogram of unfractionated Poly(ethylene xylaramide) Pre-polymer (B) on KS-804 and 805 SEC columns in series.

3.6.6.3 MALDI-TOF of Fractions

The resulting MALDI mass spectra for fractions A, B and D (Figure 3.47, A, B & D) are very similar to the results obtained for poly(ethylene xylaramide) pre-polymer (A). An explanation of the phenomena behind these mass spectra has been provided previously (see Section 3.6.5.4). For fraction C, the skewed polymer-like distribution that was observed for poly(ethylene xylaramide) pre-polymer (A) is not present for poly(ethylene xylaramide) pre-polymer (B). Note however that the repeating unit of 44Da, which is different to the hypothesised structure of the repeating unit (Figure 3.43), can still be observed in the MALDI spectra for this fraction. Therefore, the same conclusions which were drawn for fraction C of poly(ethylene xylaramide) pre-polymer (A) (see Section 3.6.5) can also be extended to the poly(ethylene xylaramide) pre-polymer (B).

| Poly(ethylene xylaramide) Pre-polymer (B) | Laser Power |
|--|-------------|
| Unfractionated | 55% |
| Fraction A | 60% |
| Fraction B | 57.5% |
| Fraction C | 60% |
| Fraction D | 42.5% |

Table 3.33: MALDI-TOF Laser Power used to Ionise Poly(ethylene xylaramide) Pre-polymer (B) Fraction

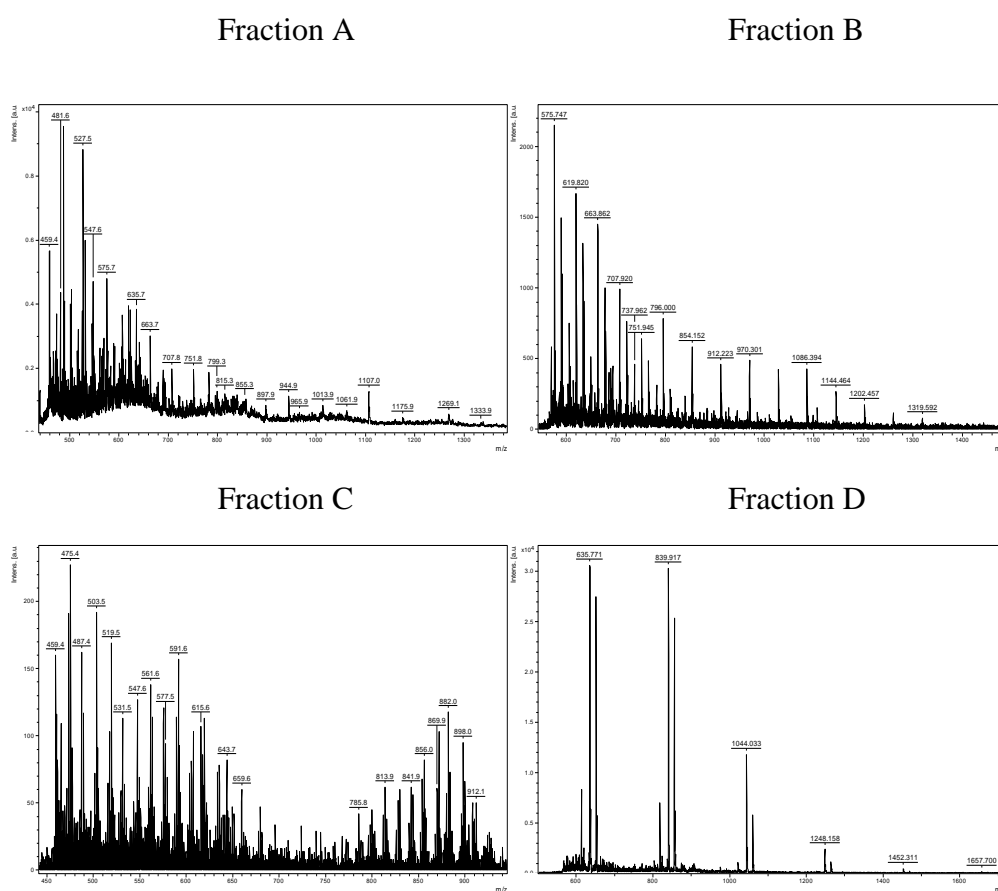


Figure 3.47: Mass Spectra of Poly(ethylene xylaramide) Pre-polymer (B) Fractions from SEC (see Figure 3.46).

| Poly(ethylene xylaramide) pre-polymer (B) | Polytools™ calculations from the MALDI-TOF spectrum | | | ¹ H NMR end group analysis M _n |
|---|---|----------------|----------------|--|
| | M _n | M _w | Polydispersity | |
| Unfractionated | 701 | 839 | 1.13 | 1831 |
| Fraction A | - | - | - | 1166 |
| Fraction B | - | - | - | 732 |
| Fraction C | - | - | - | - |
| Fraction D | 825 | 869 | 1.05 | 684 |

Table 3.34: Polytools™ Calculations of M_n using Peak Height and Peak Integral and ¹H End Group Calculations of M_n for each Poly(ethylene xylaramide) Pre-polymer (B) Fraction.

3.6.6.4 NMR Spectroscopy

The resulting ^1H NMR spectra for fractions A and B are both not only similar to each other, but are also very similar to that observed for the unfractionated poly(ethylene xylaramide) pre-polymer (B) (Figure 3.45). Moreover, this result is also very similar to what is observed for poly(ethylene xylaramide) pre-polymer (A). For fraction C, a similar ^1H NMR spectrum was obtained to that found for fraction C for poly(ethylene xylaramide) pre-polymer (A). Therefore, the same conclusion that was obtained for fraction C of poly(ethylene xylaramide) pre-polymer (A) can be extended to that for poly(ethylene xylaramide) pre-polymer (B) (see also Section 3.6.5.4).

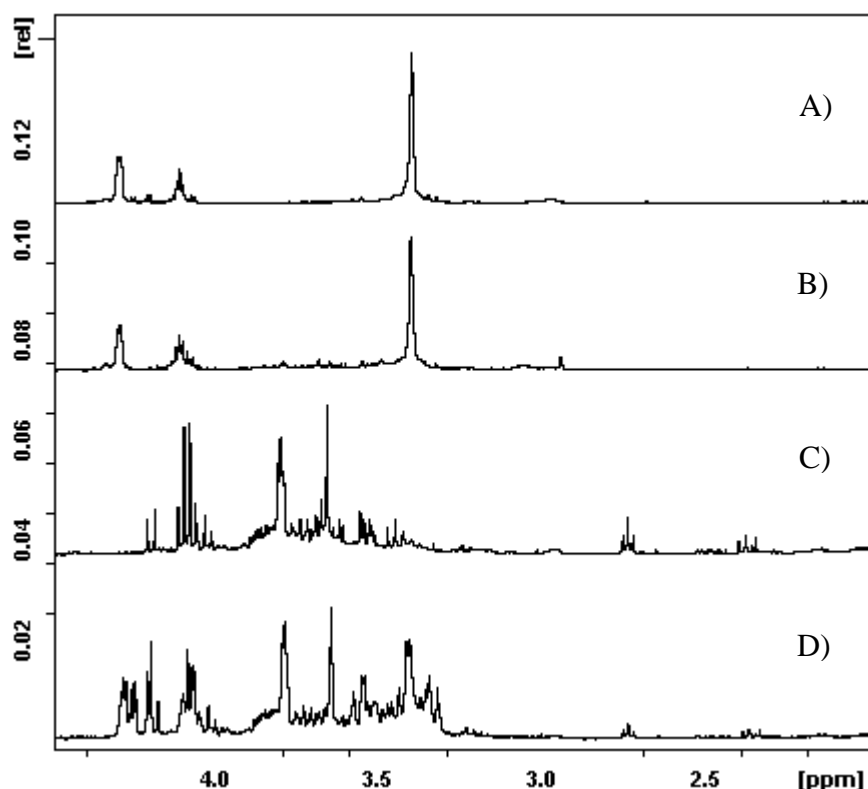


Figure 3.48: NMR of A) Fraction A 1250 scans, B) Fraction B 1250 scans, C) Fraction C 500 scan and D) Fraction D 1500 scans.

From the resulting ^1H NMR performed on fraction D, it is observed that there are greater amounts of signal corresponding to smaller non polymer organic material than that which was detected for poly(ethylene xylaramide) pre-polymer (A) (Figure 3.40D). This gives an indication that most of the peaks observed on columns KS-801 and KS-802 are due to this smaller non polymer organic material.

Comparing the calculated M_n values from the ^1H NMR end group analysis performed for each unfractionated xylaramide sample, it can be observed that pre-polymer (B) has a higher M_n than that for pre-polymer (A) (Table 3.13). This concurs with the results from the SEC in which fraction A and B are larger in poly(ethylene xylaramide) pre-polymer (B).

However, the SEC chromatogram and weights from fractionation shows a large amount of low molecular weight material in poly(ethylene xylaramide) pre-polymer (B) which is collected in fraction D. Moreover, it is not fully understood how much of fraction D is made up of the actual polymer itself and that of smaller mass material. Therefore, if very little of the of fraction D did contain the poly(ethylene xylaramide) pre-polymer (B), then this would mean higher molecular weight fractions of this polymer would dominate the sample. In order to determine if greater proportions of higher molecular weight fractions are present in the unfractionated poly(ethylene xylaramide) pre-polymer (B), T_2 relaxation rates can be utilised as a preliminary indicator. This is because the overall T_2 relaxation rate is inversely proportional to the amount of higher molecular weight fractions within the polymer mixture. A more detailed explanation of this phenomena will be discussed below (see Section 3.7)

| Poly(ethylene xylaramide) pre-polymer | T_2 Relaxation Rate (sec^{-1}) |
|---------------------------------------|---|
| (A) | 230 |
| (B) | 240 |

Table 3.35: T_2 Relaxation Rates for Unfractionated poly(ethylene xylaramide) pre-polymer (A) and (B).

Comparison of the T_2 relaxation rates for each xylaramide sample (Table 3.35) shows that poly(ethylene xylaramide) pre-polymer (B) has a much lower (~ 10 sec) T_2 relaxation rate than that observed for poly(ethylene xylaramide) pre-polymer (A). This result suggests that poly(ethylene xylaramide) pre-polymer (B) contains a greater amounts of extremely high molecular weight fractions than that of poly(ethylene xylaramide) pre-polymer (A). Therefore, despite the SEC results showing fraction D being the most prominent peak for poly(ethylene xylaramide) pre-polymer (B), the proportion of a lower molecular weight polymer in this fraction is minimal. Hence, this suggests that the majority of this fraction is comprised of smaller mass non polymer organic material.

3.6.6.5 Conclusions

Due to the similarity of the results, the same conclusions that were obtained for fractions A-D of the poly(ethylene xylaramide) pre-polymer (A) can be extended to poly(ethylene xylaramide) pre-polymer (B). However, it should be appreciated that there are some slight differences between the two xylaramide polymers. For instance, comparison of the SEC results show that fractions A and B for poly(ethylene xylaramide) pre-polymer (B) have shorter retention times than the corresponding fractions for poly(ethylene xylaramide) pre-polymer (A). Consequently, the molecular weights of these fractions are bigger than those obtained for poly(ethylene xylaramide) pre-polymer (A).

This phenomena could also explain why the M_n calculation via ^1H NMR end-group analysis is higher for poly(ethylene xylaramide) pre-polymer (B) than that obtained for pre-polymer (A). An additional factor is the composition of fraction D, this is because the SEC results for poly(ethylene xylaramide) pre-polymer (B) has a larger peak D than that observed for poly(ethylene xylaramide) pre-polymer (A). This suggests that there should be more of the lower molecular weight polymers present in this fraction. The SEC results from columns KS-801 and KS-802 also seems to provide further justification for this hypothesis.

However, the T_2 relaxation rates determined from both ethylene xylaramide polymers contradicts this suggestion. This is because pre-polymer (B) has a much lower T_2 relaxation rate for fraction D than pre-polymer (A). However poly(ethylene xylaramide) pre-polymer (B) contains large amounts of small non polymer organic material.

3.7 Relaxation Rates and Molecular Weight of Individual Polymers and Mixtures of Polymer Fractions of Varying Molecular Weight

If each PHPA sample is comprised of polymer fractions of varying molecular weights (see Section 3.2), the contribution that each individual fraction has to the overall relaxation rate in an unfractionated PHPA sample is largely unknown. Therefore, understanding the relaxation rate contribution that each individual fraction provides is important as it gives an indication of what could be occurring for the M_n calculation. via ^1H NMR end-group analysis (see Section 3.2).

The number average molecular weight M_n is obtained from ^1H NMR end group analysis from the integration of the ^1H signals of the methylene groups adjacent to the terminal and non-terminal nitrogens in each PHPA sample. The integral that is obtained for a given signal via ^1H NMR is dependent on the area of the signal, not the signal amplitude [40]. Furthermore, the T_1 and T_2 relaxation rates are related to a signal's amplitude and resolution, respectively. Therefore, as the signal integral is only dependent on the area, it would be expected that changes in T_1 relaxation would have a negligible effect on the signal integral.

Conversely, the signal resolution is inversely proportional to T_2 , meaning any changes to T_2 will affect the line width of a signal, and hence the signal's

broadness. Therefore, as high molecular weight polymers will produce small T_2 rates (and vice versa for low molecular weight polymers), in theory it should be possible to use ^1H NMR to determine the individual effect of a given PHPA on the overall relaxation rate.

Fractionated dextrans, over a wide range of known molecular weights, were used to determine what influence the individual samples have on a mixture of dextran fractions of varied molecular weights. Dextrans are made up of many D-glucopyranose molecules (see Section 3.1) and the ^1H NMR spectrum observed for each dextran fraction is essentially the same (Figure 3.49). The ^1H NMR signals for C2-H, C3-H, C4-H, C5-H and C6-H for a dextran sample are mostly overlapped and are therefore unsuitable for determining relaxation rates. The C1-H signal, which is further downfield and relatively isolated, was the most suitable signal for T_1 and T_2 relaxation time calculations.

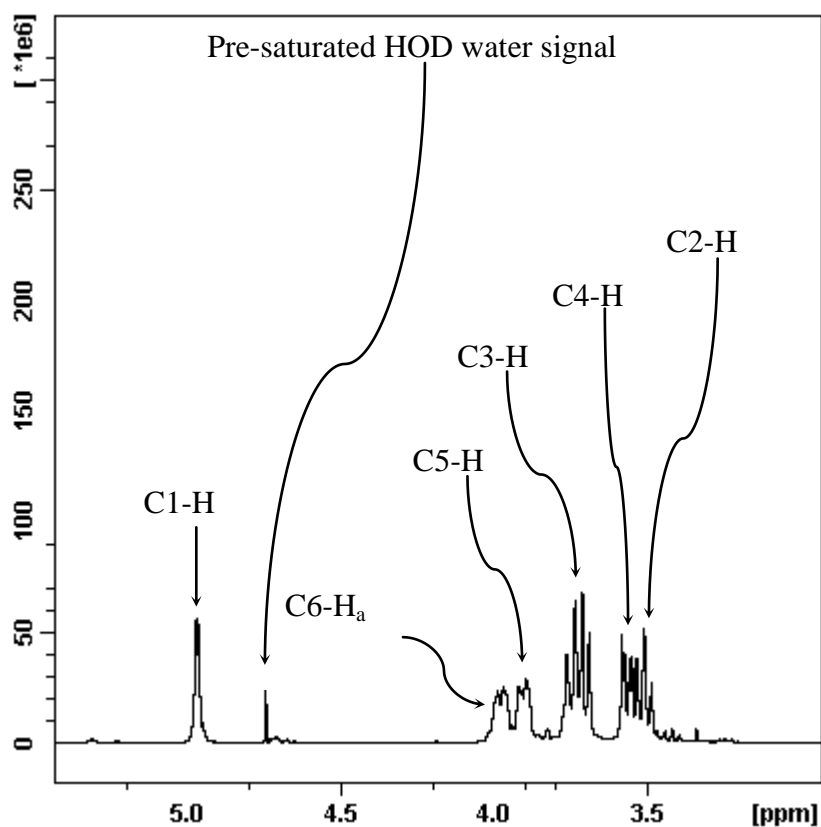


Figure 3.49: Fully labelled ^1H NMR of Dextrans

| Dextran | T ₂ Relaxation Rate (sec ⁻¹) | |
|----------------|---|--------|
| | 30°C | 50°C |
| | | |
| 1200 | 119.70 | 192.36 |
| 4440 | 86.06 | 141.83 |
| 9840 | 78.48 | 130.43 |
| 43,500 | 64.17 | 102.57 |
| 70,000 | 62.39 | 98.84 |
| 110,000 | 61.80 | 97.23 |
| 401,300 | 59.11 | 94.56 |
| 1:1 Equivalent | 75.97 | 114.37 |
| Simulated | 74.18 | 112.00 |

Table 3.36: T₂ relaxation rates for each individual Fractionated Dextrans and the two mixtures.

In order to determine the effect that each fraction has on the overall relaxation rate of an unfractionated PHPA, two mixtures of fractionated dextrans of different ratios were prepared and examined. The first dextran mixture was a 1:1 equivalent ratio of all the dextran fractions. These were used to evaluate the effect that dextran molecular weight has on the dextran mixture's overall relaxation rates.

The second mixture simulated the ratios observed for a PHPA sample in SEC; the percentage areas for each peak from the SEC results of poly(tetramethylene D-glucaramide) post-polymer were used to simulate the fraction weights of an unfractionated PHPA sample. It was assumed that the % areas for each peak represented the ratio of the weights of the individual PHPA fractions.

The T_2 relaxation time for the fractionated dextrans and the two mixtures at two different temperatures are given in Table 3.36. From these results at 30°C, the relaxation rate for the simulated mixture is slightly lower than the 1:1 mixture. This is to be expected as in this mixture there are more of the higher molecular weight dextrans in the mixture. However the difference between the two mixtures relaxation rate is not appropriate considering the change in proportions. It also can be observed that neither higher nor lower molecular weight dextrans are having a dominant influence on the overall relaxation rate in either mixtures. Therefore at this temperature it can be assumed that the overall relaxation times for each mixture represent an average of the individual polymer.

However upon elevation of the temperatures to 50°C, changes to the relative values of the T_2 relaxation measurements of the mixtures (see over). But as a single point measurement it would make it appear that the polymer was much bigger, which explains the results observed earlier in the thesis with poly(tetramethylene D-glucaramide) post-polymer at higher temperatures (Figure 3.21).

To understand what affects these relaxation rates have on the molecular weight determination for each sample the T_2 data for the fractionated dextrans will be plotted against molecular mass. Since the composition of the mixtures is known the number average molecular mass for these two mixtures can be calculated using equation 3.1:

$$M_n = \frac{\sum w_i}{\sum \frac{w_i}{M_i}} Mn = \frac{\sum_i w_i}{\sum \frac{w_i}{M_i}} \quad (3.1)$$

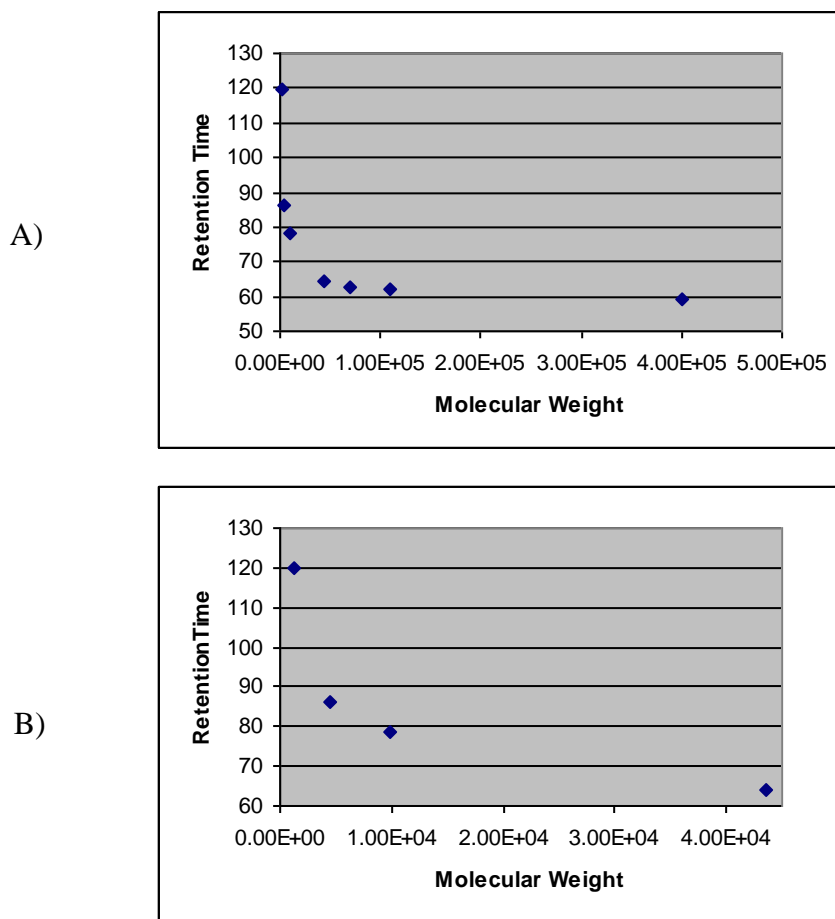


Figure 3.50: A) T_2 data for the fractionated dextrans plotted against molecular mass at 30°C B) The region 0 to 41,000 expanded.

For the 1:1 mixture this calculates to 5790 and for the simulated mixture it calculates to 6079. Figure 3.26 shows T_2 data for the fractionated dextrans at 30°C plotted against number average molecular mass. The T_2 values at 30°C for the two mixtures when applied to the graph (Figure 3.50) yield molecular weights of approximately 12,000 and 15,000 for the 1:1 and simulated materials respectively. Thus the molecular masses obtained from the plot for the mixtures do not agree with the calculated results.

| Method used to Obtain M_n | Mixture | |
|-----------------------------|---------|-----------|
| | 1:1 | simulated |
| Calculated M_n | 5790 | 6079 |
| From 30°C Plot | 12,000 | 15,000 |
| From 50°C Plot | 31,000 | 32,000 |

Table 3.37: Calculations of M_n for each Dextran Mixture.

Upon elevation of temperature to 50°C the number average molecular masses obtained for the mixtures increase (see Table 3.36). The increase in the molecular mass determined for the mixtures relaxation rates is a result of the greater influence the higher molecular masses dextrans are having on the overall relaxation time of the mixtures.

We can conclude from this that T_2 relaxation rates of mixtures are not reasonable indicators of number average molecular mass, as the molecular masses determined for the mixtures are a lot greater than the calculated results. However the number average molecular mass formula by its nature is strongly biased toward the lower molecular weight material even when the distribution is skewed as with the PHPA toward large molecular mass material [8].

Using these results for the fractionated dextrans and their two mixtures, an understanding of the behaviour each fraction has in PHPA samples during DP calculations under different conditions from end-group analysis can be obtained. The dextran mixtures show what effect each individual PHPA fraction is potentially causing at 30°C, and also why the DP for each PHPA sample increases upon heating. At low temperatures, the higher molecular weight PHPA fractions have negligible influence on the overall T_2 relaxation rates, and what is observed for the mixtures relaxation times appear to be a numerical average of all the dextran fractions relaxation times.

When temperature is elevated, due to the thermally active process of a polymer's molecular chain motion, the T_2 relaxation rates for higher molecular weight PHPA fractions increase. The dextran results show that upon increased temperature this causes the T_2 relaxation time for the mixtures to change towards the higher molecular weight dextrans. This in turn causes an increase in the calculated M_n . Such a phenomenon can be used to provide a simple explanation for what is occurring in Figure 3.21 for unfractionated poly(tetramethylene D-glucaramide) post-polymer.

4 Conclusions

4.1 Degradation of PHPA

A major issue associated with PHPA polymers is their ability to hydrolyse in water and under elevated temperatures. Therefore, this should have severe implications for polymer analysis because each PHPA sample is 1) prepared and run in deionised water, and 2) passed through columns which have elevated temperatures. However, ^1H NMR degradation experiments at room temperature and 50°C demonstrate that the polymer hydrolysis is insignificant. This because, within the time frame of preparation and analysis, the PHPA sample showed no decrease in the DP at room temperature (Figure 3.2). Similar results were observed for the degradation experiments performed at 50°C , however, a slight decrease in DP for each PHPA sample was observed over the time frame of the experiment (Figure 3.3). From these results, it was concluded that PHPA hydrolysis was not occurring within the analysis time frame.

4.2 Analysis of PHPA Fractions

4.2.1 PHPA Fractions collected around V_0 Region in SEC

The SEC results for each polymer showed multiple peaks on each KS column for all the PHPA samples. Interestingly, peaks were observed around the V_0 region for all the columns, even columns with extremely high exclusion limits. Initially, it was thought that smaller ionised polymers were responsible for this result. However, results from ICP-MS (Table 3.3), together with the fact these peaks were included on the columns KS805 and 806, and on the column setup used to fractionate each PHPA sample, suggests that these fractions were not due to ionised polymers. This was further confirmed by MALDI whereby higher laser powers were required to ionise these fractions (Table 3.16, Table 3.20, Table 3.23, Table 3.27, Table 3.30 and Table 3.33), which in turn caused fragmentation of the

samples. These results instead suggest that these fractions are high molecular weight polymers.

The hypothesis that these fractions are extremely high molecular weight polymers was further demonstrated by NMR. From ^1H NMR degradation experiments performed at 50°C , poly(tetramethylene D-glucaramide) post-polymer at different temperatures (i.e., from 30°C to 70°C) it was observed that DP increased. This phenomenon was suggested to results from changes in the relaxation times of the higher molecular weight fractions in the PHPA samples. Using the theory of T_2 relaxation rates, and the affect that the molecular weight of a polymer has on it (see section 1.4.4.2), fractions collected for poly(tetramethylene D-glucaramide) post-polymer and poly(3',6'-dioxaoctamethylene D-glucaramide) pre-polymer were used to give further evidence that fraction collected around V_0 were indeed extremely high molecular weight fractions. The resulting T_2 relaxation rates that were measured for these PHPA fraction showed that, as expected, the smaller molecular weight polymers gave higher T_2 relaxation rates than the higher molecular weight polymers (Table 3.18 and Table 3.25). Such results are similar to T_2 relaxation rate experiments that were performed on dextrans of known molecular weights, as quoted in the literature [42]. Coupling the results, for these fractions, from the SEC, T_2 relaxation rates and MALDI strongly suggests that the fractions collected around the V_0 region are due to extremely high molecular weight polymers.

4.2.2 MALDI and ^1H NMR End-group Analysis of each PHPA

Fraction

The SEC result showed that the majority (>55%) of the unfractionated PHPA samples was comprised of polymer fractions around V_0 . From conservative use of the dextran calibration curve (see Section 3.4.3), it can be assumed that the molecular weights for these fractions are greater than 100,000. For example, the molecular weight predicted for fraction A of poly(3',6'-dioxaoctamethylene D-glucaramide) pre-polymer is in excess of 2,000,000 (see Section 3.6.3.5).

With regards to results from MALDI, the high composition of these fractions within the overall sample suggests that only fragments of the extremely high molecular weight polymer are observed in the mass spectra. Furthermore, ^1H NMR end-group analysis is only applicable for polymers with molecular weights up to 20,000. Consequently, accurate determination of the molecular weights for these fractions via ^1H NMR end-group analysis is not possible. The inability to use MALDI and ^1H NMR end-group analysis for higher molecular fractions can also be extended to unfractionated PHPA samples due to the large amount of these higher molecular weight fractions in these samples. Therefore, in order to determine accurate estimates of the molecular weights for the higher weight fractions, or the unfractionated PHPA samples, LS techniques could be used. This is because LS is not necessarily limited by the molecular weight of a polymer sample.

For PHPA fractions of lower molecular weights, both MALDI and ^1H NMR end-group analysis produced molecular weights that were mostly in agreement. The exceptions to this were fractions D and F for poly(3',6'-dioxaoctamethylene D-glucaramide) pre-polymer (Figure 3.30). This is because fragmentation was presumed to be occurring in the MALDI, based on the laser power that was used to ionise these fractions (Table 3.23). Despite this, these results demonstrate that both MALDI and ^1H NMR end-group analysis are capable of accurately determining the molecular weight of the lower weight PHPA fractions.

For several of the lower molecular weight fractions, ^1H NMR observed very little, if any, signals that correspond to the PHPA polymer of interest (see Section 3.6.3.4, 3.6.4.4, 3.6.5.4 and 3.6.6.4). However, the MALDI mass spectra did observe that a PHPA polymer was present in these fraction samples. From this, it was concluded that these fractions contained significant amounts of small, non-polymer organic material. Note that the exact composition and proportion of the organic material within these polymer samples is still largely unknown. This is because such investigation is outside the scope of this research project.

4.3 Further Work that can be done

4.3.1 Light Scattering

In order to accurately determine the molecular weight of high weight polymers, further investigations into the analysis of molecular weights from PHPA fractions should be undertaken using either a LS photometer, or coupled SEC/LS detector. Such investigations could provide methods by which to determine the molecular weights of fractions collected around the V_0 region; a region in which both MALDI and ^1H NMR end-group analysis is limited. Furthermore, LS analysis could be undertaken on the lower molecular weight polymer fractions to verify the results obtained by MALDI and ^1H NMR end-group analysis.

4.3.2 Determination of Non-polymer Organic Material from PHPA polymers in Smaller Fractions

Further investigation should be undertaken to determine how much of the unfractionated PHPA samples is comprised of small non-polymer organic material. As previously mentioned (see Section 3.6.3.5), fractionation using columns KS-801 and 802 could provide an answer to the relative composition of small non-polymer organic material to the PHPA polymer of interest.

5 Appendix

5.1 Equations used to Calculate Molecular Weight of Polymers in Solution for Laser Light Scattering

Light scattering measurements are a measure of the total amount of scattered light. This is deduced from the decrease in the intensity of the light beam I_o as it passes through the polymer sample. This can be described in terms of Beer's law for absorption of light:

$$\frac{I}{I_o} = e^{-\tau l} \quad 5.1$$

where τ is the measure of the decrease of the intensity of the light beam per unit length (l) of a given solution. This is known as Turbidity of the solution.

The turbidity (τ) (also known as intensity of scattered light) can be used to calculate M_w using the following equations:

$$\frac{Hc}{\tau} = \frac{1}{M_w P_\theta} (1 + 2Bc + Cc^2 + \dots) \quad 5.2$$

where the constants H and τ can be respectively expressed as:

$$H = \left[\frac{32\pi^2}{3} \right] \left[\eta_o^2 \frac{(dn/dc)^2}{\lambda^4 N} \right] \text{ and } \tau = K' n^2 \left(\frac{i_{90}}{i_o} \right) \quad 5.3$$

where n_o is the refractive index of the solvent, n is the refractive index of the solution, c is the polymer concentration, λ is the light source wavelength, B , C etc are virial constants, these are related to the interaction of the solvent, P_θ is the particle scattering factor, N is Avogadro's number and d_n/dc is the rate of change of refractive index as a function of concentration.

For polymer solutions which contain polymers of low to moderate molecular weight, P_θ is equal to 1. This means equation 5.2 can be reduced to:

$$\frac{Hc}{\tau} = \frac{1}{M_w} (1 + 2Bc + Cc^2 + \dots) \quad 5.4$$

At low polymer concentrations equation 5.4 is now reduced to give:

$$\frac{Hc}{\tau} = \frac{1}{M_w} + \frac{2Bc}{M_w} \quad 5.5$$

This equation can be used as an equation for a straight line ($y = mx + c$), where "c"-containing terms beyond the 2Bc term are small

5.2 Explanation on how Polymers Molecular Weights are Determined using Universal Calibration Curve

Universal calibration is based on the limiting viscosity number (LVN) and molecular weight of a polymer, these are both proportional to hydrodynamic volume. Molecular weight is determined by constructing a *universal calibration line* by plotting log LVN of unknown polymer vs. retention time for a polymer standard. Molecular weight is found from the retention time of a polymer sample using the calibration line [8].

5.3 Raw Data for Each Polyhydroxypolyamide ¹H NMR Degradation Experiments

5.3.1 Poly(tetramethylene D-glucaramide) post-polymer

5.3.1.1 Degradation Experiments at Room Temperature

| Time (Mins) | Degree of Polymerisation (DP) Determined From ¹ H NMR End Group Analysis | |
|-------------|---|------------|
| | First Run | Second Run |
| | | |
| 2.83 | 13.75 | 13.42 |
| 13.50 | 13.70 | 13.64 |
| 24.17 | 13.58 | 13.76 |
| 34.83 | 13.68 | 13.45 |
| 45.50 | 13.65 | 13.59 |
| 56.17 | 13.74 | 13.74 |
| 66.83 | 13.83 | 13.63 |
| 77.50 | 13.61 | 13.68 |
| 88.17 | 13.68 | 13.71 |
| 98.83 | 13.76 | 13.64 |
| 109.50 | 13.70 | 13.61 |
| 120.17 | 13.66 | 13.68 |
| 130.83 | 13.63 | 13.52 |
| 141.50 | 13.72 | 13.81 |
| 152.17 | 13.67 | 13.66 |
| 162.83 | 13.76 | 13.76 |
| 173.50 | 13.73 | 13.61 |
| 184.17 | 13.64 | 13.68 |
| 194.83 | 13.81 | 13.56 |
| 205.50 | 13.65 | 13.86 |

| | | |
|--------|-------|-------|
| 216.17 | 13.73 | 13.70 |
| 226.83 | 13.72 | 13.85 |
| 237.50 | 13.73 | 13.68 |
| 248.17 | 13.65 | 13.63 |
| 258.83 | 13.84 | 13.61 |

5.3.1.2 Degradation Experiments at 50°C

| Time (Mins) | Degree of Polymerisation (DP) Determined From ¹ H NMR End Group Analysis | |
|-------------|---|------------|
| | First Run | Second Run |
| 2.83 | 17.22 | 17.39 |
| 13.50 | 17.12 | 17.28 |
| 24.17 | 17.04 | 17.11 |
| 34.83 | 16.75 | 17.03 |
| 45.50 | 16.86 | 16.98 |
| 56.17 | 16.94 | 16.91 |
| 66.83 | 16.20 | 16.82 |
| 77.50 | 16.22 | 16.75 |
| 88.17 | 15.58 | 16.48 |
| 98.83 | 15.27 | 16.31 |
| 109.50 | 15.65 | 16.18 |
| 120.17 | 15.27 | 16.01 |
| 130.83 | 15.15 | 15.89 |
| 141.50 | 15.10 | 15.71 |
| 152.17 | 14.86 | 15.54 |
| 162.83 | 14.64 | 15.47 |
| 173.50 | 14.14 | 15.30 |
| 184.17 | 14.18 | 15.18 |
| 194.83 | 14.09 | 15.11 |
| 205.50 | 14.12 | 14.55 |
| 216.17 | 14.07 | 14.43 |

| | | |
|--------|-------|-------|
| 226.83 | 14.08 | 14.13 |
| 237.50 | 13.75 | 13.92 |
| 248.17 | 13.56 | 13.84 |
| 258.83 | 13.35 | 13.64 |

5.3.2 Poly(tetramethylene D-glucaramide) pre-polymer

5.3.2.1 Degradation Experiments at Room Temperature

| Time (Mins) | Degree of Polymerisation (DP) Determined From ¹ H NMR End Group Analysis | |
|-------------|---|------------|
| | First Run | Second Run |
| | | |
| 2.83 | 9.46 | 9.21 |
| 13.50 | 9.35 | 9.35 |
| 24.17 | 9.33 | 9.45 |
| 34.83 | 9.33 | 9.54 |
| 45.50 | 9.67 | 9.32 |
| 56.17 | 9.70 | 9.65 |
| 66.83 | 9.70 | 9.32 |
| 77.50 | 9.29 | 9.41 |
| 88.17 | 9.27 | 9.37 |
| 98.83 | 9.33 | 9.63 |
| 109.50 | 9.29 | 9.45 |
| 120.17 | 9.27 | 9.21 |
| 130.83 | 9.27 | 9.30 |
| 141.50 | 8.94 | 9.15 |
| 152.17 | 9.27 | 9.25 |
| 162.83 | 9.27 | 9.27 |
| 173.50 | 9.29 | 9.61 |
| 184.17 | 9.23 | 9.22 |
| 194.83 | 9.25 | 9.29 |
| 205.50 | 9.25 | 9.16 |
| 216.17 | 9.21 | 9.48 |

| | | |
|--------|------|------|
| 226.83 | 9.27 | 9.45 |
| 237.50 | 9.25 | 9.23 |
| 248.17 | 8.90 | 9.24 |
| 258.83 | 9.25 | 9.15 |

5.3.2.2 Degradation Experiments at 50°C

| Time (Mins) | Degree of Polymerisation (DP) Determined From ¹ H NMR End Group Analysis | |
|-------------|---|------------|
| | First Run | Second Run |
| | | |
| 2.83 | 14.96 | 14.72 |
| 13.50 | 14.53 | 14.33 |
| 24.17 | 14.25 | 14.02 |
| 34.83 | 13.95 | 13.92 |
| 45.50 | 13.81 | 13.81 |
| 56.17 | 13.55 | 13.68 |
| 66.83 | 13.20 | 13.33 |
| 77.50 | 13.02 | 13.18 |
| 88.17 | 12.98 | 13.01 |
| 98.83 | 12.85 | 12.89 |
| 109.50 | 12.70 | 12.78 |
| 120.17 | 12.38 | 12.55 |
| 130.83 | 12.30 | 12.22 |
| 141.50 | 12.12 | 12.06 |
| 152.17 | 11.95 | 11.91 |
| 162.83 | 11.82 | 11.74 |
| 173.50 | 11.75 | 11.52 |
| 184.17 | 11.63 | 11.40 |
| 194.83 | 11.22 | 11.18 |
| 205.50 | 11.01 | 11.02 |
| 216.17 | 10.75 | 10.85 |
| 226.83 | 10.42 | 10.67 |

| | | |
|--------|-------|-------|
| 237.50 | 10.13 | 10.45 |
| 248.17 | 9.90 | 10.22 |
| 258.83 | 9.74 | 10.04 |

5.3.3 Poly(3',6'-dioxaoctamethylene D-glucaramide) pre-polymer

5.3.3.1 Degradation Experiments at Room Temperature

| Time (Mins) | Degree of Polymerisation (DP) Determined From ¹ H NMR End Group Analysis | |
|-------------|---|------------|
| | First Run | Second Run |
| 2.83 | 13.70 | 13.65 |
| 13.50 | 13.49 | 13.42 |
| 24.17 | 13.57 | 13.53 |
| 34.83 | 13.48 | 13.43 |
| 45.50 | 13.25 | 13.64 |
| 56.17 | 13.98 | 13.28 |
| 66.83 | 13.29 | 13.65 |
| 77.50 | 13.15 | 13.41 |
| 88.17 | 13.97 | 13.64 |
| 98.83 | 13.48 | 13.35 |
| 109.50 | 13.50 | 13.28 |
| 120.17 | 13.79 | 13.51 |
| 130.83 | 13.17 | 13.22 |
| 141.50 | 13.84 | 13.65 |
| 152.17 | 13.93 | 13.74 |
| 162.83 | 13.51 | 13.62 |
| 173.50 | 13.83 | 13.11 |
| 184.17 | 13.79 | 13.25 |
| 194.83 | 13.42 | 13.89 |
| 205.50 | 13.50 | 13.44 |
| 216.17 | 13.83 | 13.47 |
| 226.83 | 13.50 | 13.13 |

| | | |
|--------|-------|-------|
| 237.50 | 13.98 | 13.29 |
| 248.17 | 13.56 | 13.34 |
| 258.83 | 13.45 | 13.52 |

5.3.3.2 Degradation Experiments at 50°C

| Time (Mins) | Degree of Polymerisation (DP) Determined From ¹ H NMR End Group Analysis | |
|-------------|---|------------|
| | First Run | Second Run |
| | | |
| 2.83 | - | 14.89 |
| 13.50 | 14.66 | 14.62 |
| 24.17 | 14.58 | 14.57 |
| 34.83 | 14.53 | 14.50 |
| 45.50 | 14.48 | 14.42 |
| 56.17 | 14.47 | 14.40 |
| 66.83 | 14.41 | 14.42 |
| 77.50 | 14.34 | 14.35 |
| 88.17 | 14.30 | 14.28 |
| 98.83 | 14.27 | 14.27 |
| 109.50 | 14.21 | 14.10 |
| 120.17 | 14.16 | 14.15 |
| 130.83 | 14.09 | 14.06 |
| 141.50 | 14.11 | 14.01 |
| 152.17 | 14.06 | 13.98 |
| 162.83 | 13.94 | 14.00 |
| 173.50 | 13.92 | 13.90 |
| 184.17 | 13.86 | 13.85 |
| 194.83 | 13.77 | 13.78 |
| 205.50 | 13.68 | 13.77 |
| 216.17 | 13.65 | 13.74 |
| 226.83 | 13.61 | 13.70 |
| 237.50 | 13.58 | 13.69 |

| | | |
|--------|-------|-------|
| 248.17 | 13.50 | 13.66 |
| 258.83 | 13.49 | 13.63 |

5.3.3.3

5.3.4 Poly(ethylene D-glucaramide) post-polymer

5.3.4.1 Degradation Experiments at Room Temperature

| Time (Mins) | Degree of Polymerisation (DP) Determined From ^1H NMR End Group Analysis | |
|-------------|---|------------|
| | First Run | Second Run |
| 2.83 | 6.35 | 6.32 |
| 13.50 | 6.39 | 6.45 |
| 24.17 | 6.25 | 6.12 |
| 34.83 | 6.31 | 6.24 |
| 45.50 | 6.28 | 6.29 |
| 56.17 | 6.37 | 6.32 |
| 66.83 | 6.24 | 6.28 |
| 77.50 | 6.20 | 6.39 |
| 88.17 | 6.14 | 6.45 |
| 98.83 | 6.20 | 6.12 |
| 109.50 | 6.18 | 6.14 |
| 120.17 | 6.17 | 6.21 |
| 130.83 | 6.38 | 6.29 |
| 141.50 | 6.21 | 6.14 |
| 152.17 | 6.15 | 6.28 |
| 162.83 | 6.21 | 6.50 |
| 173.50 | 6.23 | 6.38 |
| 184.17 | 6.17 | 6.21 |
| 194.83 | 6.07 | 6.17 |
| 205.50 | 6.16 | 6.38 |
| 216.17 | 6.16 | 6.33 |
| 226.83 | 6.18 | 6.20 |
| 237.50 | 6.13 | 6.01 |

| | | |
|--------|------|------|
| 248.17 | 6.06 | 6.20 |
| 258.83 | 6.15 | 6.11 |

5.3.4.2

5.3.4.3 Degradation Experiments at 50°C

| Time (Mins) | Degree of Polymerisation (DP) Determined From ¹ H NMR End Group Analysis | |
|-------------|---|------------|
| | First Run | Second Run |
| 2.83 | 7.78 | 7.98 |
| 13.50 | 7.68 | 7.92 |
| 24.17 | 7.65 | 7.85 |
| 34.83 | 7.66 | 7.77 |
| 45.50 | 7.58 | 7.65 |
| 56.17 | 7.56 | 7.64 |
| 66.83 | 7.51 | 7.61 |
| 77.50 | 7.42 | 7.56 |
| 88.17 | 7.38 | 7.51 |
| 98.83 | 7.37 | 7.45 |
| 109.50 | 7.34 | 7.43 |
| 120.17 | 7.28 | 7.41 |
| 130.83 | 7.26 | 7.34 |
| 141.50 | 7.21 | 7.31 |
| 152.17 | 7.14 | 7.24 |
| 162.83 | 7.05 | 7.21 |
| 173.50 | 6.98 | 7.15 |
| 184.17 | 6.97 | 7.11 |
| 194.83 | 6.91 | 7.02 |
| 205.50 | 6.93 | 7.01 |
| 216.17 | 6.85 | 6.94 |
| 226.83 | 6.80 | 6.89 |
| 237.50 | 6.79 | 6.83 |

| | | |
|--------|------|------|
| 248.17 | 6.75 | 6.77 |
| 258.83 | 6.75 | 6.74 |

5.3.5 Poly(ethylene xylaramide) pre-polymer (A)

5.3.5.1 Degradation Experiments at Room Temperature

| Time (Mins) | Degree of Polymerisation (DP) Determined From ¹ H NMR End Group Analysis | |
|-------------|---|------------|
| | First Run | Second Run |
| | | |
| 2.83 | 4.87 | 4.65 |
| 13.50 | 4.74 | 4.21 |
| 24.17 | 4.31 | 4.98 |
| 34.83 | 4.68 | 4.56 |
| 45.50 | 4.53 | 4.78 |
| 56.17 | 4.48 | 4.32 |
| 66.83 | 4.53 | 4.65 |
| 77.50 | 4.60 | 4.52 |
| 88.17 | 4.60 | 4.63 |
| 98.83 | 4.59 | 4.72 |
| 109.50 | 4.52 | 4.62 |
| 120.17 | 4.53 | 4.51 |
| 130.83 | 4.81 | 4.49 |
| 141.50 | 4.68 | 4.71 |
| 152.17 | 4.61 | 4.62 |
| 162.83 | 4.53 | 4.53 |
| 173.50 | 4.77 | 4.59 |
| 184.17 | 4.64 | 4.62 |
| 194.83 | 4.78 | 4.78 |
| 205.50 | 4.86 | 4.41 |
| 216.17 | 4.59 | 4.62 |
| 226.83 | 4.69 | 4.76 |

| | | |
|--------|------|------|
| 237.50 | 4.73 | 4.51 |
| 248.17 | 4.82 | 4.50 |
| 258.83 | 4.69 | 4.89 |

5.3.5.2

5.3.5.3 Degradation Experiments at 50°C

| Time (Mins) | Degree of Polymerisation (DP) Determined From ¹ H NMR End Group Analysis | |
|-------------|---|------------|
| | First Run | Second Run |
| 2.83 | 6.31 | 6.35 |
| 13.50 | 6.22 | 6.31 |
| 24.17 | 6.21 | 6.20 |
| 34.83 | 6.14 | 6.17 |
| 45.50 | 6.02 | 6.11 |
| 56.17 | 5.98 | 6.01 |
| 66.83 | 5.96 | 5.91 |
| 77.50 | 5.90 | 5.86 |
| 88.17 | 5.85 | 5.80 |
| 98.83 | 5.81 | 5.78 |
| 109.50 | 5.72 | 5.73 |
| 120.17 | 5.65 | 5.62 |
| 130.83 | 5.57 | 5.56 |
| 141.50 | 5.43 | 5.48 |
| 152.17 | 5.39 | 5.42 |
| 162.83 | 5.31 | 5.32 |
| 173.50 | 5.21 | 5.31 |
| 184.17 | 5.16 | 5.21 |
| 194.83 | 5.11 | 5.18 |
| 205.50 | 5.02 | 5.12 |
| 216.17 | 4.96 | 4.99 |
| 226.83 | 4.92 | 4.92 |

| | | |
|--------|------|------|
| 237.50 | 4.83 | 4.88 |
| 248.17 | 4.75 | 4.74 |
| 258.83 | 4.69 | 4.68 |

5.3.5.4

5.3.6 Poly(ethylene xylaramide) pre-polymer (B)

5.3.6.1 Degradation Experiments at Room Temperature

5.3.6.2

| Time (Mins) | Degree of Polymerisation (DP) Determined From ¹ H NMR End Group Analysis | |
|-------------|---|------------|
| | First Run | Second Run |
| | | |
| 2.83 | 8.96 | 8.71 |
| 13.50 | 9.26 | 9.12 |
| 24.17 | 8.70 | 8.98 |
| 34.83 | 9.34 | 9.02 |
| 45.50 | 8.70 | 9.23 |
| 56.17 | 9.33 | 9.15 |
| 66.83 | 8.85 | 8.98 |
| 77.50 | 8.96 | 8.75 |
| 88.17 | 8.50 | 9.12 |
| 98.83 | 8.46 | 9.32 |
| 109.50 | 8.78 | 8.81 |
| 120.17 | 8.94 | 8.83 |
| 130.83 | 8.80 | 8.95 |
| 141.50 | 9.42 | 9.20 |
| 152.17 | 9.07 | 9.32 |
| 162.83 | 8.65 | 8.89 |
| 173.50 | 8.67 | 8.63 |
| 184.17 | 8.55 | 8.97 |
| 194.83 | 8.67 | 8.75 |

| | | |
|--------|------|------|
| 205.50 | 8.50 | 9.02 |
| 216.17 | 8.46 | 8.62 |
| 226.83 | 8.94 | 8.75 |
| 237.50 | 8.80 | 9.09 |
| 248.17 | 8.70 | 8.86 |
| 258.83 | 8.56 | 8.42 |

5.3.6.3 Degradation Experiments at 50°C

| Time (Mins) | Degree of Polymerisation (DP) Determined From ¹ H NMR End Group Analysis | |
|-------------|---|------------|
| | First Run | Second Run |
| 2.83 | 10.32 | 10.56 |
| 13.50 | 10.23 | 10.32 |
| 24.17 | 10.20 | 10.15 |
| 34.83 | 10.14 | 10.08 |
| 45.50 | 10.09 | 9.95 |
| 56.17 | 10.02 | 9.84 |
| 66.83 | 10.00 | 9.72 |
| 77.50 | 9.96 | 9.63 |
| 88.17 | 9.85 | 9.56 |
| 98.83 | 9.80 | 9.41 |
| 109.50 | 9.74 | 9.32 |
| 120.17 | 9.60 | 9.22 |
| 130.83 | 9.52 | 9.15 |
| 141.50 | 9.38 | 9.03 |
| 152.17 | 9.36 | 9.01 |
| 162.83 | 9.29 | 8.91 |
| 173.50 | 9.22 | 8.78 |
| 184.17 | 9.20 | 8.71 |
| 194.83 | 9.14 | 8.64 |
| 205.50 | 9.11 | 8.51 |

| | | |
|--------|------|------|
| 216.17 | 9.02 | 8.43 |
| 226.83 | 8.89 | 8.31 |
| 237.50 | 8.84 | 8.25 |
| 248.17 | 8.78 | 8.19 |
| 258.83 | 8.76 | 8.10 |

5.4 Raw Data for Poly(tetramethylene D-glucaramide) post-polymer Temperature Experiments

| Temperature (°C) | Degree of Polymerisation (DP) Determined From ¹ H NMR End Group Analysis | |
|---------------------|---|------------|
| | First Run | Second Run |
| | | |
| 30 | 8.76 | 8.45 |
| 40 | 9.22 | 9.67 |
| 50 | 11.41 | 11.21 |
| 60 | 13.51 | 13.47 |
| 70 | 17.50 | 17.02 |

5.5 Raw Data for T_1 and T_2 Relaxation Rate Measurements for each Poly(tetramethylene D-glucaramide) post-polymer Fraction

| T_1 Relaxation Rate (sec) | Fraction A | Fraction B | Fraction C | Fraction D | Fraction E | Fraction F |
|-----------------------------|------------|------------|------------|------------|------------|------------|
| First Measurement | 1.168 | 1.164 | - | 1.318 | 1.354 | 1.518 |
| Second Measurement | 1.140 | 1.157 | - | 1.316 | 1.358 | 1.517 |
| Third Measurement | 1.149 | 1.152 | - | 1.309 | - | 1.502 |
| Fourth Measurement | 1.162 | 1.155 | - | 1.315 | - | 1.511 |
| Fifth Measurement | 1.157 | 1.162 | - | 1.302 | - | 1.517 |

| T_2 Relaxation Rate (sec) | Fraction A | Fraction B | Fraction C | Fraction D | Fraction E | Fraction F |
|-----------------------------|------------|------------|------------|------------|------------|------------|
| First Measurement | 147.6 | 144.8 | - | 173.8 | - | 200.5 |
| Second Measurement | 147.8 | 144.8 | - | 173.9 | - | 200.4 |
| Third Measurement | 147.8 | 144.6 | - | 173.8 | - | 200.2 |
| Fourth Measurement | 147.7 | 144.7 | - | 173.8 | - | 200.5 |
| Fifth Measurement | 147.6 | 144.6 | - | 176 | - | 200.4 |

5.6 Raw Data for T_2 Relaxation Rate Measurements for each Poly(3',6'-dioxaoctamethylene D-glucaramide) pre-polymer Fraction

| T_2 Relaxation Rate (sec) | Fraction A | Fraction B | Fraction C | Fraction D | Fraction E | Fraction F | Fraction G |
|-----------------------------|------------|------------|------------|------------|------------|------------|------------|
| First Measurement | 192.2 | 194.9 | 209.3 | 219.7 | 228.1 | - | - |
| Second Measurement | 191.3 | 194.5 | 209.5 | 219.8 | 226.7 | - | - |
| Third Measurement | 191.4 | 194.3 | 208.8 | 219.1 | 228.2 | - | - |
| Fourth Measurement | 192.3 | 194.4 | 208.6 | 219.5 | 228.1 | - | - |
| Fifth Measurement | 192.0 | 195.4 | 209.3 | 218.9 | 227.9 | - | - |

5.7 Raw Data for T_2 Relaxation Rate Measurements for each Dextran

| T_2 Relaxation Rate (sec ⁻¹) at 30°C | Dextran 1220 | Dextran 4440 | Dextran 9840 | Dextran 43,500 | Dextran 70,000 | Dextran 110,000 | Dextran 401,300 | Dextran 1:1 Mix | Dextran Simulated |
|---|-----------------|-----------------|-----------------|-------------------|-------------------|--------------------|--------------------|--------------------|----------------------|
| First Measurement | 119.7 | 58.59 | 79.82 | 63.31 | - | 61.53 | 61.53 | 76.95 | 72.88 |
| Second Measurement | 200.0 | 86.07 | 77.03 | 64.91 | 60.94 | 61.59 | 61.59 | 75.47 | 73.69 |
| Third Measurement | 119.4 | 86.61 | 78.40 | - | 63.33 | 62.72 | 62.59 | 75.39 | 74.50 |
| Fourth Measurement | 119.6 | - | 78.67 | 64.17 | 63.00 | 61.8 | 61.80 | 76.05 | 74.42 |
| Fifth Measurement | 119.8 | 85.97 | 78.65 | 64.29 | 64.29 | 61.72 | 61.77 | 75.83 | - |

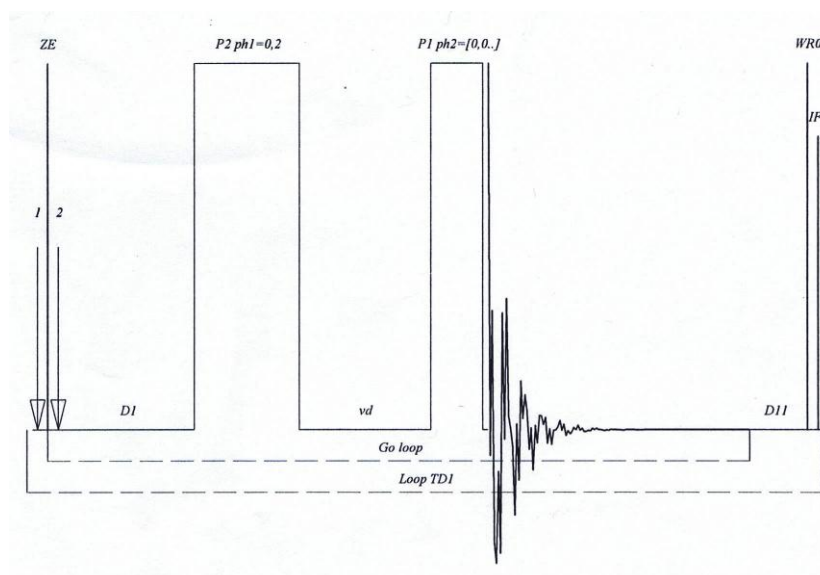
| T_2 Relaxation Rate (sec ⁻¹) at 50°C | Dextran 1220 | Dextran 4440 | Dextran 9840 | Dextran 43,500 | Dextran 70,000 | Dextran 110,000 | Dextran 401,300 | Dextran 1:1 Mix | Dextran Simulated |
|---|-----------------|-----------------|-----------------|-------------------|-------------------|--------------------|--------------------|--------------------|----------------------|
| First Measurement | 193.0 | 143.1 | 130.7 | 103.3 | 98.29 | 97.14 | 94.85 | 114.2 | 112.0 |
| Second Measurement | 192.7 | 141.4 | - | 102.2 | 98.88 | 97.07 | 94.20 | 114.7 | 112.0 |
| Third Measurement | 192.0 | 142.3 | 130.3 | 102.2 | 99.35 | 97.52 | 94.64 | 114.2 | 112.2 |
| Fourth Measurement | 192.5 | 141.6 | 130.3 | 102.1 | 99.03 | 97.29 | - | 114.5 | 111.8 |
| Fifth Measurement | 192.3 | 142.0 | 130.4 | 102.9 | 96.62 | - | 94.51 | 114.1 | - |

5.8 Commands to Reduce the Effect of HOD water Peak on T_2 Relaxation Rate Measurements

To prevent the HOD water signal affecting signals used to measure relaxation rates, the use of the command *asb2.water* can alleviate this problem from this signal.

5.9 Pulse Programs used to measure T_1 Relaxation Rate

T_1 Measurements using Inversion Recovery from TOPSPIN software



“p2 = p1*2”

“d11=30m”

1 ze

2 d1

p2 ph1

vd

p1 ph1

go=2 ph31

d11 wr #0 if #0 ivd

lo to 1 times td1

exit

ph1 = 0 2

ph2 = 0 0 2 2 1 1 3 3

ph31 = 0 0 2 2 1 1 3 3

; p11 : f1 channel - power level for pulse (default)

; p1 : f1 channel - 90 degree high power pulse

; p2 : f1 channel - 180 degree high power pulse

; d1 : relaxation delay; 1-5 * T1

; d11 : delay for disk I/O [30msec]

; vd : variable delay, from vd-list

; NS: 8 * n

; DS : 4

;td1: number of experiments = number of delays in vd-list

;define VDLIST

; this pulse program produces a ser-file (PARMOD = 2D)

VDLIST used for each Measurement

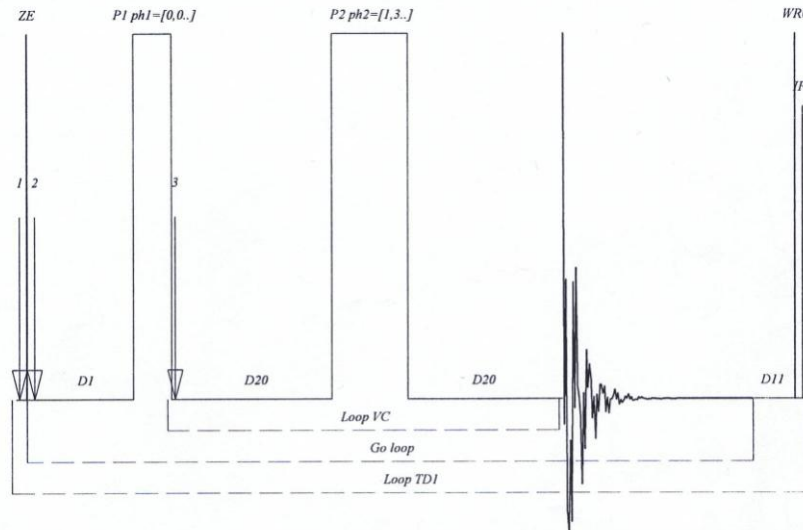
10sec, 8sec, 4sec, 2sec, 1sec, 0.7sec, 0.5sec, 0.3sec, 0.1sec

Parameters used for each Measurement

| | |
|-----|---------|
| d1 | 10sec |
| d11 | 0.03sec |
| NS | 32 |
| DS | 2 |

5.10 Pulse Programs used to measure T_2 Relaxation Rate

T_2 Measurement using Carr-Purcell-Meiboom-Gill sequence



"p2 = p1*2"

"d11 = 30m"

```

1 ze
2 d1
  p2 ph1
  3 d20
  p2 ph2
  d20
  lo to 3 times c
  go=2 ph31
  d11 wr #0 if #0 ivc
  lo to 1 times td1
exit

```

ph1= 0 0 2 2 1 1 3 3

ph2= 1 3 1 3 0 2 0 2

ph31= 0 0 2 2 1 1 3 3

```

; p11 : f1 channel - power level for pulse (default)
; p1 : f1 channel - 90 degree high power pulse
; p2 : f1 channel - 180 degree high power pulse
; d1 : relaxation delay; 1-5 * T1
; d11 : delay for disk I/O [30msec]
; d20 : fixed echo time to allow elimination of diffusion and J-mod. effects
; vc : variable loop counter, taken from vc-list
; NS: 8 * n
; DS : 16
;td1: number of experiments = number of values in vc-list

; define VCLIST

; this pulse program produces a ser-file (PARMOD = 2D)

; d20: d20 should be << 1/J, but (50 * p2)
; vc : vc should contain even numbers to provide for cancellation of 180 degree
pulse error

```

VCLIST used for each Measurement

62, 162, 262, 362, 462, 562, 662, 762, 862, 962, 1062 and 1162

Parameters used for each Measurement

| | |
|-----|----------|
| d1 | 10sec |
| d11 | 0.002sec |
| d20 | 0.002sec |

6 References

1. Hiemenz, P.C. and T.P. Lodge, *Polymer Chemistry, 2nd ed.* 2nd ed. 2007, Boca Raton: CRC Press.
2. Stevens, M.P., *Polymer Chemistry, An Introduction, 3rd ed.* 1999, New York: Oxford University Press, Inc.
3. Sperling, L.H., *Introduction to Physical Polymer Science. 4th ed.* 4th ed. 2006, New Jersey: John Wiley and Sons, Inc.
4. Jarman, B., *Synthesis of Polyhydroxypolyamides Based on Galactaric Acid and X-Ray Crystal Analysis of Their Precursors*, in *Chemistry*. 2006, University of Waikato: Hamilton.
5. Carpenter, C.A., *Mannaric Acid and Mannaric Acid Polyamides: Synthesis and Characterization*, in *Chemistry*. 2008, University of Montana: Missoula.
6. Gnanou, Y. and M. Fontanille, *Organic and Physical Chemistry Of Polymers*. 2008, New Jersey: John Wiley and Sons, Inc.
7. Holding, S.R. and E. Meehan, *Molecular Weight Characterisation of Synthetic Polymers*, in *Rapra Review Reports*. 1995.
8. Charles E. Carraher, J., *Polymer Chemistry, 7th ed.* 2008, Boca Raton: CRC Press.
9. Young, R.J., *Introduction to Polymers*. 1981, London: Chapman and Hall Ltd.
10. Seymour, R.B., *Introduction to Polymer Chemistry*. 1971, New York: McGraw-Hill.
11. Parris, N.A., *Instrumental Liquid Chromatography, A Practical Manual on High Performance Liquid Chromatographic Methods*. Journal of Chromatography Library. 1976, Amsterdam: Elsevier Scientific Publishing Company.
12. Nielen, M.W.F., *MALDI Time-of-Flight Mass Spectrometry of Synthetic Polymers*. Mass Spectrometry Reviews, 1999. **18**(5): p. 309-344.
13. Nielen, M.F. and S. Malucha, *Characterization of Polydisperse Synthetic Polymers by Size-exclusion Chromatography/Matrix-assisted Laser Desorption/Ionization Time-of-flight Mass Spectrometry*. Rapid Communications in Mass Spectrometry, 1997. **11**(11): p. 1194-1204.
14. Hanton, S.D. and X.M. Liu, *GPC Separation of Polymer Samples for MALDI Analysis*. Analytical Chemistry, 2000. **72**(19): p. 4550-4554.

15. Lehrle, R.S. and D.S. Sarson, *Degradation and Selective Desorption of Polymer can Cause Uncertainty in MALDI (Matrix-Assisted Laser Desorption Ionisation) Measurements*. *Polymer Degradation and Stability*, 1996. **51**(2): p. 197-204.
16. Hanton, S.D., *Mass Spectrometry of Polymers and Polymer Surfaces*. *Chemical Reviews*, 2001. **101**(2): p. 527-569.
17. Scrivens, J.H. and A.T. Jackson, *Characterisation of Synthetic Polymer Systems*. *International Journal of Mass Spectrometry*, 2000. **200**(2): p. 261-276.
18. Dalluge, J.J., *Matrix-assisted laser desorption ionization-mass spectrometry (MALDI-MS)*. *Analytical and Bioanalytical Chemistry* 2002. **372**(1): p. 18-19.
19. Montaudo, G., et al., *Characterization of Polymers by Matrix-assisted Laser Desorption Ionization-Time of Flight Mass Spectrometry. End Group Determination and Molecular Weight Estimates in Poly(ethylene glycols)*. *Macromolecules*, 1995. **28**(13): p. 4562-4569.
20. Montaudo, G., *Molecular and Structural Characterization of Polydisperse Polymers and Copolymers by Combining MALDI-TOF Mass Spectrometry with GPC Fractionation*. *Macromolecules*, 1995. **28**(24): p. 7983-7989.
21. Axelsson, J., et al., *Mass Discrimination Effects in an Ion Detector and Other Causes for Shifts in Polymer Mass Distributions Measured by Matrix-Assisted Laser Desorption/Ionization Time-of-Flight Mass Spectrometry*. *Macromolecules*, 1996. **29**(27): p. 8875-8882.
22. Mayran, S. and E. Jacques, *Mass-Selected Reagent Ion Chemical Ionization and Multiple Tandem Mass Spectrometry Techniques in an Ion Trap Mass Spectrometer for Structural Analysis*. *Rapid Communications in Mass Spectrometry*, 1998. **11**(11): p. 1185 - 1193.
23. Schriemer, D.C. and L. Li, *Detection of High Molecular Weight Narrow Polydisperse Polymers up to 1.5 Million Daltons by MALDI Mass Spectrometry*. *Analytical Chemistry*, 1996. **68**(13): p. 2721-2725.
24. Jackson, C., B. Larsen, and C. McEwen, *Comparison of Most Probable Peak Values As Measured for Polymer Distributions by MALDI Mass Spectrometry and by Size Exclusion Chromatography*. *Analytical Chemistry*, 1996. **68**(8): p. 1303-1308.
25. Sakurada, N., et al., *Characterization of poly(methyl methacrylate) by Matrix-assisted Laser Desorption/Ionization Mass Spectrometry. A Comparison with Supercritical Fluid Chromatography and Gel Permeation Chromatography*. *Rapid Communications in Mass Spectrometry*, 1998. **12**(23): p. 1895-1898.

26. Nielen, M.W.F., *Polymer Analysis by Micro-Scale Size-Exclusion Chromatography/MALDI Time-of-Flight Mass Spectrometry with a Robotic Interface*. Analytical Chemistry, 1998. **70**(8): p. 1563-1568.
27. Berne, B.J. and R. Pecora, *Dynamic Light Scattering*. 1976, New Jersey: John Wiley and Son, Inc.
28. Chu, B., *Laser Light Scattering*. 1974, New York: Academic Press.
29. Hasse, H., et al., *Osmotic Virial Coefficients of Aqueous Poly(ethylene glycol) from Laser-Light Scattering and Isopiestic Measurements*. Macromolecules, 1995. **28**(10): p. 3540-3552.
30. Nicholson, J.W., *The Chemistry of Polymers, 3rd ed.* 2006, London: Royal Society of Chemistry.
31. Scholte, T.G., *Light Scattering of Concentrated Polydisperse Polymer Solutions*. Journal of Polymer Science: Part C, 1972. **39**: p. 281-291.
32. Wu, C., *Laser Light-Scattering Characterization of the Molecular Weight Distribution of Dextran*. Macromolecules, 1993. **26**(15): p. 3821-3825.
33. Wyatt, P.J., *Light Scattering and Absolute Characteristic of Macromolecules*. Analytica Chimica Acta, 1993. **272**: p. 1-40.
34. Honghui Zhu, T. Yalcin, and L. Li, *Analysis of the Accuracy of Determining Average Molecular Weights of Narrow Polydispersity Polymers by Matrix-Assisted Laser Desorption Ionization Time-of-Flight Mass Spectrometry*. American Society for Mass Spectrometry, 1998. **9**(4): p. 275-281.
35. Brown, R.P., *Laser Light Scattering as GPC Detector*. Polymer Testing, 1983. **3**(4): p. 267-289.
36. Kennedy, J.F., *Light Scattering and Chromatography in Combination*. Monographs on the Physics and Chemistry of Materials, 1996. **53**: p. 494-523.
37. Ibbett, R.N., *NMR Spectroscopy of Polymers*. 1993, London: Blackie Academic & Professional.
38. Mirau, P.A., *A Practical Guide to Understanding the NMR of Polymers*. 2005, New York: Wiley-Interscience.
39. Hunt, B.J. and M.I. James, *Polymer Characterisation*. 1993, London: Blackie Academic & Professional.
40. Silverstein, R.M., F.X. Webster, and D.J. Kiemle, *Spectrometric Identification of Organic Compounds, 7th ed.* 7th ed. 2005, New Jersey: John Wiley and Sons, Inc.
41. Wilkins, A., *Lecture Notes from Chem504 Honours Lectures*.

42. Kimmich, R., G. Schnur, and M. Köpf, *Progress in Nuclear Magnetic Resonance Spectroscopy*. The Tube Concept of Macromolecular Liquids in the Light of NMR Experiments, 1988. **20**(4): p. 385-421.
43. Kimmich, R. and H.W. Weber, *Anomalous Segment Diffusion in Polymers and NMR Relaxation Spectroscopy*. *Macromolecules*, 1993. **26**: p. 2597.
44. Brown, J.M., *Equilibration of D-Glucaric Acid in Aqueous Solution*, in *Chemistry*. 2007, University of Waikato: Hamilton.
45. Kiely, D.E., L. Chen, and T.-H. Lin, *Hydroxylated Nylons Based on Unprotected Esterified D-Glucaric Acid by Simple Condensation Reactions*. *Journal of American Chemical Society*, 1994. **116**: p. 571-578.
46. Kiely, D.E., L. Chen, and T.-H. Lin, *Synthetic Polyhydroxypolyamides from Galactaric, Xylaric, D-Glucaric, and D-Mannaric Acids and Alkylenediamine Monomers—Some Comparisons*. *Journal of Polymer Science: Part A: Polymer Chemistry*, 2000. **38**(3): p. 594-603.
47. Chen, L. and D.E. Kiely, *Synthesis of Stereoregular Head, Tail Hydroxylated Nylons Derived from D-Glucose*. *Journal of Organic Chemistry*, 1996. **61**(17): p. 5847-5851.
48. Kiely, D.E., et al., *Synthesis of Poly(galactaramides) from Alkylene- and Substituted Alkylenediammonium Galactarates*. *Journal of Carbohydrate Chemistry*, 2009. **28**(6): p. 348-368.
49. Carter, A., D.W. Morton, and D.E. Kiely, *Synthesis of Some Poly(4-alkyl-4-azaheptamethylene-Dglucaramides)*. *Journal of Polymer Science: Part A: Polymer Chemistry*, 2000. **38**(21): p. 3892-3899.
50. Morton, D.W. and D.E. Kiely, *Synthesis of Poly(azaalkylene aldaramide)s and Poly(oxaalkylene aldaramide)s Derived from D-Glucaric and D-Galactaric Acids*. *Journal of Polymer Science: Part A: Polymer Chemistry*, 2000. **38**(3).
51. Styron, S.D., et al., *MM3(96) Conformational Analysis of D-Glucaramide and X-Ray Crystal Structures of Three D-Glucaric Acid Derivatives—Models of Synthetic Poly(Alkylene D-Glucaramides)* *Journal of Carbohydrate Chemistry*, 2002. **21**: p. 27-51.
52. Kiely, D.E., *Unpublished Work from the Shafizadeh Rocky Mountain Center for Wood and Carbohydrate Chemistry*.
53. Hsu, N.-Y., et al., *Matrix-Assisted Laser Desorption/Ionization Mass Spectrometry of Polysaccharides with 2',4',6'-Trihydroxyacetophenone as Matrix*. *Rapid Communications in Mass Spectrometry*, 2007. **21**(13): p. 2137-2146.

54. Bashir, S., et al., *Matrix-Assisted Laser Desorption/Ionization Time-of-Flight Mass Spectrometry of Dextran and Dextrin Derivatives*. *European Journal of Mass Spectrometry*, 2003. **9**(1): p. 61-70.
55. Hinton, M.R., *Xylaric Acid, D-Arabinaric Acid (D-Lyxaric Acid), L-Arabinaric Acid (L-Lyxaric Acid), and Ribaric Acid-1,4-Lactone; Synthesis and Isolation of Polyhydroxypolyamides there from in Chemistry*. 2008, University of Montana: Missoula.
56. Barrow, G.M., *Physical Chemistry, 6th ed.* 1996: WCB/McGraw-Hill.
57. Craver, C.D. and C.E. Carraher, *Applied Polymer Science: 21st Century*. 2000, Amsterdam: Elsevier.
58. Nicholson, J.W., *The Chemistry of Polymers*. 1991, London: Royal Society of Chemistry.
59. Bletsos, I.V. and D.M. Hercules, *Molecular Weight Distributions of Polymers Using Time-of-Flight Secondary-Ion Mass Spectrometry*. *Analytical Chemistry*, 1991. **63**(18): p. 1953-1960.
60. Chuang, I.-S. and G.E. Maciel, *Natural-abundance ^{15}N Cross-polarization/Magic-angle Spinning Nuclear Magnetic Resonance Study of Urea-formaldehyde Resins*. *Polymer*, 1994. **35**(8): p. 1621-1628.
61. Cmelík, R., M. Stikarovská, and J. Chmelík, *Different Behavior of Dextrans in Positive-ion and Negative-ion Mass Spectrometry*. *Journal of Mass Spectrometry*, 2004. **39**(12): p. 1467-1473.
62. Grcev, S., P. Schoenmakers, and P. Iedema, *Determination of Molecular Weight and Size Distribution and Branching Characteristics of PVAc by Means of Size Exclusion Chromatography/Multi-Angle Laser Light Scattering (SEC/MALLS)*. *Polymer*, 2004. **45**(1): p. 39-48.
63. Hagelin, G., et al., *Characterization of Low Molecular Weight Polymers by Matrix-assisted Laser Desorption/Ionization Mass Spectrometry. A Comparison with Gel Permeation Chromatography*. *Rapid Communications in Mass Spectrometry*, 1998. **12**(1): p. 25-27.
64. Halbeek, H.V. and L. Poppe, *Conformation and Dynamics of Glycoprotein Oligosaccharides as Studied by ^1H NMR Spectroscopy*. *Magnetic Resonance in Chemistry*, 1992. **30**(1): p. 74-86.
65. Jahns, T. and D.E. Kiely, *Abiotic Hydrolysis of Some Poly-D-glucaramides and Subsequent Microbial Utilization/Degradation*. *Journal of Polymers and the Environment*, 2006. **14**(2): p. 165-169.
66. M.Andreis and J.L. Koenig, *Applications of Nitrogen-15 NMR to Polymers*. *Advances in Polymer Science*, 1995. **124**: p. 193-237.

67. Mccall, D.W., *Nuclear Magnetic Resonance Studies of Molecular Relaxation Mechanisms*. The Journal of Elastomers and Plastics, 1976. **8**(1): p. 60-80.
68. Meier, M.A.R., et al., *Automated Multiple-Layer Spotting for Matrix-assisted Laser Desorption/Ionization Time-of-Flight Mass Spectrometry of Synthetic Polymers Utilizing Ink-Jet Printing Technology*. Rapid Communications in Mass Spectrometry, 2003. **17**(20): p. 2349-2353.
69. Meier, M.A.R. and U.S. Schubert, *Evaluation of a New Multiple-Layer Spotting Technique for Matrix-Assisted Laser Desorption/Ionization Time-of-Flight Mass Spectrometry of Synthetic Polymers*. Rapid Communications in Mass Spectrometry, 2003. **17**(7): p. 713-716.
70. Thijs, H.M.L., M.A.R. Meier, and U.S. Schubert, *Application Possibilities of Preparative Size Exclusion Chromatography to Analytical Problems in Polymer Science*. e-Polymers, 1997. **46**: p. 1-10.
71. Viswanathan, A. and D.E. Kiely, *Mechanisms for the Formation of Diamides and Polyamides by Aminolysis of D-Glucaric Acid Esters*. Journal of Carbohydrate Chemistry, 2003. **22**(9): p. 903-918.
72. Zhang, Z. and A.G. Marshall, *A Universal Algorithm for Fast and Automated Charge State Deconvolution of Electrospray Mass-to-Charge Ratio Spectra*. American Society for Mass Spectrometry, 1998. **9**: p. 225-233.
73. Chuang, I.-S. and G.E. Maciel, *NMR Characterization of Complex Organic Resin*, in *Annual Reports on NMR Spectroscopy*. 1994.